

Supplementary Information

Three-Dimensional Structural Alignment Based Discovery and Molecular Basis of AtoB, Catalyzing Linear Tetracyclic Formation

*Ke Ma,^a Jie Liu,^a Zequan Huang,^a Mengyue Wu,^a Dong Liu,^a Jinwei Ren,^b Aili Fan,^{*a} and Wenhan Lin^{*a,c}*

a. State Key Laboratory of Natural and Biomimetic Drugs, School of Pharmaceutical Sciences, Peking University, Beijing 100191, China.

b. State Key Laboratory of Mycology, Institute of Microbiology, Chinese Academy of Sciences, Beijing 100101, China.

c. Ningbo Institute of Marine Medicine, Peking University, Ningbo 315832 Zhejiang, China.

* Corresponding authors: fanaili@bjmu.edu.cn; whlin@bjmu.edu.cn

TABLE OF CONTENTS

Experimental Procedures	6
Strains and culture conditions.	6
General Chemical Analysis.....	6
Gene cloning, DNA fragment construction, and plasmid construction	6
Bioinformatics analysis.....	7
Fungal transformation in <i>A.nidulans</i> and <i>A. ochraceus</i>	7
Feeding experiments with <i>A.nidulans</i>	7
Protein expression and purification.....	7
<i>In vitro</i> assays of AtoB and its mutant variants	8
AtoB protein expression and purification for crystallization	8
Crystallization and structure determination of AtoB	9
Large-scale fermentation, extraction, Isolation and characterization of compounds.....	9
The protein sequence of AtoB.....	11
Supplementary Tables	12
Table S1. Predicted protein functions and blast results of <i>ato</i> cluster.	12
Table S2. Fungal strains used in this study.	13
Table S3. PCR primers used in this study.....	14
Table S4. Plasmids used in this study.	17
Table S5. Data collection, phasing, and refinement statistics.....	18
Table S6. Relative enzymatic activities of wild-type AtoB and its variants.....	19
Table S7. ^1H and ^{13}C NMR data of compounds 4a and 4b	20
Table S8. ^1H and ^{13}C NMR data of compounds 6a and 6b in acetone- <i>d</i> ₆	21
Table S9. ^1H and ^{13}C NMR data of compounds 3 , 7 , and 8 in DMSO- <i>d</i> ₆	22
Table S10. ^1H and ^{13}C NMR data of compounds 9-11	23
Table S11. ^1H and ^{13}C NMR data of compounds 12-14 in acetone- <i>d</i> ₆	24
Table S12. ^1H and ^{13}C NMR data of compounds 15-17	25
Table S13. ^1H and ^{13}C NMR data of compounds 19 , 21 , and 23	26
Supplementary Figures.....	27
Figure S1. Phylogenetic tree of AtoB and others NTF2-like enzymes in cluster 2.	27
Figure S2. Comparison of the <i>ato</i> cluster and the reported fungal meroterpenoid gene clusters that encoding homologous proteins.....	29

Figure S3. Biosynthesis of aspertetranone and functions of <i>ato</i> genes.....	30
Figure S4. Metabolites of $\Delta atoB\Delta atoM$ and An- <i>ato</i> CEHKGDLIF.....	32
Figure S5. The overall structures of AtoB (A), AtoB complex with compound 19 (B) and omitting map (C and D) of the complex.....	33
Figure S6. Comparing the hydrophilic amino acid residues in the active cavity of AtoB (A), BvnE (B), SdnG (C), Trt14 (D), and NsrQ (E).	34
Figure S7. The dimer interface of AtoB (A), BvnE (B), SdnG (C), Trt14 (D), and NsrQ (E).	35
Figure S8. SDS-PAGE analysis of purified AtoB (19.8 kDa).	36
Figure S9. 1H NMR spectrum of 3 (DMSO- <i>d</i> ₆ , 500 MHz).....	37
Figure S10. ^{13}C NMR spectrum of 3 (DMSO- <i>d</i> ₆ , 125 MHz).....	37
Figure S11. HSQC spectrum of 3	38
Figure S12. HMBC spectrum of 3	38
Figure S13. ROESY spectrum of 3	39
Figure S14. 1H NMR spectrum of 4a (acetone- <i>d</i> ₆ , 500 MHz).....	39
Figure S15. ^{13}C NMR spectrum of 4a (acetone- <i>d</i> ₆ , 125 MHz).....	40
Figure S16. 1H NMR spectrum of 4b (DMSO- <i>d</i> ₆ , 500 MHz).....	40
Figure S17. ^{13}C NMR spectrum of 4b (DMSO- <i>d</i> ₆ , 125 MHz).....	41
Figure S18. HSQC spectrum of 4b	42
Figure S19. HMBC spectrum of 4b	42
Figure S20. ROESY spectrum of 4b	43
Figure S21. 1H NMR spectrum of 6a (acetone- <i>d</i> ₆ , 500 MHz).....	44
Figure S22. ^{13}C NMR spectrum of 6a (acetone- <i>d</i> ₆ , 125 MHz).....	44
Figure S23. HSQC spectrum of 6a	44
Figure S24. HMBC spectrum of 6a	45
Figure S25. ROESY spectrum of 6a	45
Figure S26. 1H NMR spectrum of 6b (acetone- <i>d</i> ₆ , 500 MHz).....	46
Figure S27. ^{13}C NMR spectrum of 6b (acetone- <i>d</i> ₆ , 125 MHz).....	46
Figure S28. HSQC spectrum of 6b	47
Figure S29. HMBC spectrum of 6b	47
Figure S30. ROESY spectrum of 6b	48
Figure S31. 1H NMR spectrum of 7 (DMSO- <i>d</i> ₆ , 500 MHz).....	48
Figure S32. ^{13}C NMR spectrum of 7 (DMSO- <i>d</i> ₆ , 125 MHz).....	49
Figure S33. HSQC spectrum of 7	49
Figure S34. HMBC spectrum of 7	50
Figure S35. ROESY spectrum of 7	50

Figure S36. ^1H NMR spectrum of 8 (DMSO- d_6 , 500 MHz).....	51
Figure S37. ^{13}C NMR spectrum of 8 (DMSO- d_6 , 125 MHz).....	51
Figure S38. HSQC spectrum of 8	52
Figure S39. HMBC spectrum of 8	52
Figure S40. ROESY spectrum of 8	53
Figure S41. ^1H NMR spectrum of 9 (DMSO- d_6 , 500 MHz).....	53
Figure S42. ^{13}C NMR spectrum of 9 (DMSO- d_6 , 125 MHz).....	54
Figure S43. HSQC spectrum of 9	54
Figure S44. HMBC spectrum of 9	55
Figure S45. ROESY spectrum of 9	55
Figure S46. ^1H NMR spectrum of 10 (acetone- d_6 , 500 MHz)	56
Figure S47. ^{13}C NMR spectrum of 10 (acetone- d_6 , 125 MHz)	56
Figure S48. HSQC spectrum of 10	57
Figure S49. HMBC spectrum of 10	57
Figure S50. ROESY spectrum of 10	58
Figure S51. ^1H NMR spectrum of 11 (acetone- d_6 , 500 MHz)	58
Figure S52. ^{13}C NMR spectrum of 11 (acetone- d_6 , 125 MHz)	59
Figure S53. HSQC spectrum of 11	59
Figure S54. HMBC spectrum of 11	60
Figure S55. ROESY spectrum of 11	60
Figure S56. ^1H NMR spectrum of 12 (acetone- d_6 , 500 MHz)	61
Figure S57. ^{13}C NMR spectrum of 12 (acetone- d_6 , 125 MHz)	61
Figure S58. HSQC spectrum of 12	62
Figure S59. HMBC spectrum of 12	62
Figure S60. ROESY spectrum of 12	63
Figure S61. ^1H NMR spectrum of 13 (acetone- d_6 , 500 MHz)	63
Figure S62. ^{13}C NMR spectrum of 13 (acetone- d_6 , 125 MHz)	64
Figure S63. HSQC spectrum of 13	64
Figure S64. HMBC spectrum of 13	65
Figure S65. ROESY spectrum of 13	65
Figure S66. ^1H NMR spectrum of 14 (acetone- d_6 , 500 MHz)	66
Figure S67. ^{13}C NMR spectrum of 14 (acetone- d_6 , 125 MHz)	66
Figure S68. HSQC spectrum of 14	67
Figure S69. HMBC spectrum of 14	67
Figure S70. ROESY spectrum of 14	68

Figure S71. ^1H NMR spectrum of 15 (acetone- d_6 , 500 MHz)	68
Figure S72. ^{13}C NMR spectrum of 15 (acetone- d_6 , 125 MHz)	69
Figure S73. HSQC spectrum of 15	69
Figure S74. HMBC spectrum of 15	70
Figure S75. ROESY spectrum of 15	70
Figure S76. ^1H NMR spectrum of 16 (chloroform- d , 500 MHz).....	71
Figure S77. ^{13}C NMR spectrum of 16 (chloroform- d , 125 MHz).....	71
Figure S78. HSQC spectrum of 16	72
Figure S79. HMBC spectrum of 16	72
Figure S80. ^1H NMR spectrum of 17 (acetone- d_6 , 500 MHz)	73
Figure S81. ^{13}C NMR spectrum of 17 (acetone- d_6 , 125 MHz)	73
Figure S82. HSQC spectrum of 17	74
Figure S83. HMBC spectrum of 17	74
Figure S84. ROESY spectrum of 17	75
Figure S85. ^1H NMR spectrum of 19 (DMSO- d_6 , 500 MHz).....	75
Figure S86. ^{13}C NMR spectrum of 19 (DMSO- d_6 , 125 MHz).....	76
Figure S87. HSQC spectrum of 19	76
Figure S88. HMBC spectrum of 19	77
Figure S89. ^1H NMR spectrum of 21 (acetone- d_6 , 500 MHz)	77
Figure S90. ^{13}C NMR spectrum of 21 (acetone- d_6 , 125 MHz)	78
Figure S91. HSQC spectrum of 21	78
Figure S92. HMBC spectrum of 21	79
Figure S93. ^1H NMR spectrum of 23 (pyridine- d_5 , 500 MHz)	79
Figure S94. ^{13}C NMR spectrum of 23 (pyridine- d_5 , 125 MHz)	80
Figure S95. HSQC spectrum of 23	80
Figure S96. HMBC spectrum of 23	81
Figure S97. ROESY spectrum of 23	81
References	82

Experimental Procedures

Strains and culture conditions.

The *Aspergillus ochraceus* strains were cultivated on PDASS (potato dextrose agar with 3.3% sea salt) plates at 28 °C and stored as 33% glycerol stock at -80 °C. *Aspergillus nidulans* LO8030 was utilized as the fungal heterologous expression host.¹ For all fungal transformation, glucose minimum medium, liquid glucose minimum medium, and sorbitol glucose minimum medium were used with correspondingly nutritional supplements. *Escherichia coli* strain DH5 α was used for plasmids construction, while BL21 (DE3) was used for protein expression. They were grown in liquid LB medium or solid medium (with 2% agar) with antibiotics appropriate for the resistance markers on the plasmid DNA.

General Chemical Analysis.

To analyze the metabolites from fungal strains, the fungal strains (Table S2) were cultivated on PDASS plates for 15 days at 28 °C. The mycelia-containing agar was collected and extracted with ethyl acetate. The ethyl acetate extract of *A. nidulans* and *A. ochraceus* were dried and dissolved in methanol and analyzed on a Waters Acquity UPLC I-Class Plus-Xevo G2 XS QTOF system equipped with an Agilent Eclipse XDB-C18 column (5 μ m, 4.6 \times 150 mm) with a flow rate of 0.4 mL min⁻¹. The mobile phase consisted of acetonitrile (A) and water with 0.01% trifluoroacetate (B) using a gradient elution of 10% to 100% A at 0-12 min and 100% A at 12-13 min. ¹H, ¹³C and 2D NMR spectra were acquired at 298K on 500 MHz Bruker FTNMR spectrometer using DMSO-*d*₆, chloroform-*d*, [D₆]acetone-*d*₆, or pyridine-*d*₅ as solvent.

Gene cloning, DNA fragment construction, and plasmid construction

The oligonucleotide sequences synthesized by Shanghai Sango Biotech were given in Table S3 and the plasmids used in this study were listed in Table S4. To construct fungal expression plasmids for *A. nidulans*, the *ato* genes (containing their own promoter and terminator) were amplified from the genomic DNA of *A. ochraceus* LZDX-32-15 by using Q5 high-fidelity DNA polymerase (New England Biolabs). The DNA fragments were then introduced into the NheI-digested pYH-WA vector by using a ClonExpress Ultra One Step Cloning Kit (Vazyme Biotech). To create the *ato* genes deletion strains in *A. ochraceus*, the deletion cassette was constructed by Double-joint PCR strategy as described previously.² For protein expression, the full-length coding sequence of AtoB was obtained by PCR from the genomic DNA of *A. ochraceus* LZDX-32-15. The DNA fragment was then assembled into the NcoI/HindIII-digested pET-28a vector by using a ClonExpress Ultra One Step Cloning Kit and verified

by sequencing. For the construction of the AtoB mutant variants, Quick-change site-directed mutagenesis method were used.³

Bioinformatics analysis

The structures of defined NTF2-like enzymes (BvnE, Trt14, SdnG, and NsrQ) and the predicted structure (using RoseTTAFold) of NTF2-like homologous were used as queries for Foldseek against the PDB, Uniprot, Swiss-Prot, CATH, GMGCL, and MGnify database.⁴⁻⁵ The cluster analysis of all 1432 sequences was carried out by CLANS (Cluster analysis of sequences) software to visualize pairwise all-against-all comparison.⁶ For the phylogenetic analysis of sequences in cluster 2, alignments were computed using ClustalW2 and the phylogenetic analysis was conducted using Fasttree with the default parameters for the Maximum Likelihood.⁷

Fungal transformation in *A.nidulans* and *A. ochraceus*

Transformation of *A.nidulans* LO8030 and *A. ochraceus* was performed by the previously reported protoplast-polyethylene glycol method.¹ The empty vectors pYH-wa was transformed into host strain LO8030 to create the control strain An-CK. The completed *ato* cluster containing plasmid pYH-wa-*ato*cluster, *atoC/E/H/K* genes containing plasmid pYH-wa-*atoCEHK*, and *atoC/E/H/K/G/D/L/I/F* genes containing plasmid pYH-wa-*atoCEHKGDLIF* were transformed into the host strain *A. nidulans* LO8030 to create the expression strains An-*ato*cluster, An-*atoCEHK* and An-*atoCEHKGDLIF*, respectively. For feeding experiments, *atoM* genes (with *gpdA* promoters and its own terminators) containing plasmid pYH-wa-*atoM* was transformed into the host strain *A. nidulans* LO8030 to create the expression strains An-*atoM*. Transformants were verified using diagnostic PCR with appropriate primers (Table S3). The transformants created in this study were provided in Table S2.

Feeding experiments with *A.nidulans*

The spores of *A.nidulans* strain An-*atoM* was evenly inoculated on PDASS plates which added with the corresponding substrates (1.0 mg of substrate, dissolved in 20 µL DMSO). The plates were incubated at 28 °C for 96 hours. The culture was extracted with an equal volume of ethyl acetate and evaporated to dryness. The extract was dissolved in methanol and analyzed by LC-MS.

Protein expression and purification

For His₆-tagged AtoB expression, the plasmid pAtoB-1 was introduced into *E. coli* BL21 (DE3) component cells following the manufacturer's instructions. An individual bacterial colony was cultured at 37 °C, 200 rpm in 10 mL of LB medium containing 50 mg mL⁻¹ kanamycin (Solar Lab) for 16 hours, then inoculated into 1 L of LB medium. A final concentration of 0.2 mM isopropylthio-β-D-galactoside

(IPTG) was added when OD₆₀₀ reached 0.7 to induce protein expression and the cells were cultured for 18 hours at 16 °C. The cells were harvested by centrifugation at 4 °C, 5000 rpm for 20 min. Supernatant was discarded, and cell pellets were suspended in 18 mL cold lysis buffer (50 mM NaH₂PO₄ pH 7.5, 300 mM NaCl, 10% glycerine, and 10 mM imidazole). A fifteen-minute ultrasonication was used to disrupt *E. coli* cells. Cell lysate was centrifuged at 4 °C, 12000 rpm for 30 min, and the supernatant was incubated with Ni-NTA agarose (GE Healthcare) for 1 hour at 4 °C. The mixture was loaded onto a pre-equilibrated column and then washed by washing buffer (50 mM NaH₂PO₄ pH 7.5, 300 mM NaCl, 10% glycerine, and 30 mM imidazole). The fused AtoB protein was eluted by elution buffer (50 mM NaH₂PO₄ pH 7.5, 300 mM NaCl, 10% glycerine, and 200 mM imidazole). The fractions containing target proteins were desalted by using PD-10 Desalting Column (GE Healthcare) and eluted with storage buffer (50 mM Tris-HCl, 20% glycerol, pH 7.5). The purified protein was stored at -80 °C.

***In vitro* assays of AtoB and its mutant variants**

The enzymatic reaction was performed with in a final volume of 100 µL containing 50 mM Tris-HCl (pH 7.5), 100 µM substrate compound, and 20 µg of purified AtoB (or its variants) for 12 hour at 30 °C. Reactions were terminated by adding 100 µL of MeOH and centrifuged at 13000 rpm for 30 minutes before analyzed by LC-MS. The enzymatic products were analyzed with a linear gradient elution of 20 to 45% acetonitrile in water containing 0.01% trifluoroacetate in 7 min, followed by 45 to 100% acetonitrile for 1 min.

AtoB protein expression and purification for crystallization

The plasmid pAtoB-2 was transformed into *E. coli* BL21(DE3). An individual bacterial colony was grown in 5 L LB medium with 50 µg mL⁻¹ kanamycin at 37 °C to OD₆₀₀ reached 0.8. The culture was cooled to 16 °C over 1 hour and induced with 0.2 mM IPTG and incubated for 18 h at 20 °C. The *E. coli* cells was collected by centrifugation at 4 °C, 5000 rpm for 20 min. The cell pellet was re-suspended in lysis buffer (50 mM NaH₂PO₄ pH 7.5, 300 mM NaCl, 10% glycerine, and 10 mM imidazole) and lysed by sonication followed by centrifugation at 4 °C, 13000 rpm for 30 min. Then, the supernatant was incubated with Ni-NTA agarose (GE Healthcare) for 1 hour at 4 °C. The AtoB protein was washed by washing buffer (50 mM NaH₂PO₄ pH 7.5, 300 mM NaCl, 10% glycerine, and 30 mM imidazole) and eluted by elution buffer (50 mM NaH₂PO₄ pH 7.5, 300 mM NaCl, 10% glycerine, and 200 mM imidazole). After preliminary isolation, PD-10 Desalting Column was used to desalt and exchange with storage buffer. Then the protein solution was incubated with His-tagged HRV 3C protease (Shanghai Sango Biotech) in a 1:20 molar ratio to remove the HIS₆ tag. The protein was dialysed overnight against 50 mM Tris pH 8.0 and 150 mM NaCl, and reloaded into a Ni-NTA column to remove HRV 3C Protease and the HIS tag. Further purification was fractionated by Superdex 200 Increase 10/300 GL columns

(GE Healthcare) eluted with 50mM Tris-HCl, 150mM NaCl 10% Glycerol 1mM TCEP pH 8.0. The eluted fractions were tested by SDS-PAGE and determined to be >95% pure. The concentration of AtoB was concentrated to 10 mg mL⁻¹ and determined by UV spectrophotometry using the calculated molar extinction coefficient.

Crystallization and structure determination of AtoB

Untagged AtoB was screened for initial crystallization conditions using a sitting drop vapour diffusion method at 4 °C. Protein was crystallized in 0.06 M magnesium chloride hexahydrate, 0.06 M Calcium chloride dihydrate, 0.1 M Sodium HEPES, 0.1M MOPS (acid), pH 6.5, 12.5% glycerol, 12.5% PEG1000, and 12.5% PEG3350. Then, crystals were cryoprotected in 0.06 M magnesium chloride hexahydrate, 0.06 M Calcium chloride dihydrate, 0.1 M Sodium HEPES, 0.1M MOPS (acid), pH 6.5, 12.5% glycerol, 12.5% PEG1000, and 12.5% PEG3350 and additional 15% glycerol, and flash frozen in liquid nitrogen. Complex structures of untagged AtoB proteins (10 mg mL⁻¹) and substrate analogs **19** (3 mM) were prepared by incubating crystals in 2 M ammonium sulfate, 0.2 M potassium sodium tartrate tetrahydrate, and 0.1 M sodium citrate (pH 5.6) at 18 °C. Crystals were cryoprotected in 2 M ammonium sulfate, 0.2 M potassium sodium tartrate tetrahydrate, and 0.1 M sodium citrate (pH 5.6) and additional 15% glycerol, and flash frozen in liquid nitrogen. X-ray diffraction data were collected at the Shanghai Synchrotron Radiation Facility (beamline BL02U1) with an X-ray wavelength of 0.97915 Å. The data were integrated and scaled using XDS and Aimless programs.⁸ The structure was solved by a molecular replacement method using BvnE (PDB ID: 6U9I) as search model (Phaser) and refined using Coot and Phenix.⁹⁻¹¹ The data collection and refinement details are presented in Table S5. The coordinates and the structure factor amplitudes for the *apo*-AtoB and AtoB complexed with ligands were deposited to the Protein Data Bank under accession codes 9JLM, 8ZED and 8ZEC.

Large-scale fermentation, extraction, Isolation and characterization of compounds

To characterize the metabolites of fungal mutants, the fungal strains were cultivated on 2.5 L (10 L for Δ atoB Δ atoM strain) PDASS medium at 28 °C for 15 days. The culture was extracted repeatedly with ethyl acetate (3×2.5 L) at room temperature. The crude extract was separated by reversed phase C18 silica column chromatography eluted with methanol-H₂O in a gradient manner (v/v, 20:80, 30:70, 40:60, 50:50, 75:25, 100:0). The fractions with target compounds were purified by semi-preparative RP-C18 HPLC using CH₃CN/H₂O as mobile phase.

Compound 3: colorless oil, UV λ_{max} (methanol) 209, 290 nm; HRESIMS m/z 361.2375 [M+H]⁺ (Calcd for C₂₂H₃₃O₄, 361.2379); for ¹H NMR and ¹³C NMR data see Table S8.

Compound 4a: colorless crystal, UV (methanol, nm): λ_{max} 209, 290; HRESIMS m/z 421.1861 [M+H]⁺ (Calcd for C₂₂H₂₉O₈, 421.1862); for ¹H NMR and ¹³C NMR data see Table S7.

Compound 4b: colorless crystal, UV (methanol, nm): λ_{\max} 209, 290; HRESIMS m/z 421.1864 [M+H]⁺ (Calcd for C₂₂H₂₉O₈, 421.1862); for ¹H NMR and ¹³C NMR data see Table S7.

Compound 6a: white amorphous powder, UV λ_{\max} (methanol) 209, 290 nm; HRESIMS m/z 421.1862 [M+H]⁺ (Calcd for C₂₂H₂₉O₈, 421.1862); for ¹H NMR and ¹³C NMR data see Table S13.

Compound 6b: white amorphous powder, UV λ_{\max} (methanol) 209, 290 nm; HRESIMS m/z 421.1866 [M+H]⁺ (Calcd for C₂₂H₂₉O₈, 421.1862); for ¹H NMR and ¹³C NMR data see Table S13.

Compound 7: colorless oil, UV λ_{\max} (methanol) 209, 290 nm; HRESIMS m/z 359.2218 [M+H]⁺ (Calcd for C₂₂H₃₁O₄, 359.2222); for ¹H NMR and ¹³C NMR data see Table S8.

Compound 8: colorless oil, UV λ_{\max} (methanol) 209, 290 nm; HRESIMS m/z 397.1996 [M+Na]⁺ (Calcd for C₂₂H₃₀O₅Na, 397.1991); for ¹H NMR and ¹³C NMR data see Table S8.

Compound 9: colorless oil, UV λ_{\max} (methanol) 209, 290 nm; HRESIMS m/z 377.2328 [M+H]⁺ (Calcd for C₂₂H₃₃O₅, 377.2328); for ¹H NMR and ¹³C NMR data see Table S9.

Compound 10: colorless oil, UV λ_{\max} (methanol) 209, 290 nm; HRESIMS m/z 375.2176 [M+H]⁺ (Calcd for C₂₂H₃₁O₅, 375.2171); for ¹H NMR and ¹³C NMR data see Table S9.

Compound 11: white amorphous powder, UV λ_{\max} (methanol) 209, 290 nm; HRESIMS m/z 413.1941 [M+Na]⁺ (Calcd for C₂₂H₃₀O₆Na, 413.1940); for ¹H NMR and ¹³C NMR data see Table S9.

Compound 12: colorless oil, UV λ_{\max} (methanol) 209, 290 nm; HRESIMS m/z 377.2327 [M+H]⁺ (Calcd for C₂₂H₃₃O₅, 377.2328); for ¹H NMR and ¹³C NMR data see Table S10.

Compound 13: white amorphous powder, UV λ_{\max} (methanol) 209, 290 nm; HRESIMS m/z 375.2174 [M+H]⁺ (Calcd for C₂₂H₃₁O₅, 375.2171); for ¹H NMR and ¹³C NMR data see Table S10.

Compound 14: white amorphous powder, UV λ_{\max} (methanol) 209, 290 nm; HRESIMS m/z 413.1942 [M+Na]⁺ (Calcd for C₂₂H₃₀O₆Na, 413.1940); for ¹H NMR and ¹³C NMR data see Table S10.

Compound 15: white amorphous powder, UV λ_{\max} (methanol) 209, 290 nm; HRESIMS m/z 393.2273 [M+H]⁺ (Calcd for C₂₂H₃₃O₆, 393.2277); for ¹H NMR and ¹³C NMR data see Table S11.

Compound 16: colorless crystal, UV λ_{\max} (methanol) 209, 290 nm; HRESIMS m/z 391.2121 [M+H]⁺ (Calcd for C₂₂H₃₁O₆, 391.2121); for ¹H NMR and ¹³C NMR data see Table S11.

Compound 17: colorless crystal, UV λ_{\max} (methanol) 209, 290 nm; HRESIMS m/z 429.1888 [M+Na]⁺ (Calcd for C₂₂H₃₀O₆Na, 429.1889); for ¹H NMR and ¹³C NMR data see Table S11.

Compound 19: colorless crystal, UV λ_{\max} (methanol) 209, 290 nm; HRESIMS m/z 407.2071 [M+H]⁺ (Calcd for C₂₂H₃₁O₇, 407.2070); for ¹H NMR and ¹³C NMR data see Table S12.

Compound 21: colorless crystal, UV λ_{\max} (methanol) 209, 290 nm; HRESIMS m/z 445.1835 [M+Na]⁺ (Calcd for C₂₂H₃₀O₈Na, 445.1838); for ¹H NMR and ¹³C NMR data see Table S12..

Compound 23: colorless crystal, UV λ_{\max} (methanol) 209, 290 nm; HRESIMS m/z 423.2018 [M+H]⁺ (Calcd for C₂₂H₃₁O₈, 423.2019); for ¹H NMR and ¹³C NMR data see Table S12.

The protein sequence of AtoB

MGSTSSTDLMALPLRERLIQTADHYFRNMESFDLETGLTGRTADCILKVL
PASFGMPDRTNEECMAAHIA TRADM TMKNFKAWRVPGSIPIVDEANRKVV
FHMEIY AEMGDGVYHNEFIFIMTT NDEGTLLEVAEYVDTAAEKKFAA
ERMARTKGS

Supplementary Tables

Table S1. Predicted protein functions and blast results of *ato* cluster.

Protein	Predicted functions	BlastP homologs	Fungal strain	Coverage/identities
AtoA	transporter	CRL18191.1	<i>Penicillium camemberti</i>	99/51 %
AtoB	NTF2-like protein	6U9I_A	<i>Penicillium brevicompactum</i>	88/40 %
AtoC	polyketide synthase	KAF7507855.1	<i>Endocarpon pusillum</i>	99/41 %
AtoD	2OG-Fe(II) oxygenase	KAB8075087.1	<i>Aspergillus leporis</i>	99/57 %
AtoE	prenyltransferase	KAF4301751.1	<i>Botryosphaeria dothidea</i>	98/58 %
AtoF	cytochrome P450	KAF3397743.1	<i>Penicillium rolfssii</i>	90/38 %
AtoG	cytochrome P450	XP_033428940.1	<i>Aspergillus tanneri</i>	82/57 %
AtoH	FAD-oxidase	A0A3G9GX61.1	<i>Talaromyces verruculosus</i>	50/51 %
AtoI	cytochrome P450	PYI00108.1	<i>Aspergillus ellipticus</i>	94/42 %
AtoJ	short-chain reductase	XP_001259639.1	<i>Aspergillus fischeri</i>	98/48 %
AtoK	terpene cyclase	A0A0E3D8Q2.1	<i>Penicillium janthinellum</i>	98/51 %
AtoL	short-chain reductase	A0A3G9HAL8.1	<i>Talaromyces verruculosus</i>	98/60 %
AtoM	cytochrome P450	KAE8162642.1	<i>Aspergillus tamarii</i>	96/48 %

Table S2. Fungal strains used in this study.

Strain	Genotype	Source
<i>Aspergillus nidulans</i>		
LO8030	<i>pyroA4, riboB2, pyrG89, nkuA::argB, sterigmatocystin cluster (AN7804-AN7825)Δ</i>	¹
An-CK	LO8030 carrying pYH-wa	this study
An-atocluster	LO8030 carrying pYH-wa-atocluster	this study
An-atoCEHK	LO8030 carrying pYH-wa-atoCEHK	this study
An-atoCEHKGDLIF	LO8030 carrying pYH-wa-atoCEHKGDLIF	this study
An-atoM	LO8030 carrying pYH-wa-atorM	this study
<i>Aspergillus ochraceus</i>		
LZDX-32-15	wild type	¹²
AoS1	$\Delta Aoku80::hygR; \Delta AopyrG::neo$ in LZDX-32-15	this study
AoS1ΔatoD	$\Delta atoD::AfpyrG$ in AoS1	this study
AoS1ΔatoF	$\Delta atoF::AfpyrG$ in AoS1	this study
AoS1ΔatoG	$\Delta atoG::AfpyrG$ in AoS1	this study
AoS1ΔatoI	$\Delta atoI::AfpyrG$ in AoS1	this study
AoS1ΔatoJ	$\Delta atoJ::AfpyrG$ in AoS1	this study
AoS1ΔatoL	$\Delta atoL::AfpyrG$ in AoS1	this study
AoS1ΔatoM	$\Delta atoM::AfpyrG$ in AoS1	this study
AoS1ΔatoBΔatoM	$\Delta atoB, atoM::AfpyrG$ in AoS1	this study
AoS1ΔatoDΔatoL	$\Delta atoD, atoL::AfpyrG$ in AoS1	this study
AoS1ΔatoFΔatoM	$\Delta atoF, atoM::AfpyrG$ in AoS1	this study
AoS1ΔatoGΔatoD	$\Delta atoG, atoD::AfpyrG$ in AoS1	this study
AoS1ΔatoGΔatoL	$\Delta atoG, atoL::AfpyrG$ in AoS1	this study
AoS1ΔatoIΔatoM	$\Delta atoI, atoM::AfpyrG$ in AoS1	this study

Table S3. PCR primers used in this study.

primer	sequences of primer (5'→3')
AtoB-for	agaaggagatataccatgggctccacctaagca
AtoB-rev	tgcgtcgagtgccgcagagccctggcttcgc
Untagged-AtoB-for	ccgctggaaatgttccaggcccctccgcaacgtctcatcc
Untagged-AtoB-rev	gtgcggccgcaagcttaagagccctggctcg
E136A	gtggccgcgtatgtgatac
E136D	ggtgtggccgcactatgtgatac
E136Q	ggtgtggccgcagtatgtgatac
E143A	cagcggctgcaaagaagttc
E143D	cagcggctgacaagaagttc
E143Q	cagcggctcaaaaagaagttc
H68A	gtatggccgcgtctatcgc
R72A	gctcatatcgctaccgcggc
R72Q	gctcatatcgctaccgcggc
R150A	gttcgctgtgaggcgatg
R150Q	gttcgctgtgaggcgatg
Y25F	gcagaccacttccgcac
Y114F	cgacggcggtttcacaatg
R59A	gtatgcccgtatgcttccac
R59Q	gtatgcccgtatgccaac
R59K	gtatgcccgtatgccaac
scr-ku80-5f-for	gctccctcaccgtctcgaaag
ku80-5f-rev	gtcgacggatcgattggatgtcccgatgtcaaggag
ku80-3f-for	ggcggtaatacggttatccaccagtgcgagaaataggcg
scr-ku80-3f-rev	atccctctgaaggccatgttccg
ku80-5f-for	cagtcagaacgcctccctg
ku80-3f-rev	ggcacaacccactgcaatc
Ku80-for	tcatgcccgtatcggaaag
Ku80-rev	gagactgtgtcacaaggacatg
scr-pyrg-5f-for	cacccatcatagcgaaatg
pyrg-5f-rev	cagcagtatcagactctgagtc
pyrg-3f-for	cgactcaggagtcgtatactgtggcgtagatccagcaactc
scr-pyrg-3f-rev	cagggtcaggacggtatc
pyrg-5f-for	gtgcaggcaagcttatcgac
pyrg-3f-rev	gcatggagggtttcttcaatcc
pyrg-for	ctaattcccccaacacgcg
pyrg-rev	atgtttccaagtgcatttgc
scr-atoB-5f-for	ctgaacagtgcgggtggaaatc
atoB-5f-rev	gtgccttcgtcagacagaatgtcgaggatcgatgttc
atoB-3f-for	catatttcgtcagacacagaataacttcgtgagaggatggcgagga
scr-atoB-3f-rev	gtggcaggaggatcataaccg
atoB-5f-for	gatatagaaggcaccaccgcca
atoB-3f-rev	ggtgttccaagacagagagagcc
atoB-rt-for	atgggctccaccaagca

atoB-rt-rev	gcgaaacttttcagccgc
scr-atoD-3f-for	gctcaacggatacacatctcg
atoD-3f-rev	catattcgtcagacacaataacttccagcaaggactccataggattc
atoD-5f-for	ggcgtaatacgttatccacagatggctatacggtcgtag
scr-atoD-5f-rev	ctagctgtccgcaaacgatag
atoD-3f-for	cgtcattgtcggtcgtag
atoD-5f-rev	caagcaggctgtggatctgac
atoD-rt-for	ctagacatccagcggtacatcg
atoD-rt-for	ctggatggcctcgaatgcg
scr-atoF-5f-for	gcctccaccagcagtgttg
atoF-5f-rev	catattcgtcagacacaataacttccaaggctagaagccattgtcc
atoF-3f-for	gtgcctcctcagacacaatgcgtggcttaacgaagtgt
scr-atoF-3f-rev	gctggctgcaacaggatc
atoF-5f-for	tggagggtggatggcttag
atoF-3f-rev	gatacctgcacgaccattcg
atoF-rt-for	atgcagacgggtatggagct
atoF-rt-rev	gcctcgctgtcaacctc
scr-atoG-5f-for	gcctcgctgtcaacctc
atoG-5f-rev	ggcgtaatacgttatccactgtgatgtgacagtcccg
atoG-3f-for	gtcgacggatcgttggaaatgctgaacagcctcatcccagaag
scr-atoG-3f-rev	gcaggagggtatggaggtc
atoG-5f-for	ctggttgcttctcgctgttag
atoG-3f-rev	caatggctgaattgcaccc
atoG-rt-for	atggtttcgagcttctgaacac
atoG-rt-rev	gctggctgcaacaggatc
scr-atoI-5f-for	agtatcctgagcatcatcg
atoI-5f-rev	catattcgtcagacacaataacttcgttggcaacactgtgtagtc
atoI-3f-for	gtgcctcctcagacacaattttcgctcaaagctgg
scr-atoI-3f-rev	tctacatgtctgataggctcg
atoI-5f-for	tgttctccatgacaaatctgagg
atoI-3f-rev	gacgtggacaggaacggtag
atoI-rt-for	gactggacttcagaaggcttg
atoI-rt-rev	ctggcgctagtagctcaagg
scr-atoJ-5f-for	gcatatgcaggctcggtatacg
atoJ-5f-rev	catattcgtcagacacaataacttcctgtctaaactcgactgactac
atoJ-3f-for	gtgcctcctcagacacaatgcgtggcatagcatataaccat
scr-atoJ-3f-rev	ctgacgacgcactgaatcg
atoJ-5f-for	gtcgactcaccgtggagac
atoJ-3f-rev	cttgcagccacccagatagac
atoJ-rt-for	cgctcgatccttggagatg
atoJ-rt-rev	tcttgctcgcaaagctgg
scr-atoL-5f-for	gcgtggcatagcatataaccat
atoL-5f-rev	gtgcctcctcagacacaatctgacgacgcactgaatcg
atoL-3f-for	catattcgtcagacacaataacttcgcctcaagtagccacccttac
scr-atoL-3f-rev	gaaggctcgaggaaggatgc

Table S4. Plasmids used in this study.

Plasmid	Description	Source
pYH-wa	<i>URA3</i> , <i>WA</i> flanking, <i>AfpyrG</i> , <i>Amp</i> , <i>gpdA(p)</i>	¹
pYH-wa-atocluster	<i>ato</i> cluster genes expression cassette in pYHWA-pyrG	this study
pYH-wa-atoCEHK	<i>atoC</i> , <i>atoE</i> , <i>atoH</i> , and <i>atoK</i> expression cassette in pYHWA-pyrG	this study
pYH-wa-atoCEHKGDLIF	<i>atoC</i> , <i>atoE</i> , <i>atoH</i> , <i>atoK</i> , <i>atoG</i> , <i>atoD</i> , <i>atoL</i> , <i>atoI</i> , and <i>atoF</i> expression cassette in pYHWA-pyrG	this study
pYH-wa-atoM	<i>atoM</i> expression cassette in pYH-wa-pyrG	this study
pAtoB-1	<i>atoB</i> expression cassette in pET-28a	this study
pAtoB-2	AtoB (Fused with HRV 3C Protease cleavage site and HIS tag) expression cassette in pET-28a	this study

Table S5. Data collection, phasing, and refinement statistics.

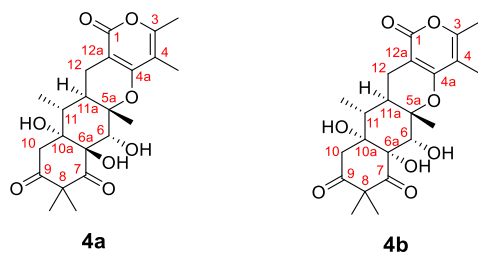
	AtoB-apo	AtoB-apo	AtoB with 19
Data collection			
PDB ID	9JLM	8ZED	8ZEC
Space group	P ₁ 2 ₁ 1	P ₁ 2 ₁ 1	P ₁ 2 ₁ 1
Cell dimensions			
<i>a, b, c</i> (Å)	51.23, 70.07, 51.83	51.56, 122.89, 69.73	44.27, 92.92, 44.27
α, β, γ (°)	90.00, 101.95, 90.00	90.00, 90.00, 90.00	90.00, 90.18, 90.00
Resolution (Å)	41.08-1.90 (1.97-1.90)	29.14-2.37(2.46-2.37)	29.71-1.65 (1.71-1.65)
<i>R</i> _{merge}	21.39 (56.82)	16.48 (42.78)	6.51 (58.78)
CC1/2 (%)	98.90 (50.30)	97.90 (84.70)	99.80 (81.50)
I / σ I	8.51 (3.90)	4.34 (2.10)	14.16 (2.88)
Completeness (%)	98.04 (92.37)	78.82 (83.11)	99.24 (99.53)
Redundancy	6.40 (5.90)	3.10 (3.00)	5.60 (5.60)
Refinement			
Resolution (Å)	41.08-1.90 (1.97-1.90)	29.14-2.37 (2.46-2.37)	29.71-1.65 (1.71-1.65)
No. reflections	27975 (2627)	27862 (2953)	42709 (4241)
<i>R</i> _{work} / <i>R</i> _{free} (%)	21.04/26.28	26.03/32.10	12.58/15.84
No. atoms			
Protein	2324	4372	2336
Ligand/ion	2	4	82
Water	305	209	220
B-factors			
Protein	12.89	33.33	26.72
Ligand/ion	19.84	29.21	29.43
Water	8.31	37.03	27.13
Ramachandran plot (%)			
Favoured	97.58	98.90	97.24
Allowed	1.73	1.10	2.41
Outliers	0.69	0.00	0.34
R.m.s. deviations			
Bond lengths (Å)	0.007	0.001	0.013
Bond angles (°)	0.91	0.39	1.89

Table S6. Relative enzymatic activities of wild-type AtoB and its variants.

Enzyme	Percentage of 4a (%) ^a	Percentage of 4b (%) ^a	Relative production of 4a (%) ^a	Relative production of 4b (%) ^a
AtoB WT	77.88±0.35	22.12±0.38	100.00±0.45	100.00±1.73
R59A	4.60±0.03	0.00	5.91±0.04	0.00
R59Q	20.82±0.44	1.16±0.02	26.74±0.56	5.22±0.08
R59K	47.95±0.54	12.29±0.27	61.57±0.67	55.56±1.56
Y114F	0.00	0.00	0.00	0.00
R72A	5.18±0.09	0.29±0.40	6.65±0.12	1.29±1.82
R72Q	39.88±1.14	1.98±0.06	51.20±1.46	8.94±0.25
E136A	0.00	0.00	0.00	0.00
E136D	0.00	0.00	0.00	0.00
E136Q	0.00	0.00	0.00	0.00
E143A	0.00	0.00	0.00	0.00
E143D	10.21±0.37	18.37±0.78	13.12±0.47	83.06±3.51
E143Q	21.46±0.39	17.57±0.93	27.55±0.49	79.42±4.19
H68A	59.61±1.36	3.83±0.03	76.53±1.75	17.33±0.15

^aData presented as means ± SD from three independent experiments

Table S7. ^1H and ^{13}C NMR data of compounds **4a** and **4b**.



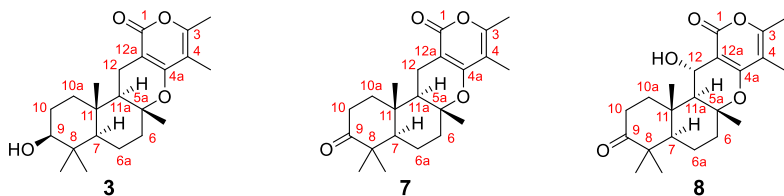
No.	4a^a		4b^b	
	δ_{C}	δ_{H} (mult., J in Hz)	δ_{C}	δ_{H} (mult., J in Hz)
1	163.8	-	162.9	-
3	156.2	-	155.4	-
3-Me	16.5	2.15, s	16.9	2.15, s
4	107.3	-	106.3	-
4-Me	9.5	1.88, s	9.2	1.84, s
4a	163.1	-	162.2	-
5a	82.4	-	80.6	-
5a-Me	20.2	1.40, s	18.6	0.72, s
6	74.4	4.59, d (4.2)	73.9	4.43, s
6a	76.8	-	76.1	-
7	208.9	-	207.9	-
8	55.9	-	56.8	-
8-Me α	26.1	1.30, s	29.1	1.37, s
8-Me β	22.8	1.28, s	20.2	1.15, s
9	209.4	-	209.1	-
10	46.1	2.69, d (17.0) 2.82, dd (17.0, 2.6)	44.0	2.53, d (13.9) 3.46, d (13.9)
10a	75.7	-	74.5	-
11	39.1	1.87, m	38.4	0.87, m
11-Me	10.3	1.06, d (6.7)	9.6	0.94, d (6.4)
11a	34.4	2.16, m	31.2	2.08, td (12.0, 5.0)
12	21.7	1.99, dd (16.5, 12.5) 2.59, dd (16.5, 5.0)	19.7	1.81, dd (16.6, 5.0) 2.34, dd (16.6, 5.0)
12a	98.6	-	96.7	-
6-OH	-	5.60, d (4.2)	-	5.84, br.s
6a-OH	-	5.66, s	-	6.37, br.s
10a-OH	-	4.70, d (2.6)	-	5.09, br.s

^a recorded in acetone- d_6 ; ^b recorded in DMSO- d_6

Table S8. ^1H and ^{13}C NMR data of compounds **6a** and **6b** in acetone- d_6 .

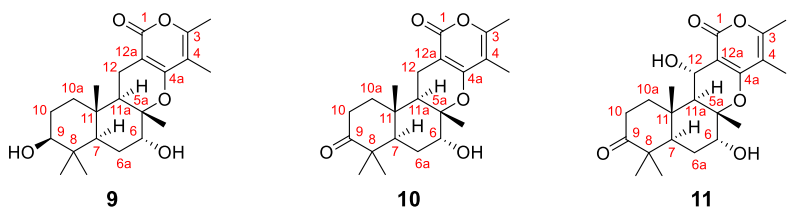
No.	6a		6b	
	δ_{C}	δ_{H} (mult., J in Hz)	δ_{C}	δ_{H} (mult., J in Hz)
1	163.7	-	162.9	-
3	156.4	-	155.5	-
3-Me	17.2	2.17, s	16.3	2.17, s
4	107.0	-	106.1	-
4-Me	9.6	1.87, s	8.7	1.88, s
4a	162.5	-	161.6	-
5a	78.1	-	76.9	-
5a-Me	14.0	1.35, s	13.0	1.34, s
6	74.4	4.35, s	77.1	4.45, s
6a	82.3	5.39, s	82.4	5.40, s
7	212.9	-	208.5	-
8	43.7	-	43.8	-
8-Me α	20.7	1.29, s	20.4	1.30, s
8-Me β	21.5	1.27, s	20.6	1.25, s
9	178.2	-	177.2	-
10	26.6	1.43, s	25.8	1.42, s
10a	99.6	-	98.6	-
11	42.5	1.65, m	41.5	1.61, m
11-Me	13.4	1.01, d (6.7)	12.5	1.01, d (6.7)
11a	40.2	1.97, m	39.4	1.96, m
12	20.6	1.90, d (15.7) 2.50 dd (15.7, 3.9)	19.9	1.95, d (16.0) 2.05, dd (16.0, 4.3)
12a	99.0	-	98.2	-
10a-OH	-	5.24, d (1.6)	-	5.41, d (1.6)

Table S9. ^1H and ^{13}C NMR data of compounds **3**, **7**, and **8** in $\text{DMSO}-d_6$.



No.	3		7		8	
	δ_{C}	δ_{H} (mult., J in Hz)	δ_{C}	δ_{H} (mult., J in Hz)	δ_{C}	δ_{H} (mult., J in Hz)
1	162.1	-	163.1	-	162.6	-
3	155.1	-	155.3	-	157.1	-
3-Me	16.9	2.13, s	16.9	2.15, s	17.0	2.18, s
4	106.0	-	106.0	-	106.2	-
4-Me	9.2	1.76, s	9.2	1.78, s	9.1	1.79, d, (1.1)
4a	163.2	-	163.1	-	162.3	-
5a	80.1	-	79.9	-	82.4	-
5a-Me	20.4	1.14, s	20.1	1.20, s	20.3	1.21, s
6	39.9	2.03, o 1.59, o	37.0	1.86, ddd (13.1, 7.4, 3.6) 1.53, o	39.5	1.96, dt (12.1, 13.0) 1.72, m
6a	19.0	1.68, o 1.41, o	20.0	1.64, m 1.51, o	20.0	1.71, o 1.50, o
7	54.2	0.94, o	53.4	1.59, o	54.0	1.61, m
8	38.4	-	46.6	-	47.1	-
8-Me α	28.1	0.91, s	26.1	1.03, s	26.1	1.03, s
8-Me β	15.9	0.69, s	21.0	0.97, s	21.1	0.98, s
9	76.5	3.01, q (4.9, 3.5)	215.4	-	215.6	-
10	27.0	1.51, m	39.2	2.08, o 1.64, o	38.8	1.66, o 2.39, ddd (14.0, 7.2, 3.7)
10a	36.9	1.58, o 1.05, m	33.5	2.60, ddd (15.9, 11.0, 7.4) 2.33, ddd (15.9, 7.0, 3.6)	33.7	2.56, ddd (15.7, 11.1, 7.2) 2.28, ddd (15.6, 6.9, 3.6)
11	36.2	-	36.0	-	37.4	-
11-Me	14.7	0.82, s	14.1	0.96, s	14.8	1.05, s
11a	50.6	1.35, m	49.6	1.51, o	55.9	1.66, o
12	16.7	2.20, dd (16.9, 4.8) 2.05, dd (16.9, 4.8)	16.8	2.25, dd (16.6, 4.8) 2.09, o	60.9	4.66, dd (9.9, 4.2)
12a	97.1	-	97.1	-	102.6	-
9-OH	-	4.39, d (5.0)	-	-	-	-
12-OH	-	-	-	-	-	4.78, d (4.2)

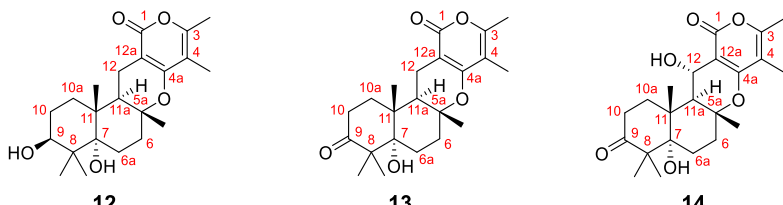
Table S10. ^1H and ^{13}C NMR data of compounds **9-11**.



No.	9^a		10^b		11^b	
	δ_{C}	δ_{H} (mult., J in Hz)	δ_{C}	δ_{H} (mult., J in Hz)	δ_{C}	δ_{H} (mult., J in Hz)
1	162.5	-	163.9	-	164.7	-
3	154.8	-	155.8	-	158.1	-
3-Me	16.8	2.13, s	17.1	2.15, s	17.2	2.20, s
4	106.5	-	107.3	-	108.0	-
4-Me	9.4	1.84, s	9.6	1.87, d (0.9)	9.5	1.89, d (1.0)
4a	163.2	-	163.2	-	163.7	-
5a	81.5	-	82.4	-	85.3	-
5a-Me	20.1	1.11, s	20.2	1.29, s	20.5	1.34, s
6	70.7	3.84, br	72.1	4.05, t (3.1)	72.5	4.00, m
6a	26.2	1.65, o	27.2	1.86, o, 1.83, m	27.6	1.81, o,
7	45.1	1.52, o	44.5	2.01, o	46.4	2.37, m
8	37.9	-	37.1	-	38.5	-
8-Me α	28.0	0.87, s	26.7	1.05, s	26.9	1.06, s
8-Me β	16.0	0.69, s	21.6	1.04, s	21.6	1.05, s
9	76.8	3.03, m	215.5	-	215.9	-
10	27.1	1.52, o	38.5	2.02, o 1.63, m	40.4	2.57, m 1.81, m
10a	37.1	1.04, o 1.05, m	34.3	2.61, ddd (16.0, 10.5, 7.6) 2.44, o	34.5	2.52, o 2.43, o
11	36.1	-	47.2	-	49.8	-
11-Me	14.3	0.82, s	14.5	1.08, s	15.4	1.16, s
11a	43.9	1.70, o	46.4	2.29, dd (11.7, 3.9)	47.5	2.18, d (10.5)
12	16.1	2.21, dd (16.7, 5.0) 2.04, dd (16.4, 13.3)	17.4	2.39, o 2.22, dd (16.8, 13.2)	63.1	4.89, d (11.0)
12a	96.6	-	98.4	-	102.6	-
6-OH	-	4.70, d (3.3)	-	-	-	4.25, d (2.3)
9-OH	-	4.39, d (5.1)	-	-	-	-
12-OH	-	-	-	-	-	4.68, d (1.3)

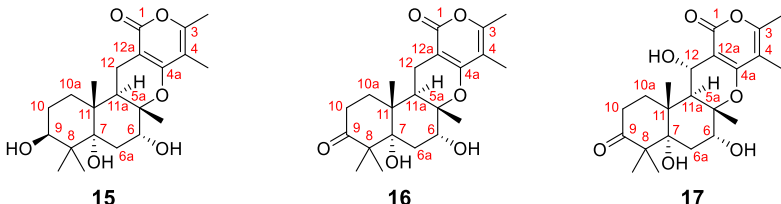
^a recorded in DMSO- d_6 ; ^b recorded in acetone- d_6

Table S11. ^1H and ^{13}C NMR data of compounds **12-14** in acetone- d_6 .



No.	12		13		14	
	δ_{C}	δ_{H} (mult., J in Hz)	δ_{C}	δ_{H} (mult., J in Hz)	δ_{C}	δ_{H} (mult., J in Hz)
1	164.2	-	164.0	-	163.5	-
3	155.7	-	155.9	-	140.4	-
3-Me	17.1	2.14, s	17.1	2.15, s	17.3	2.21, s
4	107.0	-	107.0	-	107.7	-
4-Me	9.6	1.81, d (1.0)	9.6	1.83, d (1.0)	9.4	1.86, d (1.0)
4a	163.1	-	163.0	-	158.1	-
5a	80.9	-	80.6	-	83.2	-
5a-Me	21.4	1.25, s	20.7	1.19, s	21.3	1.34, s
6	34.7	2.28, dd (13.9, 12.7) 1.82, o	34.5	2.24, o 1.88, dt (12.6, 3.5)	34.6	2.21, m 1.79, m
6a	25.5	1.94, td (14.1, 4.1) 1.75, m	25.8	2.06, o 1.77, m	25.9	2.04, o 1.78, m
7	78.0	-	79.3	-	80.1	-
8	44.6	-	53.8	-	54.0	-
8-Me α	23.3	1.07, s	23.8	1.19, s	23.8	1.20, s
8-Me β	18.3	0.95, s	22.2	1.11, s	22.1	1.11, s
9	73.1	3.87, m	215.1	-	215.5	-
10	31.7	1.70, o 1.32, m	34.2	2.61, m 2.45, o	35.1	2.35, m 2.28, m
10a	28.2	1.68, o	33.4	2.04, o 1.66, m	34.5	2.57, o 2.43, ddd (15.4, 7.5, 3.7)
11	41.2	-	41.4	-	42.9	-
11-Me	18.5	1.08, s	18.6	1.19, s	19.4	1.29, s
11a	43.5	2.51, dd (13.2, 5.0)	44.0	2.47, m	49.9	2.57, o
12	17.9	2.19, dd (16.7, 5.0) 2.09, m	17.9	2.26, o 2.20, o	62.9	4.84, d (10.6)
12a	98.8	-	98.6	-	103.1	-
7-OH	-	3.14, s	-	3.82, s	-	3.75, s
9-OH	-	3.29, d (6.0)	-	-	-	-
12-OH	-	-	-	-	-	4.55, s

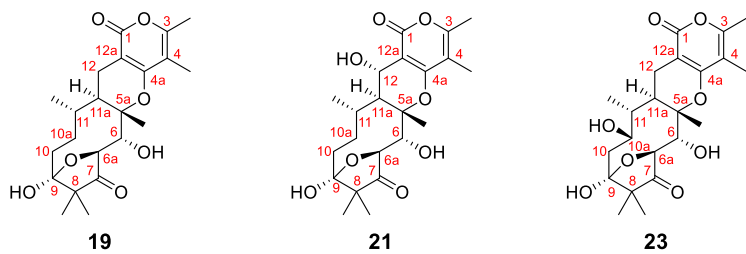
Table S12. ^1H and ^{13}C NMR data of compounds **15-17**.



No.	15^a		16^b		17^a	
	δ_{C}	δ_{H} (mult., J in Hz)	δ_{C}	δ_{H} (mult., J in Hz)	δ_{C}	δ_{H} (mult., J in Hz)
1	164.0	-	164.4	-	164.6	-
3	155.8	-	155.1	-	158.6	-
3-Me	17.1	2.15, s	17.4	2.22, s	17.3	2.21, s
4	107.3	-	106.5	-	108.0	-
4-Me	9.6	1.87, d (1.0)	9.8	1.87, d (1.0)	9.5	1.90, d (1.0)
4a	162.9	-	162.1	-	163.4	-
5a	82.0	-	81.3	-	84.7	-
5a-Me	20.8	1.30, s	20.0	1.29, s	20.7	1.39, s
6	75.0	4.22, m	74.2	4.21, t (3.1)	74.8	4.20, br
6a	28.1	1.65, m	28.4	2.14, dd (15.3, 3.1) 2.00, dd (15.3, 3.0)	29.4	2.21, o 2.05, o
7	79.6	-	79.8	-	81.6	-
8	44.6	-	53.4	-	54.2	-
8-Me α	23.5	1.13, s	22.5	1.21, s	23.7	1.17, s
8-Me β	18.2	0.91, s	23.6	1.17, s	22.4	1.15, s
9	72.2	3.87, dt (9.4, 6.1)	215.9	-	215.0	-
10	31.8	1.78, td (11.9, 7.1) 1.28, o	33.7	2.55, o	35.3	2.34, o 2.13, o
10a	28.2	2.12, o 2.05, o	33.1	2.10, m 1.67, m	34.5	2.57, m 2.34, o
11	42.4	-	41.9	-	44.1	-
11-Me	18.2	1.08, s	18.5	1.12, s	19.5	1.32, s
11a	38.9	2.58, dd (12.9, 5.2)	38.5	2.57, o	45.3	2.71, d (10.1)
12	17.6	2.30, dd (16.9, 5.2) 2.18, dd (14.5, 10.4)	17.0	2.53, o 2.33, dd (16.8, 12.9)	62.6	4.94, dd (10.1, 1.4)
12a	98.9	-	99.1	-	103.2	-
6-OH	-	-	-	-	-	5.34, br.s
7-OH	-	5.46, s	-	5.12, s	-	5.67, s
9-OH	-	3.19, d (6.0)	-	-	-	-
12-OH	-	-	-	-	-	4.53, d (1.5)

^a recorded in acetone- d_6 ; ^b recorded in chloroform- d

Table S13. ^1H and ^{13}C NMR data of compounds **19**, **21**, and **23**.



No.	19^a		21^b		23^c	
	δ_{C}	δ_{H} (mult., J in Hz)	δ_{C}	δ_{H} (mult., J in Hz)	δ_{C}	δ_{H} (mult., J in Hz)
1	163.1	-	164.6	-	164.1	-
3	155.3	-	158.0	-	155.1	-
3-Me	16.9	2.14, s	17.2	2.21, s	16.9	2.02, s
4	106.2	-	107.9	-	107.0	-
4-Me	9.2	1.84, d (1.0)	9.5	1.91, d (1.1)	9.4	1.79, s
4a	162.2	-	163.2	-	162.7	-
5a	85.8	-	87.3	-	86.3	-
5a-Me	14.9	1.09, s	15.0	1.24, s	15.4	1.55, s
6	69.7	3.81, d (10.0)	71.1	4.20, dd (10.3, 2.9)	70.7	4.30, o
6a	77.8	4.35, d (9.9)	78.5	4.48, d (6.3)	79.4	5.14, d (9.9)
7	218.3	-	220.3	-	219.7	-
8	50.8	-	52.3	-	52.5	-
8-Me α	21.1	0.97, s	21.1	1.10, s	20.5	1.39, s
8-Me β	16.6	0.91, s	16.7	1.00, s	17.1	1.22, s
9	106.2	-	107.4	-	106.8	-
10	37.6	1.87, o 1.50, o	40.6	2.06, o 1.58, o	42.7	1.75, o 2.49, dd (15.3, 8.8)
10a	33.3	1.74, dd (14.8, 9.6) 1.37, dd (14.7, 9.3)	35.4	2.01, o 1.52, dd (14.7, 9.3)	75.1	4.30, o
11	32.3	1.51, o	35.1	1.62, o	38.6	1.75, o
11-Me	19.8	0.96, d (7.3)	19.2	1.29, d (7.3)	18.4	1.23, d (7.0)
11a	37.6	3.21, m	45.7	3.61, dd (10.4, 2.9)	31.7	4.45, br
12	20.1	2.27, dd (16.4, 5.3) 2.09, o	63.8	4.66, d (10.4)	22.4	2.59, dd (16.4, 13.0) 2.88, dd (16.4, 5.3)
12a	97.4	-	103.2	-	98.9	-
6-OH	-	5.16, s	-	3.89, d (5.1)	-	-
7-OH	-	-	-	-	-	-
9-OH	-	6.15, s	-	5.25, s	-	-
12-OH	-	-	-	4.49, d (3.2)	-	-

^a recorded in DMSO-*d*₆; ^b recorded in acetone-*d*₆; ^c recorded in pyridine-*d*₅

Supplementary Figures

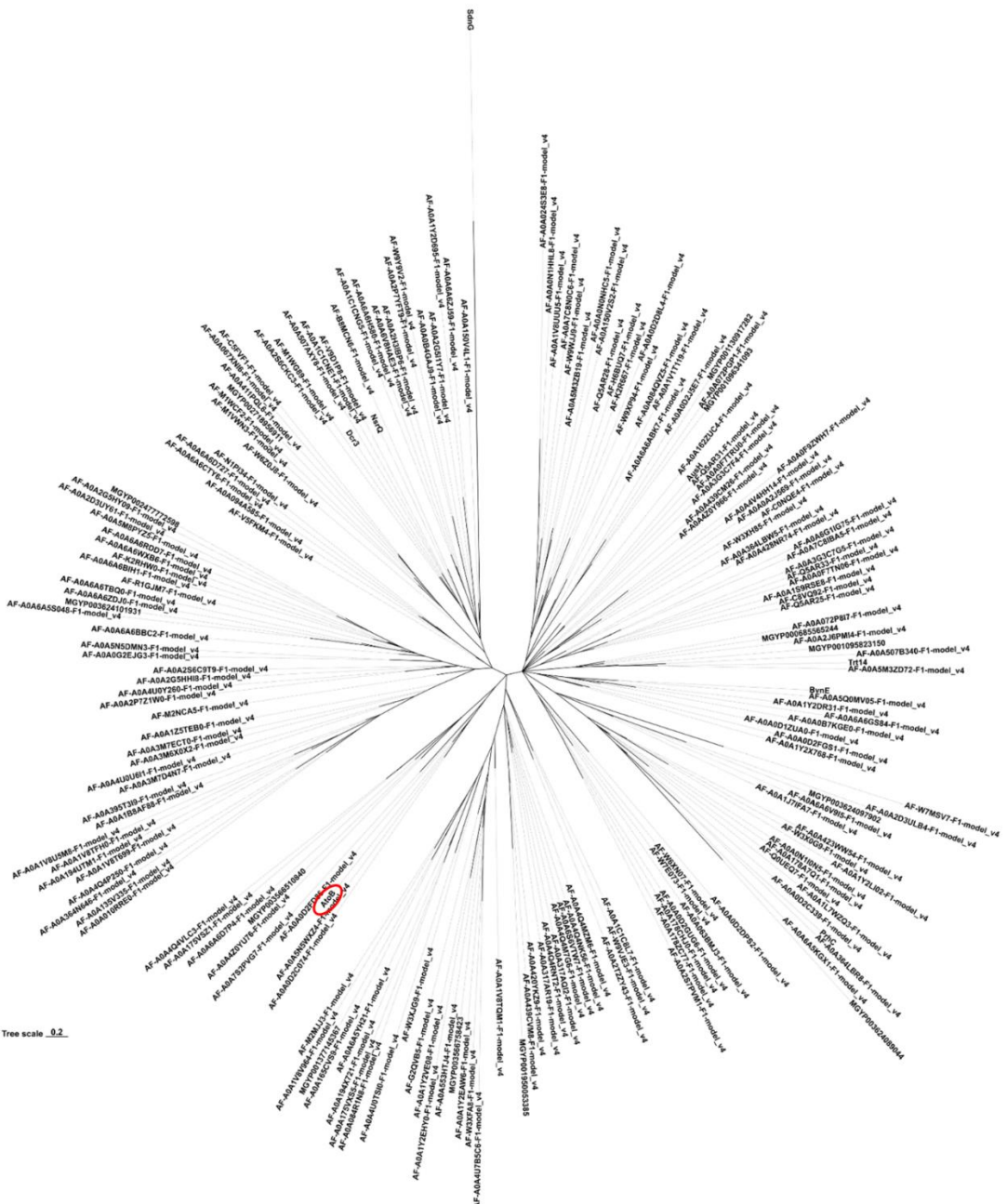


Figure S1. Phylogenetic tree of AtoB and others NTF2-like enzymes in cluster 2. Accession numbers of the sequences used are as follows: AF-A0A2S7QP61-F1-model_v4, AF-A0A2S7PVM1-F1-model_v4, AF-A0A178ZC77-F1-model_v4, AF-A0A0D2GUG6-F1-model_v4, AF-A0A178CHJ0-F1-model_v4, AF-A0A0D2C339-F1-model_v4, AF-A0A6A5KGX1-F1-model_v4, AF-A0A364LBR8-F1-model_v4, PrhC, AF-A0A423WW54-F1-model_v4, AF-W3X0G9-F1-model_v4, AF-A0A0N1I0N5-F1-model_v4, AF-A0A178A7Q1-F1-model_v4, AF-A0A1L7WZQ3-F1-model_v4, AF-A0A1Y2LI02-F1-model_v4, AF-Q0UEQ7-F1-model_v4, AF-A0A0D2DPS2-F1-model_v4, AF-A0A0A2J569-F1-model_v4, AF-A0A4V4HH14-F1-model_v4, AF-A0A0F9ZWH7-F1-model_v4, MGYP003624089044, AF-A0A1J7IFA7-F1-model_v4, AF-A0A6A6V9I5-F1-model_v4, AF-A0A2D3ULB4-F1-model_v4, MGYP003624097902, AF-A0A0D2FGS1-F1-model_v4, AF-A0A1Y2X768-F1-model_v4, AF-A0A0D1ZUA0-F1-model_v4, AF-A0A0B7KGE0-F1-model_v4.

BvnE, AF-A0A5Q0MV05-F1-model_v4, AF-A0A1Y2DR31-F1-model_v4, AF-A0A6A6GS84-F1-model_v4, AF-A0A0N0HNC5-F1-model_v4, AF-A0A150V2S2-F1-model_v4, AF-A0A5M3ZB19-F1-model_v4, AF-A0A0N1HHL8-F1-model_v4, AF-A0A1V8UUU5-F1-model_v4, AF-A0A7C8N0C6-F1-model_v4, AF-W9WJJ9-F1-model_v4, AF-A0A1V1T119-F1-model_v4, AF-A0A024S3E8-F1-model_v4, AF-A0A0D2J5E7-F1-model_v4, AF-A0A072PGP1-F1-model_v4, MGYP001096341093, MGYP001130917282, AF-A0A0D2D8L4-F1-model_v4, AF-W9XP94-F1-model_v4, AF-H6BUQ7-F1-model_v4, AF-K2R667-F1-model_v4, AF-Q5AR28-F1-model_v4, AF-C0NQE4-F1-model_v4, AF-W3XH85-F1-model_v4, AF-A0A063BMJ3-F1-model_v4, AF-W6XN07-F1-model_v4, AF-W7E073-F1-model_v4, AF-A0A364LBW5-F1-model_v4, AF-A0A428NR74-F1-model_v4, AF-A0A0F7TN06-F1-model_v4, AF-A0A3G3C7G5-F1-model_v4, AF-Q5AR33-F1-model_v4, AF-A0A1S9RSE8-F1-model_v4, AF-C8VQ92-F1-model_v4, AF-Q5AR25-F1-model_v4, AF-A0A162ZUC4-F1-model_v4, AF-A0A084QVZ5-F1-model_v4, AF-A0A6A6ABK7-F1-model_v4, AF-A0A6G1IG75-F1-model_v4, AF-A0A7C8IBA5-F1-model_v4, AF-A0A0F7TRU0-F1-model_v4, AF-A0A3G3C7F4-F1-model_v4, AF-Q5AR31-F1-model_v4, AusH, AF-A0A439CM26-F1-model_v4, AF-A0A4Z0Y966-F1-model_v4, AF-A0A2J6PMI4-F1-model_v4, AF-A0A072P8I7-F1-model_v4, MGYP000685565244, MGYP001095823150, AF-A0A507B340-F1-model_v4, Trt14, AF-A0A5M3ZD72-F1-model_v4, AF-A0A1C1C8L7-F1-model_v4, AF-W9VJE3-F1-model_v4, AF-G2QVB5-F1-model_v4, AF-A0A2T2ZY43-F1-model_v4, AF-A0A4U7B5C6-F1-model_v4, AF-W3XFA8-F1-model_v4, AF-A0A1Y2EAW6-F1-model_v4, AF-A0A553HTJ4-F1-model_v4, MGYP003566758423, AF-A0A420YKZ9-F1-model_v4, AF-A0A439CVM8-F1-model_v4, MGYP001950053385, AF-A0A4Q4MZM6-F1-model_v4, AF-A0A317AR19-F1-model_v4, AF-A0A317AQI2-F1-model_v4, AF-A0A4Q4RNT2-F1-model_v4, AF-A0A4Q4M7G6-F1-model_v4, AF-A0A4Q4NK56-F1-model_v4, AF-A0A6S6VTW7-F1-model_v4, AF-A0A1V8TQM1-F1-model_v4, AF-A0A1Y2EHY0-F1-model_v4, AF-A0A1Y2VE08-F1-model_v4, AF-A0A194X721-F1-model_v4, AF-A0A084R1N8-F1-model_v4, AF-A0A175VXS5-F1-model_v4, AF-A0A1V8V964-F1-model_v4, AF-M2MJ3-F1-model_v4, AF-A0A4U0TSI0-F1-model_v4, AF-A0A165CVS9-F1-model_v4, MGYP001377145367, AF-A0A6A5YH21-F1-model_v4, AF-W3XJG9-F1-model_v4, AF-A0A0D2FD86-F1-model_v4, AF-A0A7S2PVG7-F1-model_v4, AtoB, AF-A0A0D2C074-F1-model_v4, AF-A0A5N5WXZ4-F1-model_v4, AF-A0A6A6D7P4-F1-model_v4, AF-A0A175VSZ1-F1-model_v4, AF-A0A4Q4VLC3-F1-model_v4, AF-A0A4Z0YU76-F1-model_v4, MGYP003566510840, AF-V5FKM4-F1-model_v4, AF-A0A094A585-F1-model_v4, AF-A0A6A6D727-F1-model_v4, AF-N1PI34-F1-model_v4, AF-A0A6A6CTY6-F1-model_v4, AF-A0A1Y2D695-F1-model_v4, AF-A0A6A6ZJ59-F1-model_v4, AF-A0A150V4L1-F1-model_v4, AF-B8MCN6-F1-model_v4, AF-A0A2S6CKC3-F1-model_v4, AF-M1WG89-F1-model_v4, NsrQ, Dcr3, AF-A0A507AXY8-F1-model_v4, AF-A0A1C1CNE1-F1-model_v4, AF-V9D1P8-F1-model_v4, AF-A0A2G5I1Y7-F1-model_v4, AF-A0A0B4GAJ9-F1-model_v4, AF-A0A2P7YFT9-F1-model_v4, AF-W9Y9V2-F1-model_v4, AF-A0A1C1CNG5-F1-model_v4, AF-A0A6A6H580-F1-model_v4, AF-A0A2H3IBP6-F1-model_v4, AF-A0A6V8HAE3-F1-model_v4, AF-A0A6A6BBC2-F1-model_v4, AF-A0A2P7Z1W0-F1-model_v4, AF-A0A4U0Y260-F1-model_v4, AF-A0A2G5HHI8-F1-model_v4, AF-A0A2S6C9T9-F1-model_v4, AF-A0A0G2EJG3-F1-model_v4, AF-A0A5N5DMN3-F1-model_v4, AF-A0A2D3UY61-F1-model_v4, AF-A0A5M8PYZ5-F1-model_v4, SdnG, AF-A0A2G5HY09-F1-model_v4, MGYP002477772598, AF-A0A6A6TBQ0-F1-model_v4, AF-A0A6A6ZDJ0-F1-model_v4, AF-A0A6A5S048-F1-model_v4, MGYP003624101931, AF-R1GJM7-F1-model_v4, AF-A0A6A6RDD7-F1-model_v4, AF-A0A6A6WXB6-F1-model_v4, AF-A0A6A6BIH1-F1-model_v4, AF-K2RHW0-F1-model_v4, AF-M2NCA5-F1-model_v4, AF-W6Z0J8-F1-model_v4, AF-M1VWN3-F1-model_v4, AF-M1WCF2-F1-model_v4, MGYP002718956911, AF-A0A411PQL6-F1-model_v4, AF-A0A067XNI6-F1-model_v4, AF-C5FVF1-F1-model_v4, AF-A0A194UTM1-F1-model_v4, AF-A0A1V8T699-F1-model_v4, AF-A0A1V8TFH0-F1-model_v4, AF-A0A1V8U5M8-F1-model_v4, AF-A0A010RRE0-F1-model_v4, AF-A0A135V335-F1-model_v4, AF-A0A364N646-F1-model_v4, AF-A0A4Q4P250-F1-model_v4, AF-A0A1B8AF88-F1-model_v4, AF-A0A395T3I9-F1-model_v4, AF-A0A3M7D4N7-F1-model_v4, AF-A0A4U0U6I1-F1-model_v4, AF-A0A1Z5TEB0-F1-model_v4, AF-A0A3M6X0X2-F1-model_v4, AF-A0A3M7ECT0-F1-model_v4. Chiplot program was used.¹³

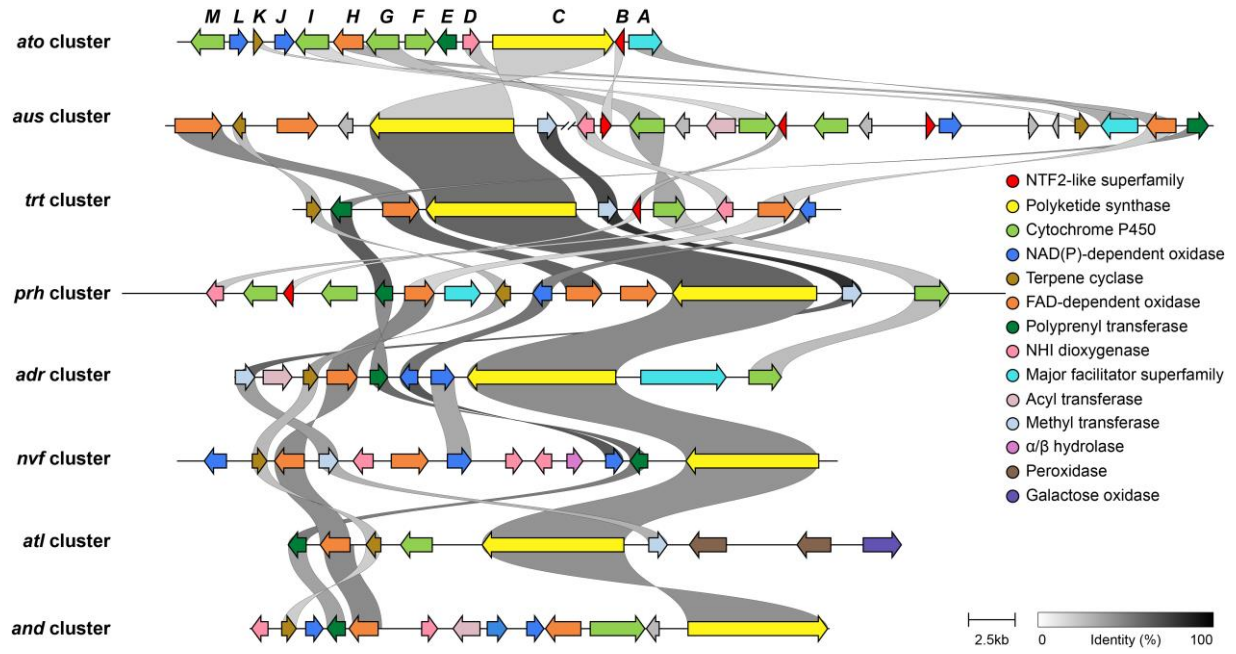


Figure S2. Comparison of the *ato* cluster and the reported fungal meroterpenoid gene clusters that encoding homologous proteins

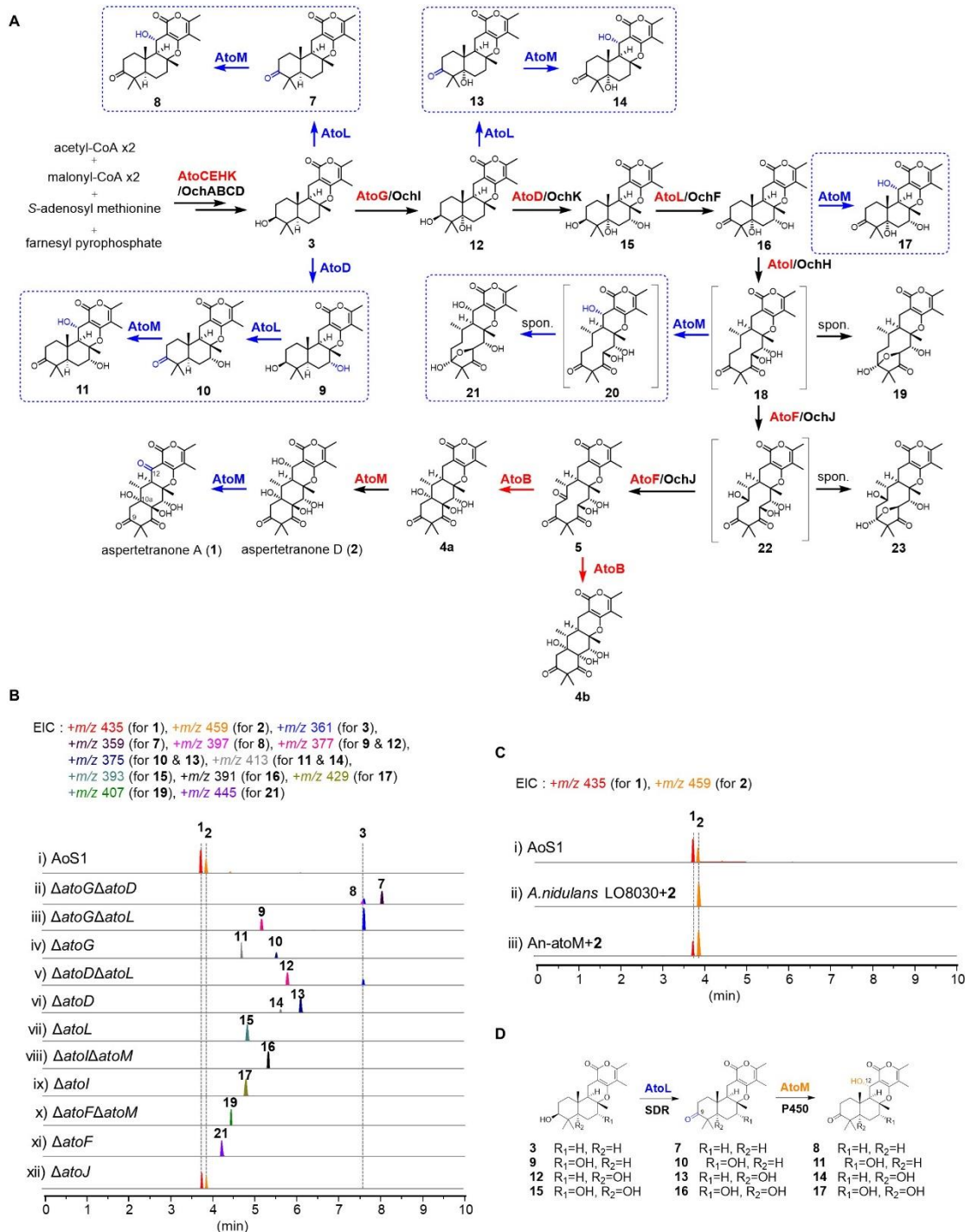


Figure S3. Biosynthesis of aspertetranone and functions of *ato* genes. (A) The branching biosynthetic pathway of aspertetranones. (B) LC-MS analysis of the metabolites of *A. ochraceus* strains. When cytochrome P450 *atoG* and 2OG-Fe(II) oxygenase *atoD* were both disrupted, the resulting strain $\Delta atoG\Delta atoD$ generated **3** together with unforeseen **7** and **8**. These results suggested that AtoM would accept both linear and angular intermediates with a ketone group at C-9 in the biosynthetic pathway of aspertetranones. This was supported by the production of **10** and **11** in $\Delta atoG$ strain, while **9** was obtained from $\Delta atoG\Delta atoL$ strain. Similarly, **13** and **14** were detected in $\Delta atoD$ strain and their precursor **12** was generated from $\Delta atoD\Delta atoL$ strain. Then, production of **15**, **16**, and **17** was observed in $\Delta atoL$, $\Delta atoI\Delta atoM$, and $\Delta atoI$ strains, respectively. Furthermore, $\Delta atoF\Delta atoM$ and $\Delta atoF$ strains produced **19** and **21**, respectively, considering as the spontaneous products of ketalization. These findings indicated

that ketone group at C-9 was obligatory for AtoM. However, the constructed Δa_{toJ} strain showed no change comparing to AoS1. (C) LC-MS analysis of feeding experiment. For the final step in synthesis of **1**, we assumed that AtoM was involved. The feeding experiments indicated AtoM also catalyzed the ketolation at C-12. (D) Substrate heterogeneities of short-chain dehydrogenase AtoL and cytochrome P450 AtoM.

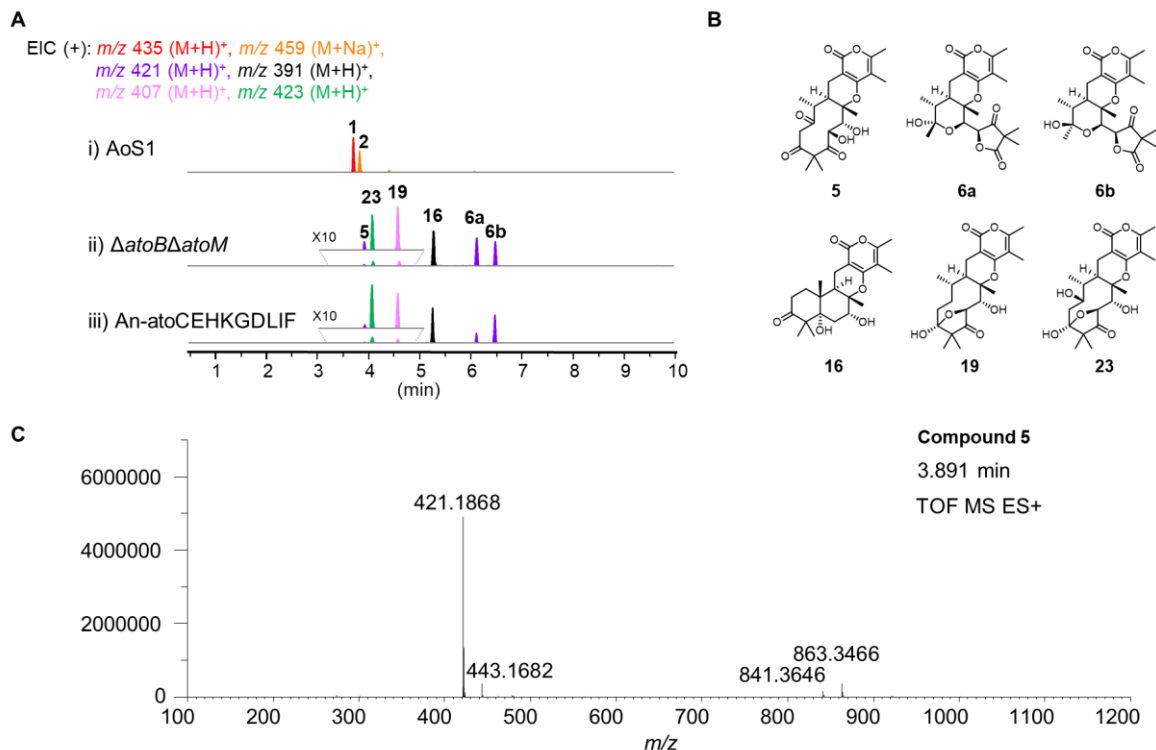


Figure S4. Metabolites of $\Delta atoB\Delta atoM$ and An-atoCEHKGDLIF. (A) LC-MS analysis of AoS1, $\Delta atoB\Delta atoM$, and An-atoCEHKGDLIF strains. (B) Sturctures of compounds from $\Delta atoB\Delta atoM$ strain. (C) MS spectrum of isolated **5**.

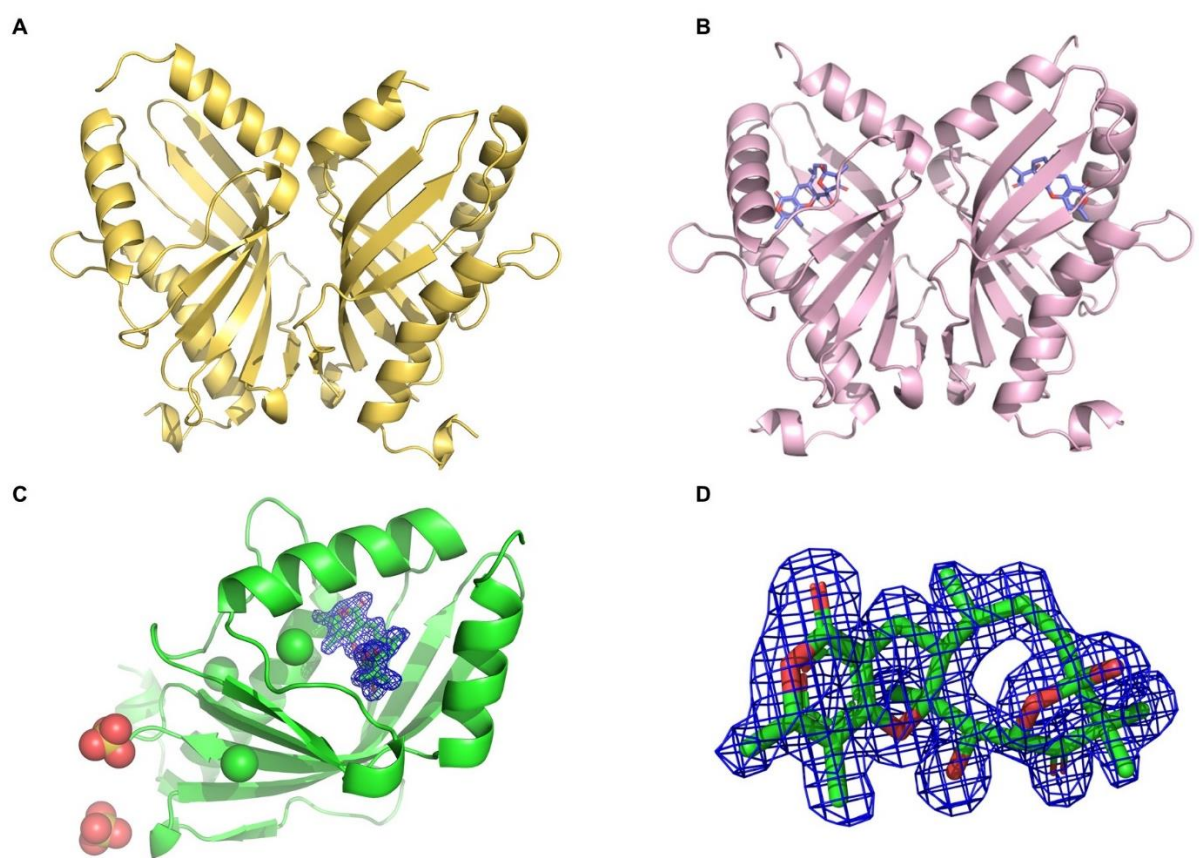


Figure S5. The overall structures of AtoB (A), AtoB complex with compound 19 (B) and omitting map (C and D) of the complex.

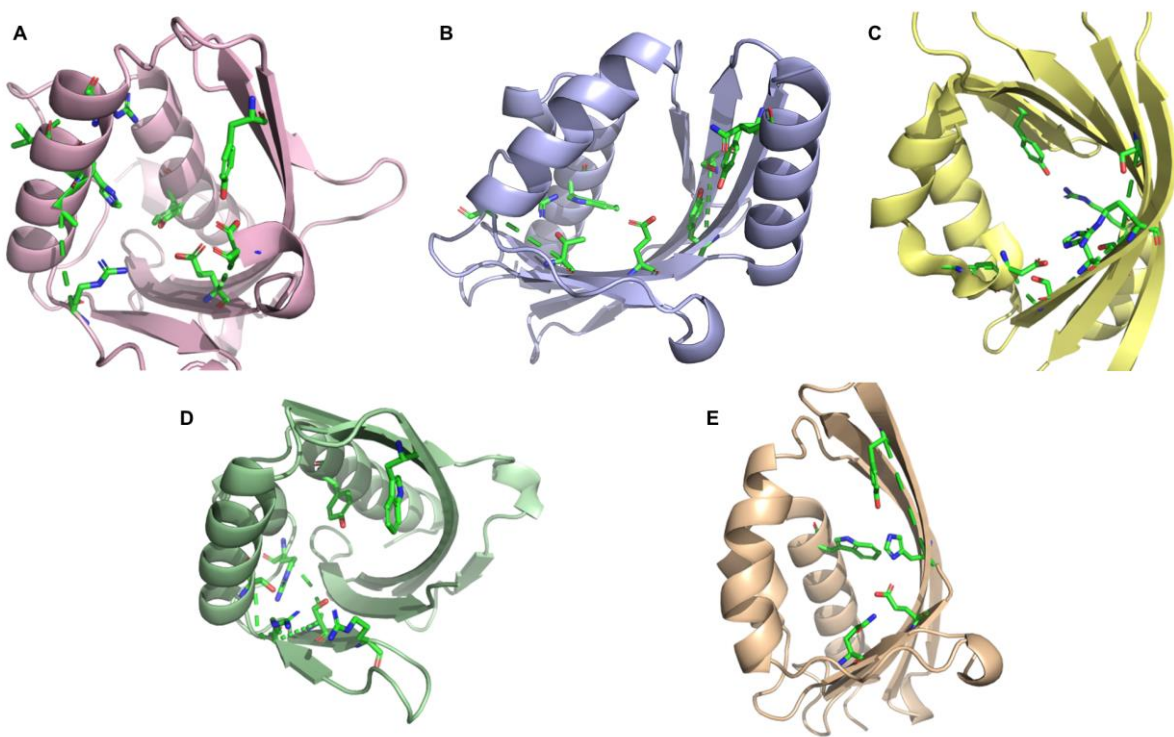


Figure S6. Comparing the hydrophilic amino acid residues in the active cavity of AtoB (A), BvnE (B), SdnG (C), Trt14 (D), and NsrQ (E).

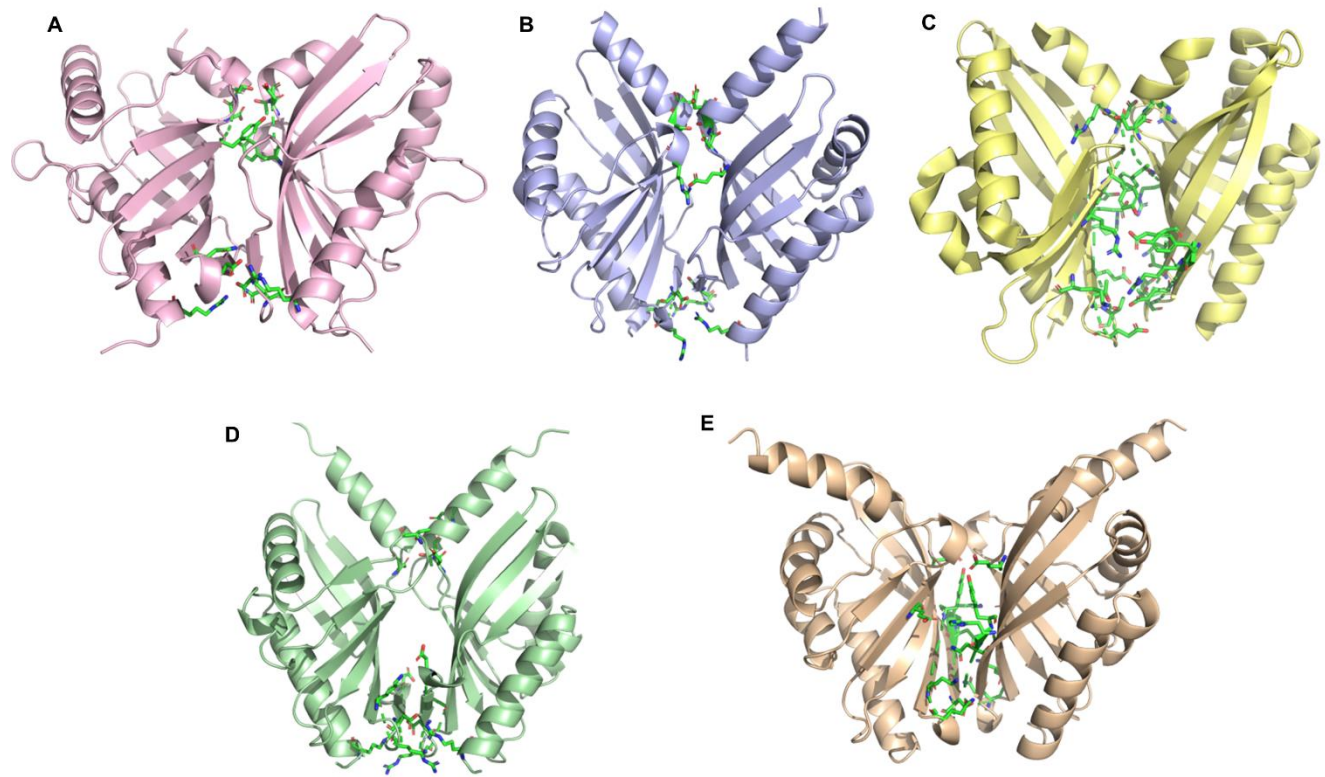


Figure S7. The dimer interface of AtoB (A), BvnE (B), SdnG (C), Trt14 (D), and NsrQ (E).

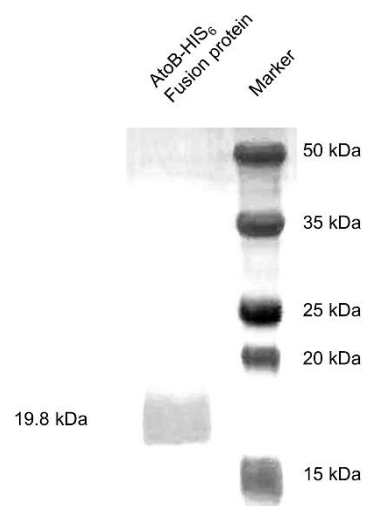


Figure S8. SDS-PAGE analysis of purified AtoB (19.8 kDa).

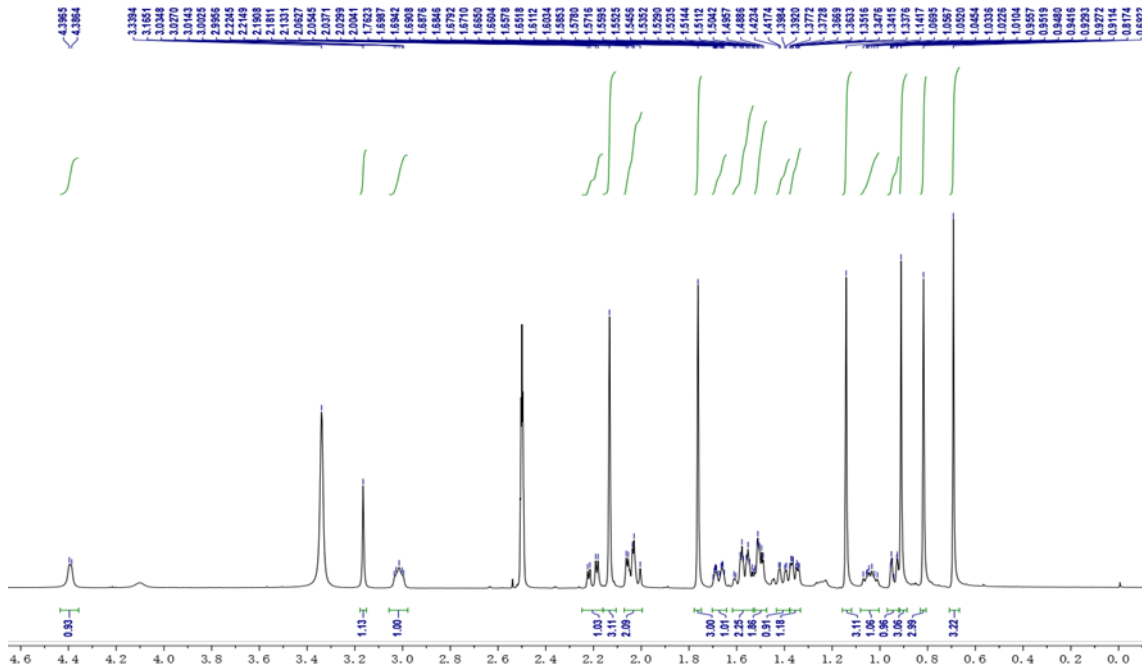


Figure S9. ^1H NMR spectrum of 3 (DMSO- d_6 , 500 MHz).

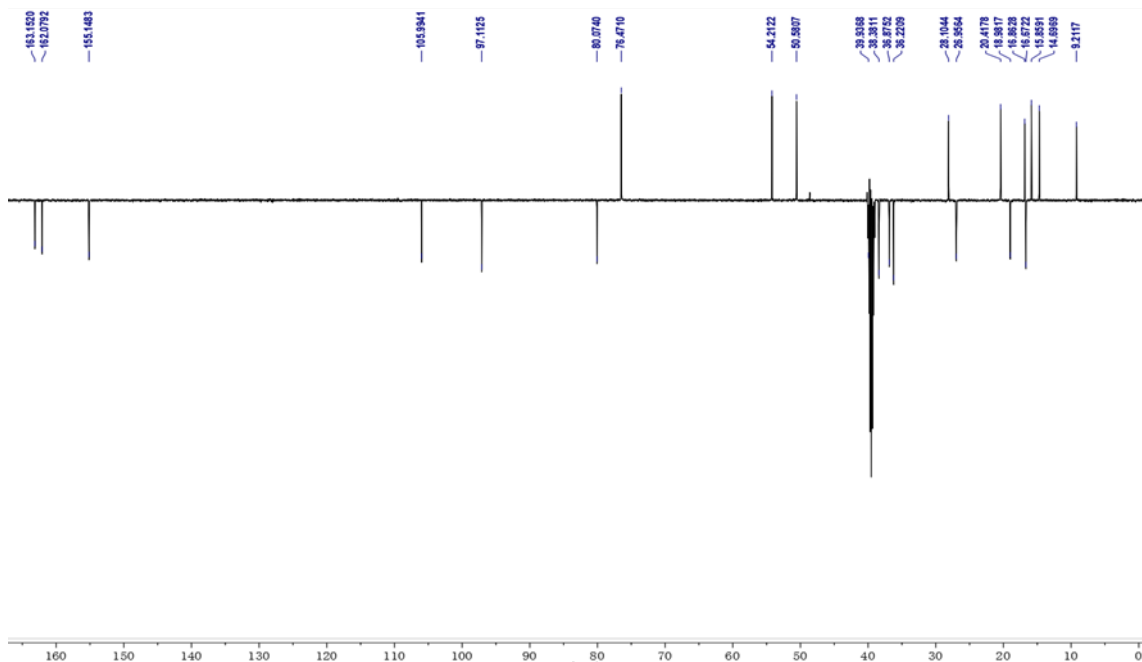


Figure S10. ^{13}C NMR spectrum of 3 (DMSO- d_6 , 125 MHz).

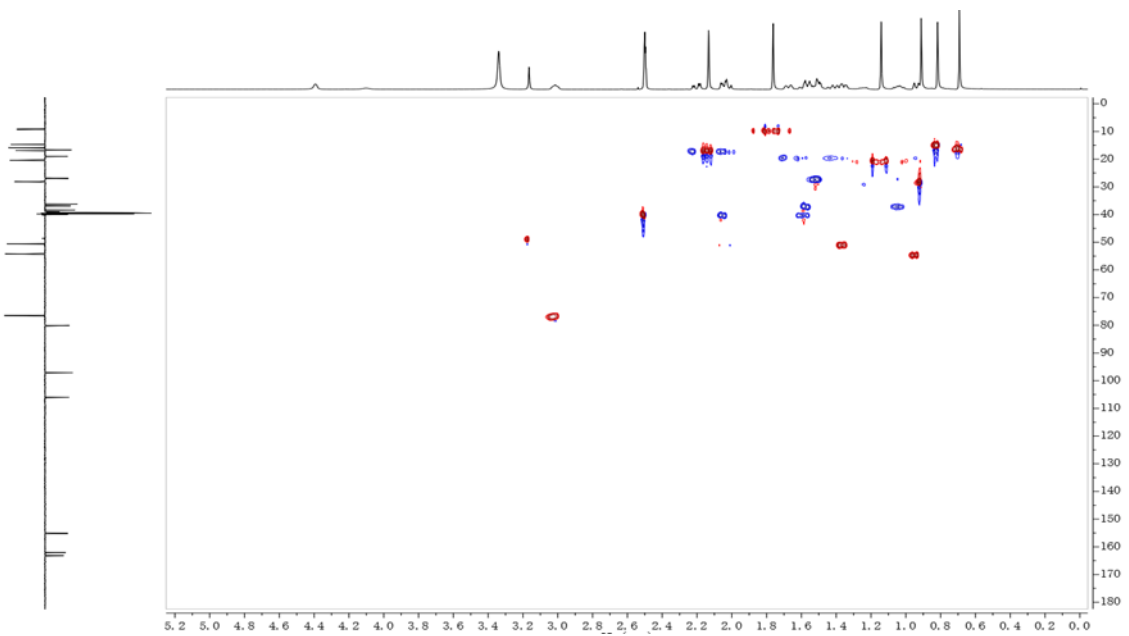


Figure S11. HSQC spectrum of 3.

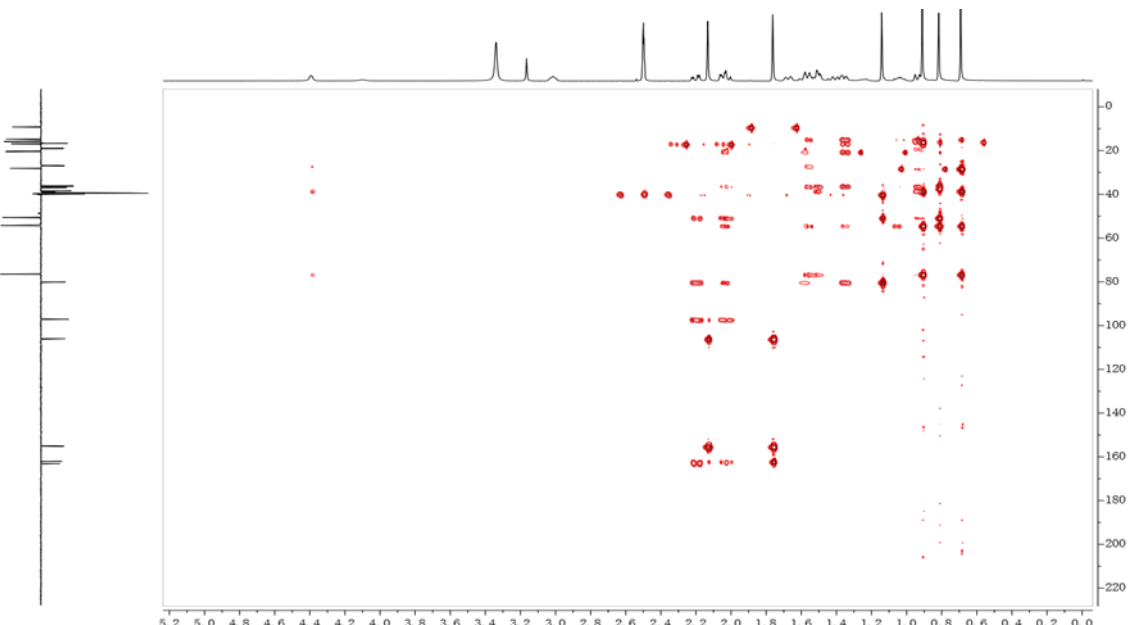


Figure S12. HMBC spectrum of 3.

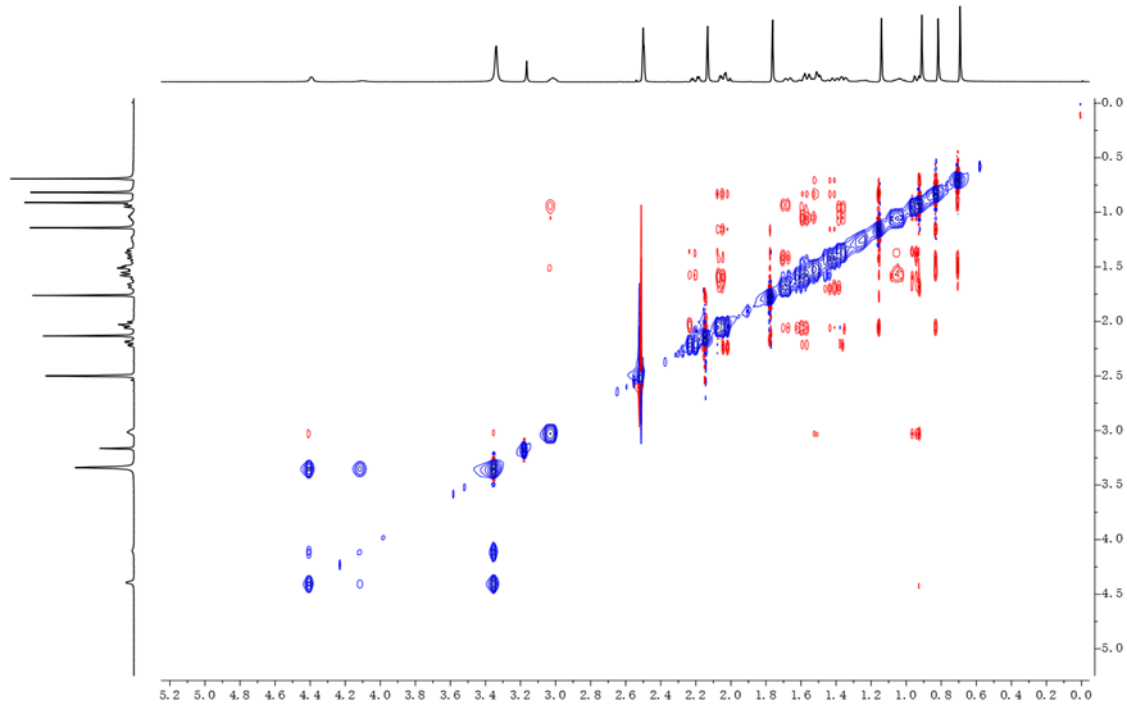


Figure S13. ROESY spectrum of 3.

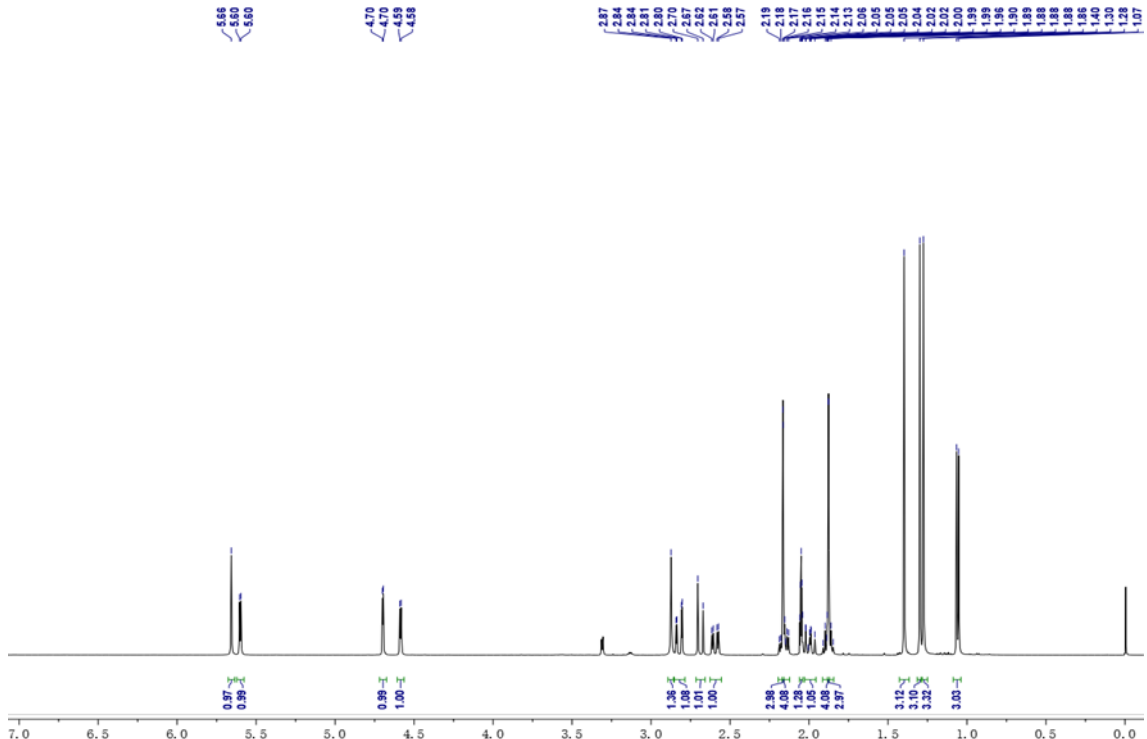


Figure S14. ^1H NMR spectrum of 4a (acetone- d_6 , 500 MHz).

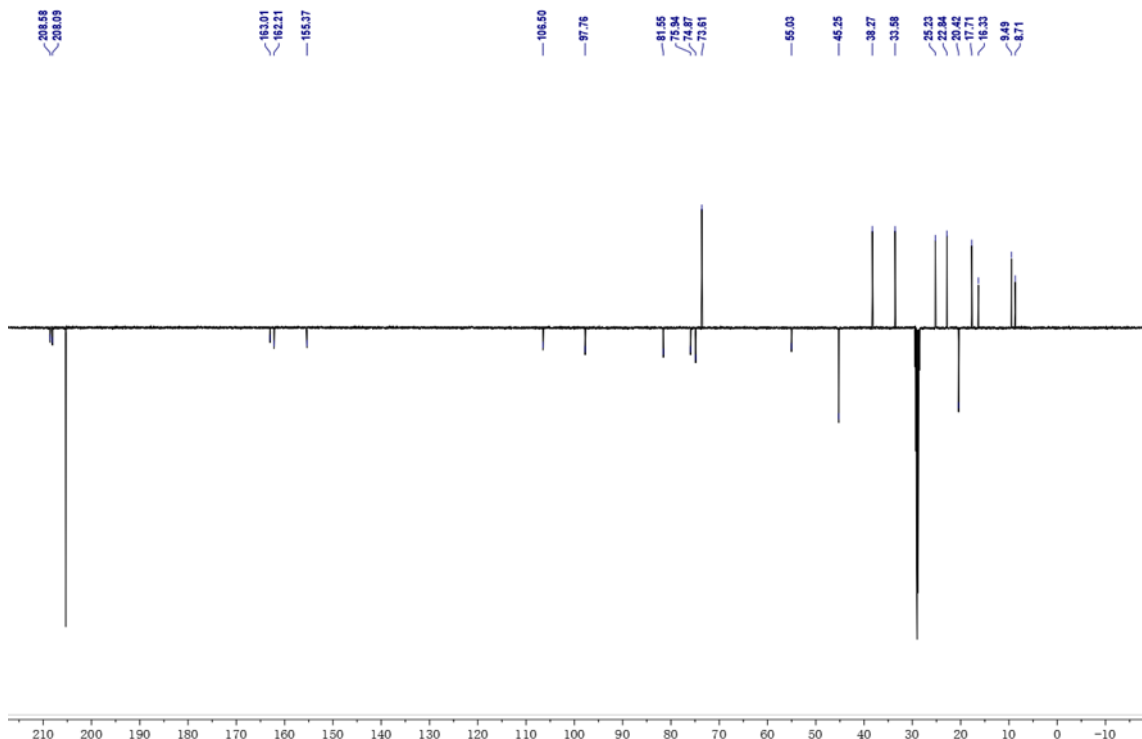


Figure S15. ^{13}C NMR spectrum of 4a (acetone- d_6 , 125 MHz).

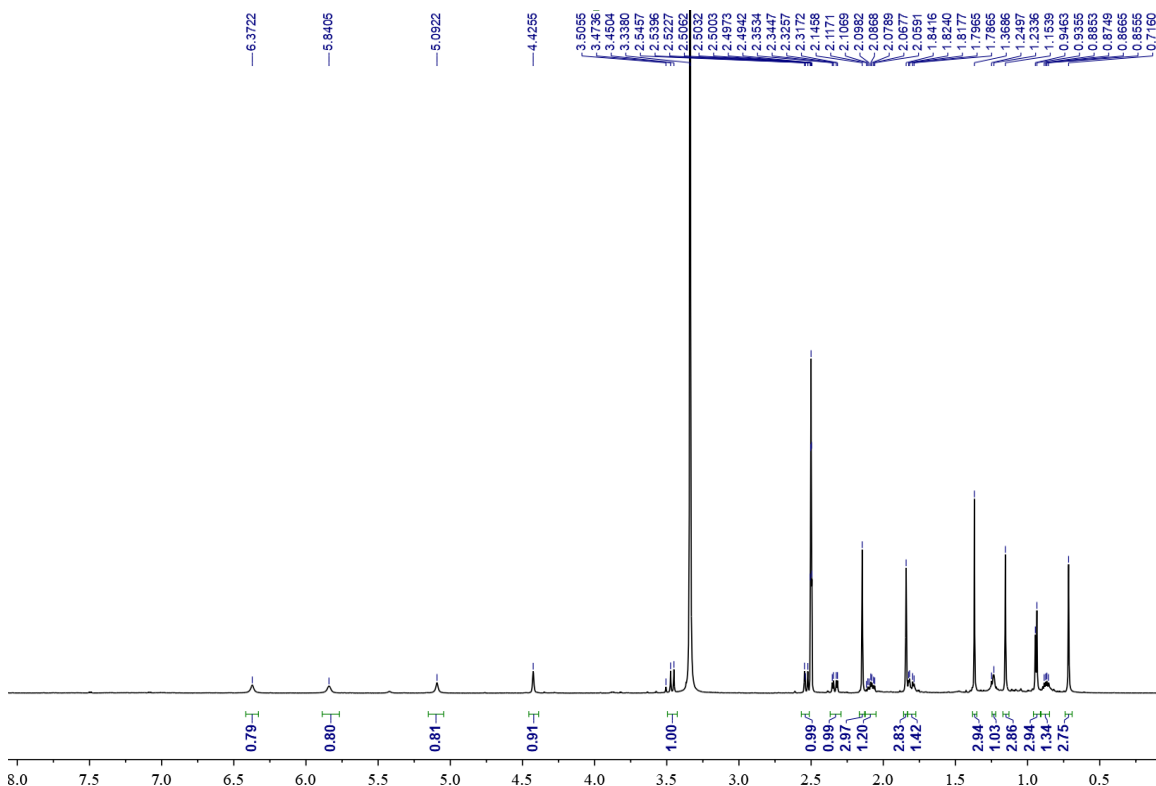


Figure S16. ^1H NMR spectrum of 4b (DMSO- d_6 , 500 MHz).

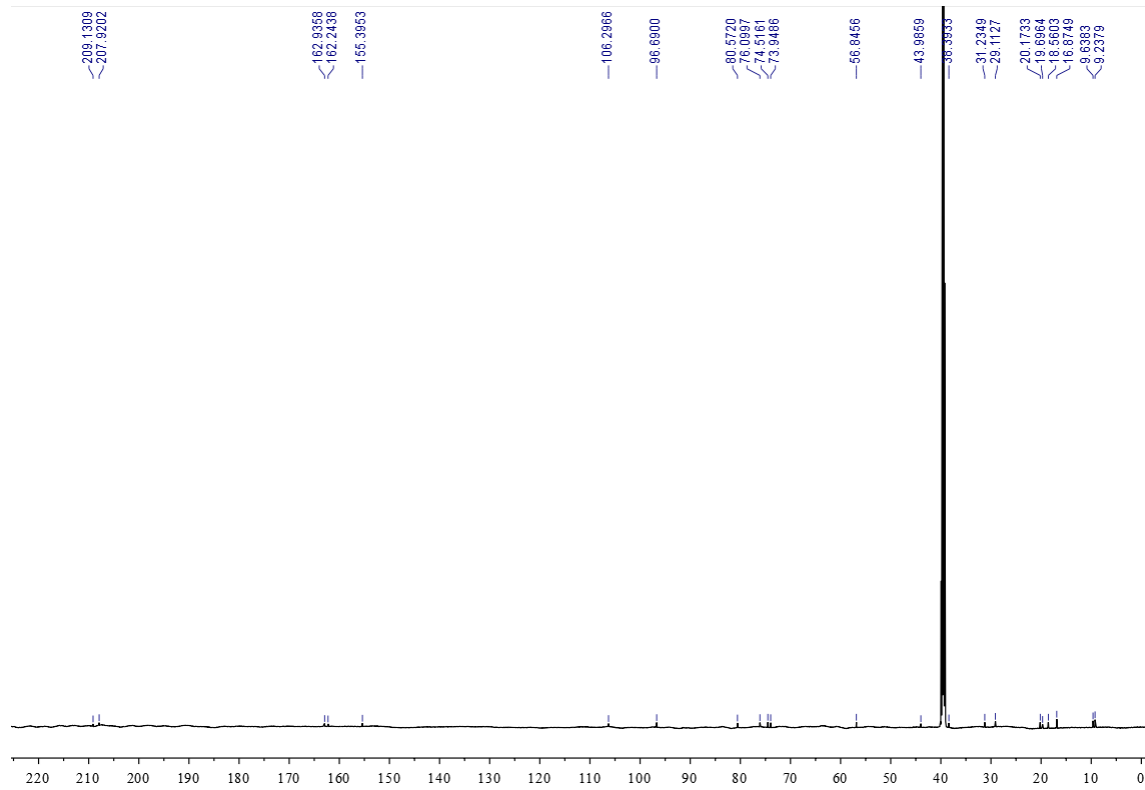


Figure S17. ¹³C NMR spectrum of 4b (DMSO-*d*₆, 125 MHz).

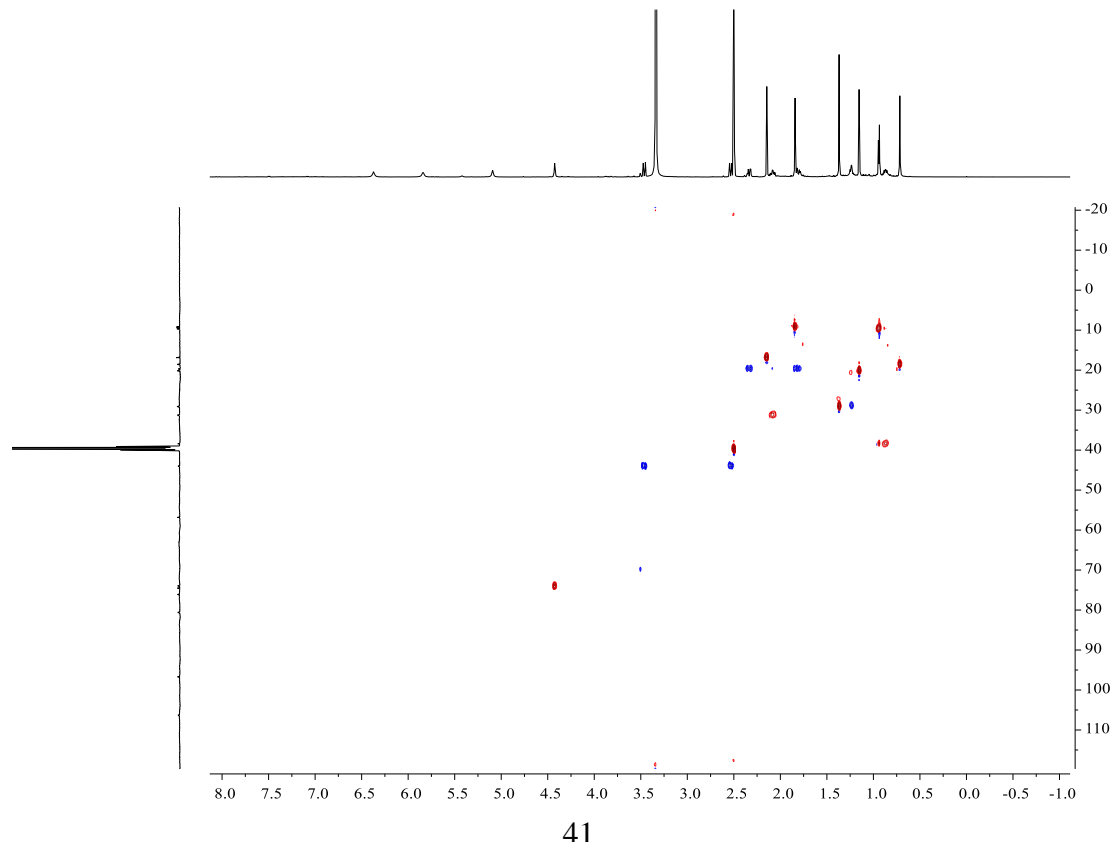


Figure S18. HSQC spectrum of 4b.

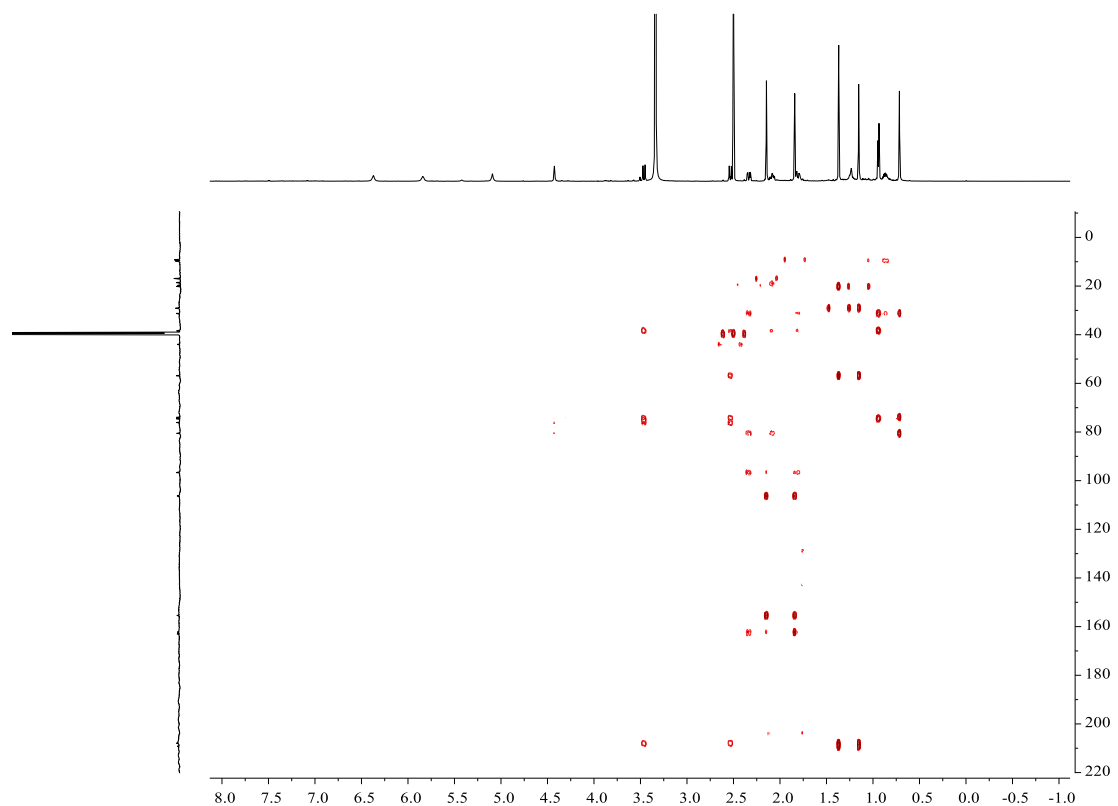


Figure S19. HMBC spectrum of 4b.

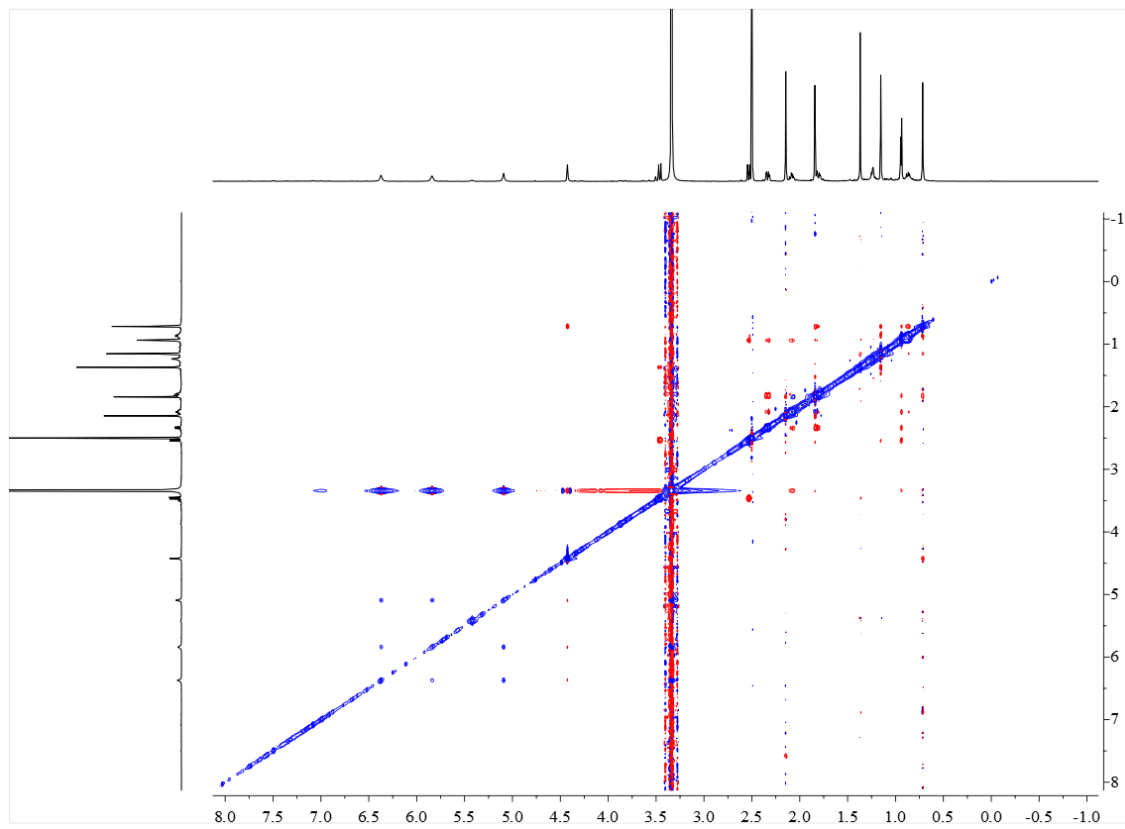


Figure S20. ROESY spectrum of 4b.

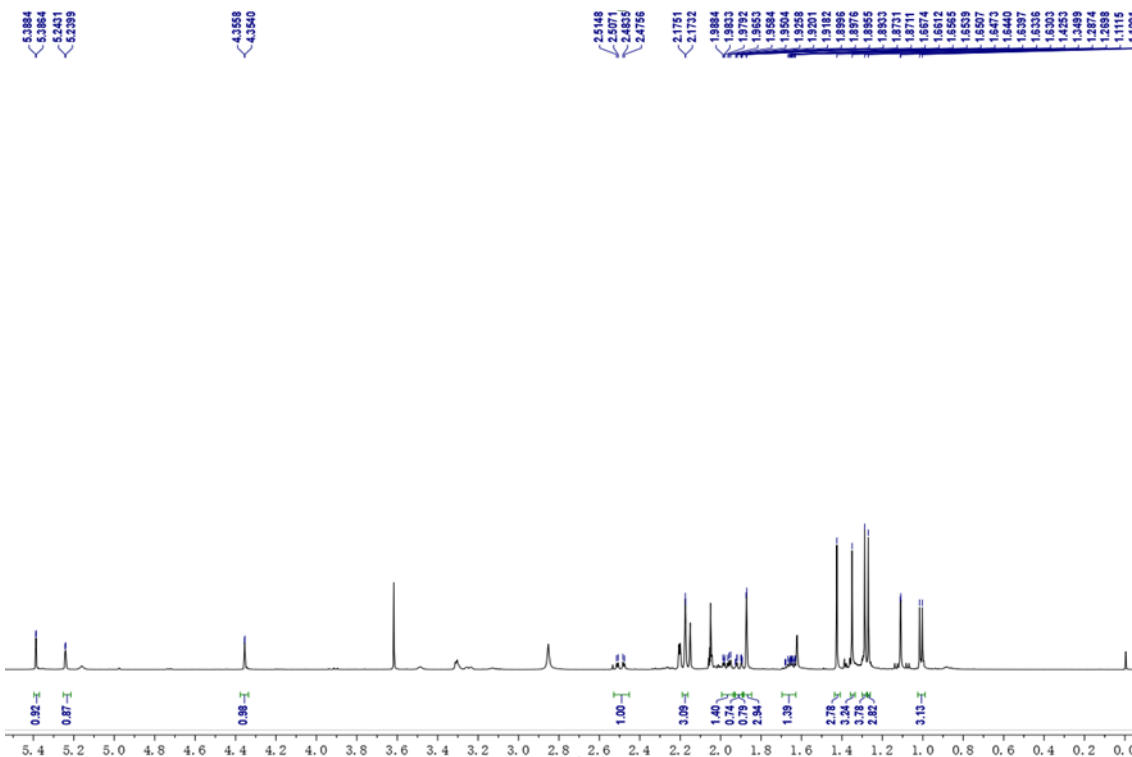


Figure S21. ^1H NMR spectrum of 6a (acetone- d_6 , 500 MHz).

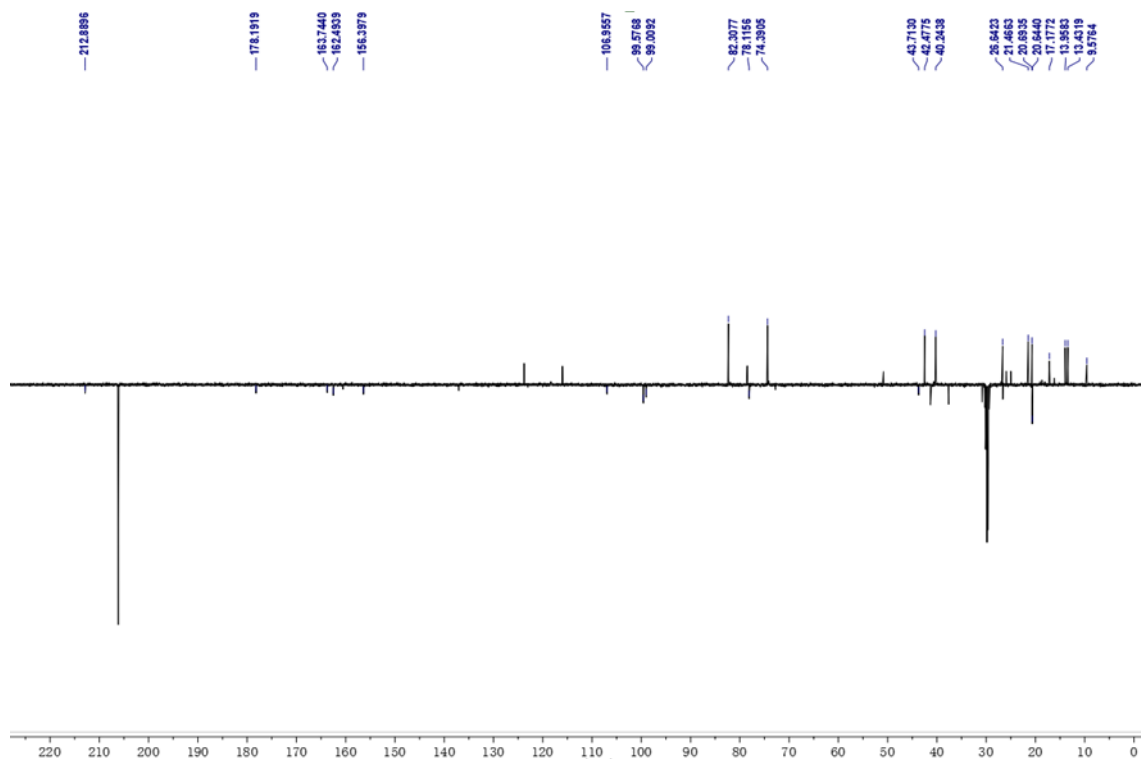


Figure S22. ^{13}C NMR spectrum of 6a (acetone- d_6 , 125 MHz).

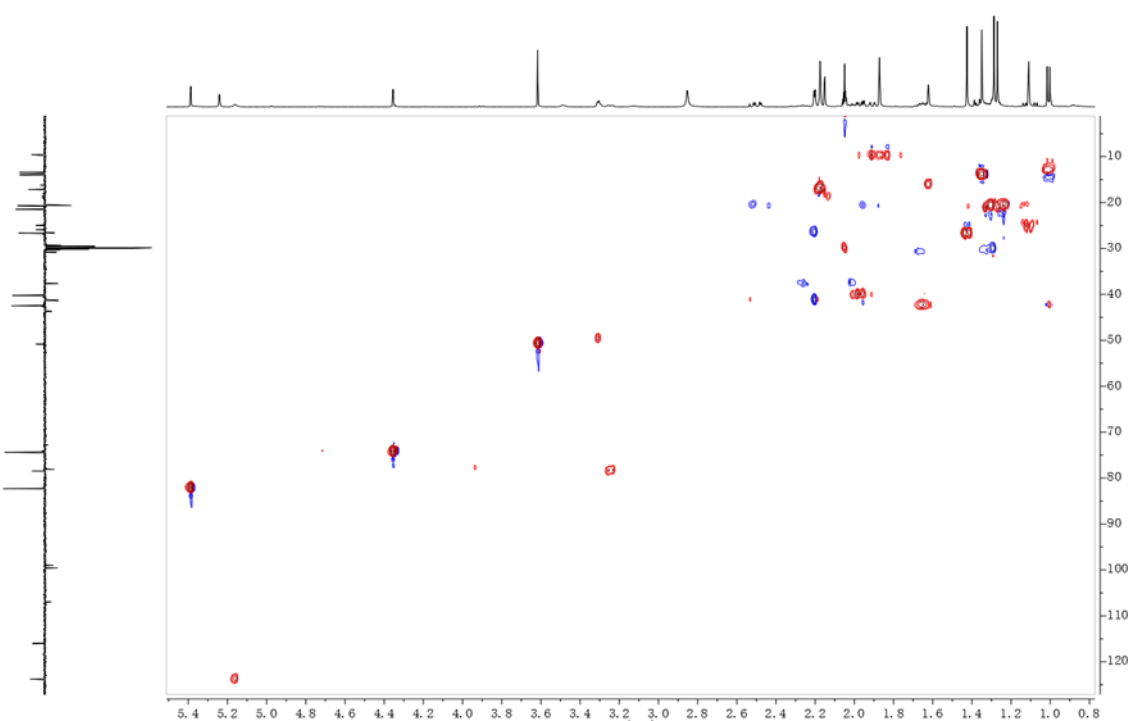


Figure S23. HSQC spectrum of 6a.

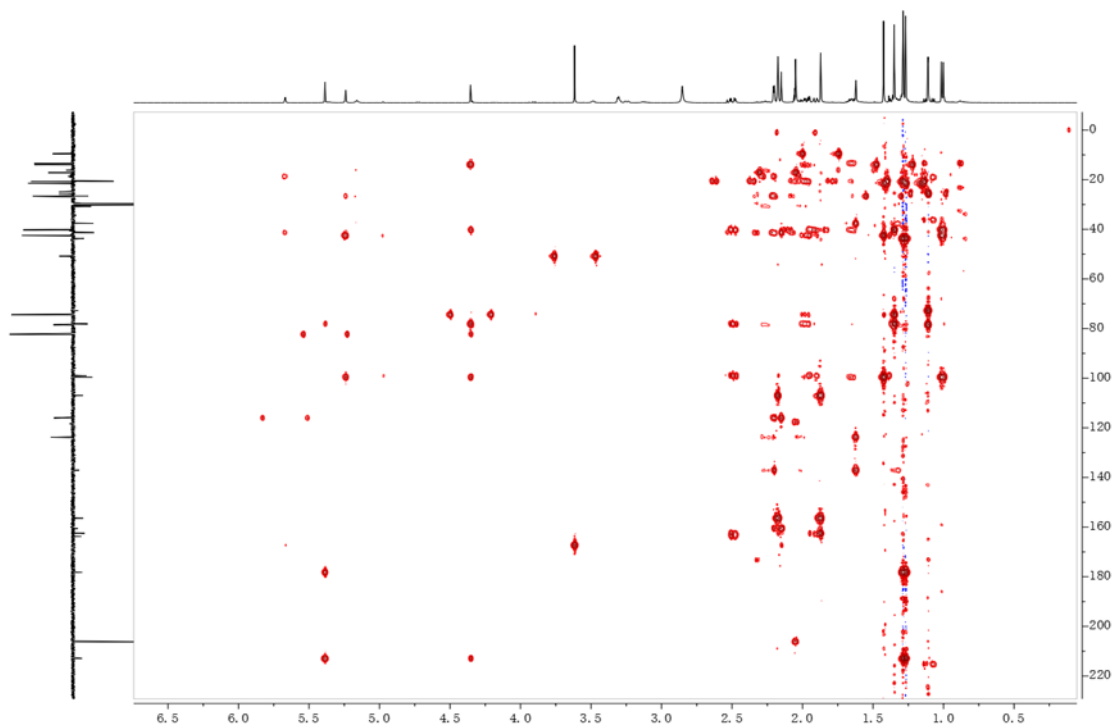


Figure S24. HMBC spectrum of 6a.

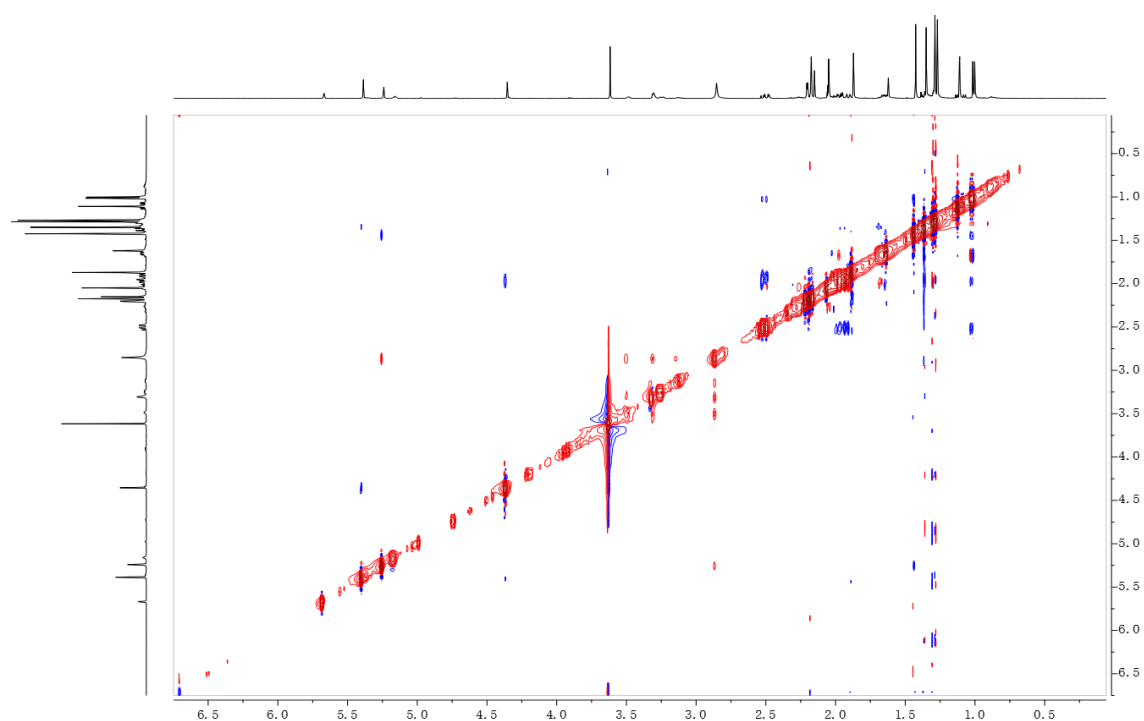


Figure S25. ROESY spectrum of 6a.

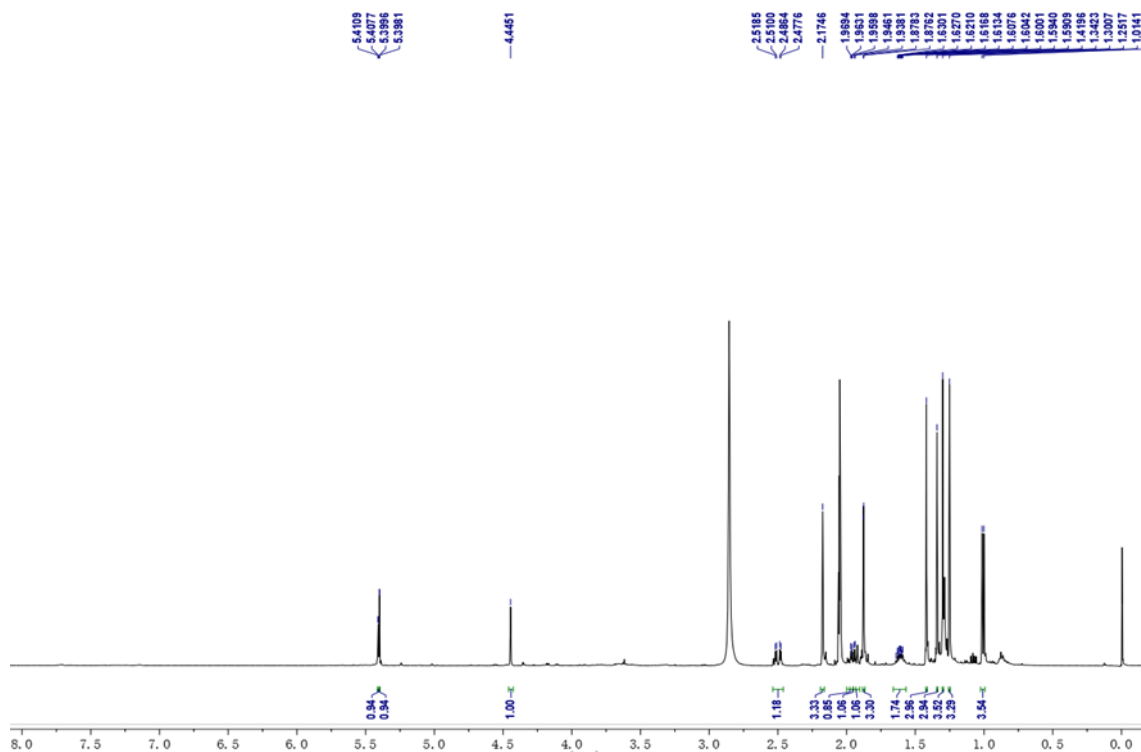


Figure S26. ^1H NMR spectrum of **6b** (acetone- d_6 , 500 MHz).

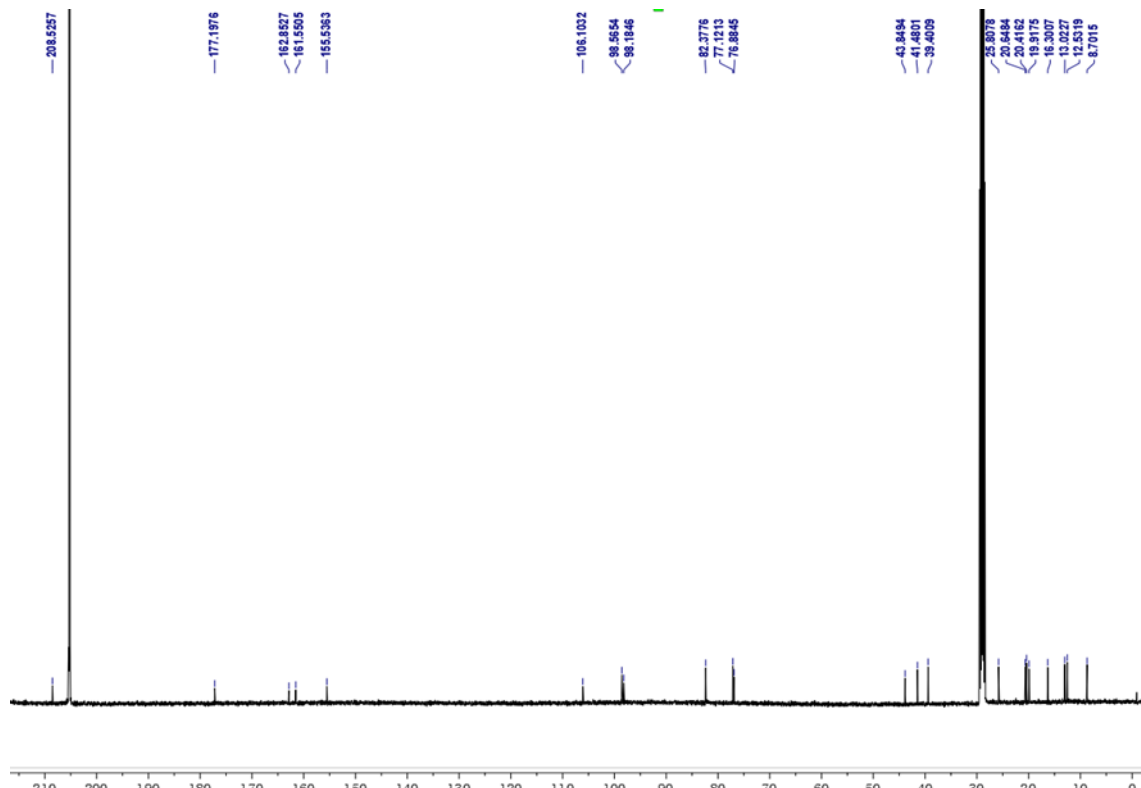


Figure S27. ^{13}C NMR spectrum of **6b** (acetone- d_6 , 125 MHz).

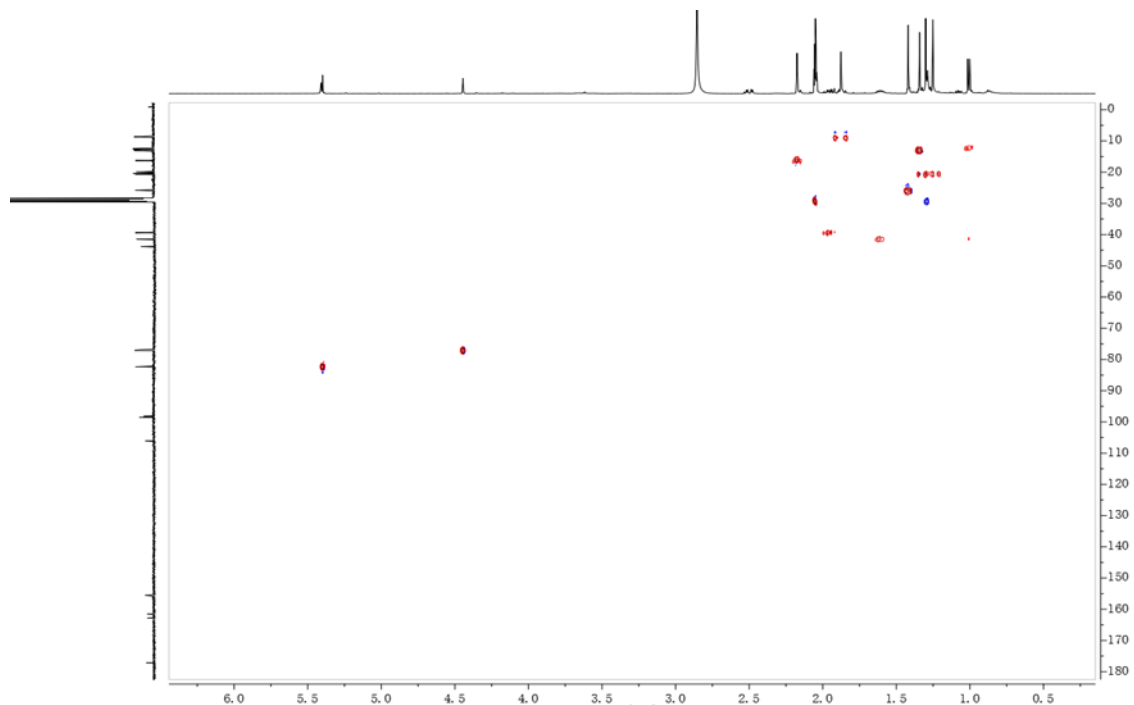


Figure S28. HSQC spectrum of 6b.

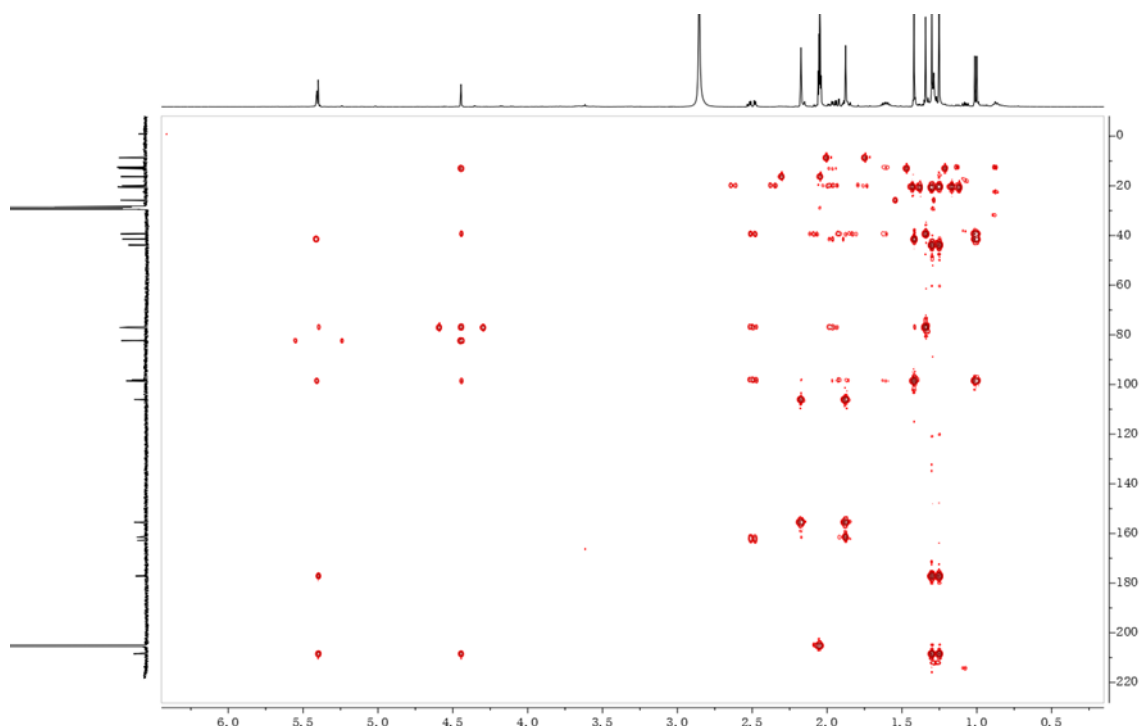


Figure S29. HMBC spectrum of 6b.

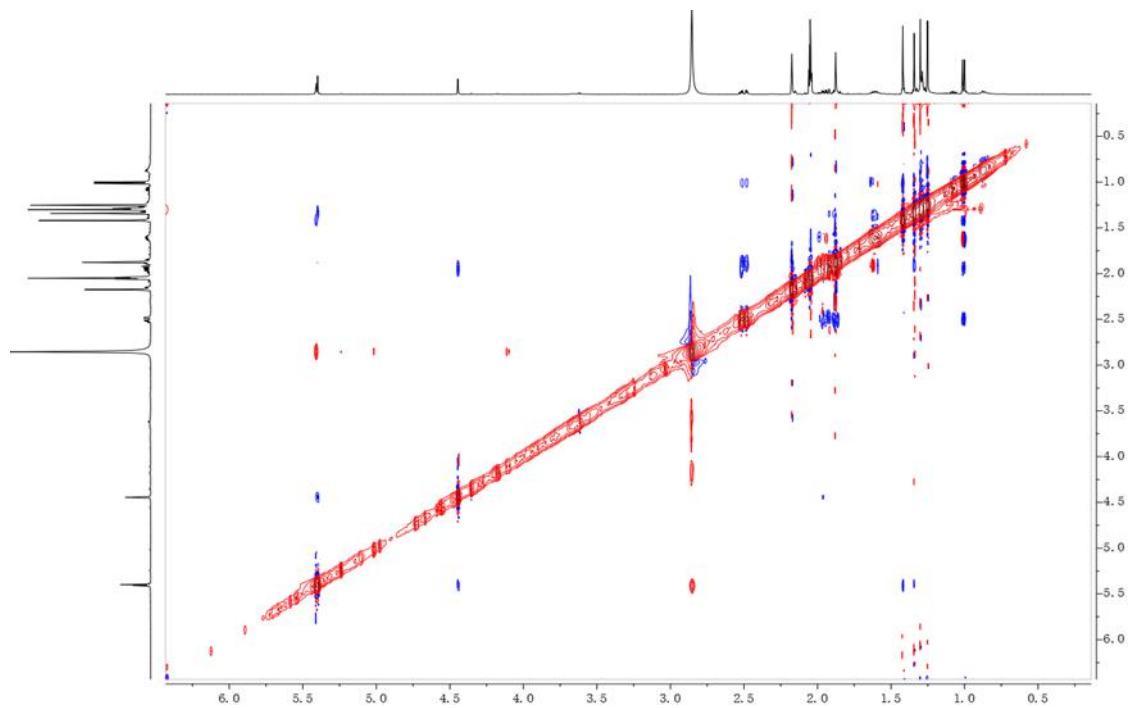


Figure S30. ROESY spectrum of 6b.

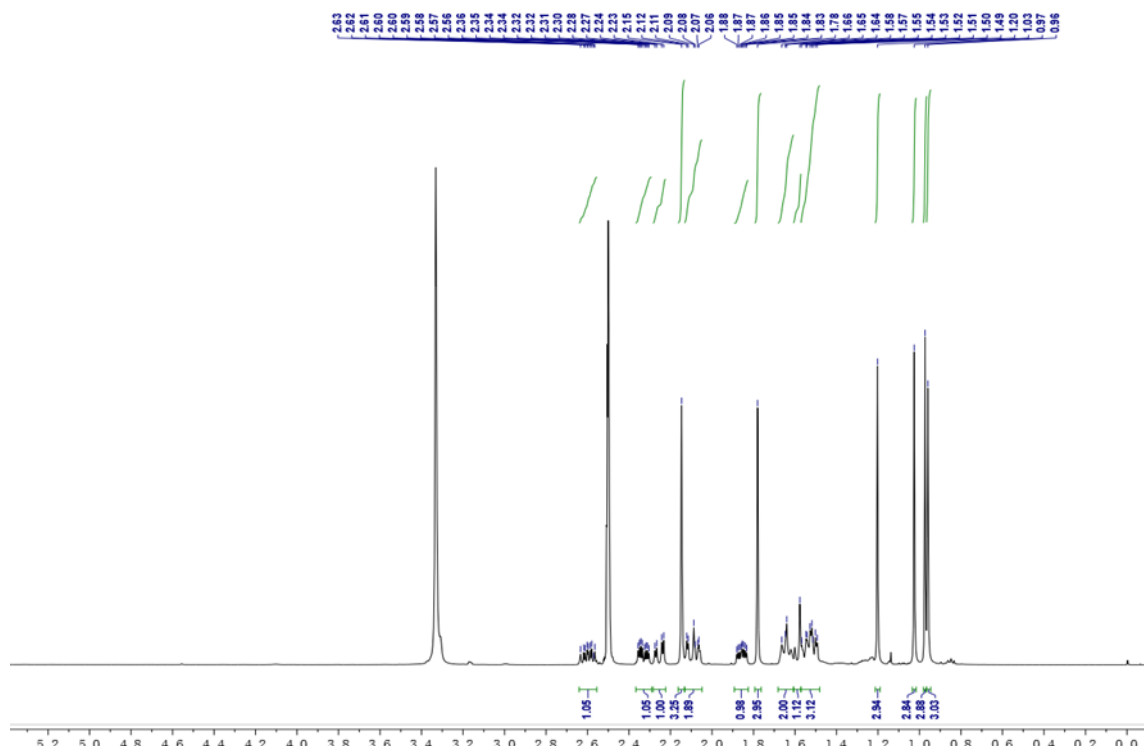


Figure S31. ^1H NMR spectrum of 7 (DMSO- d_6 , 500 MHz).

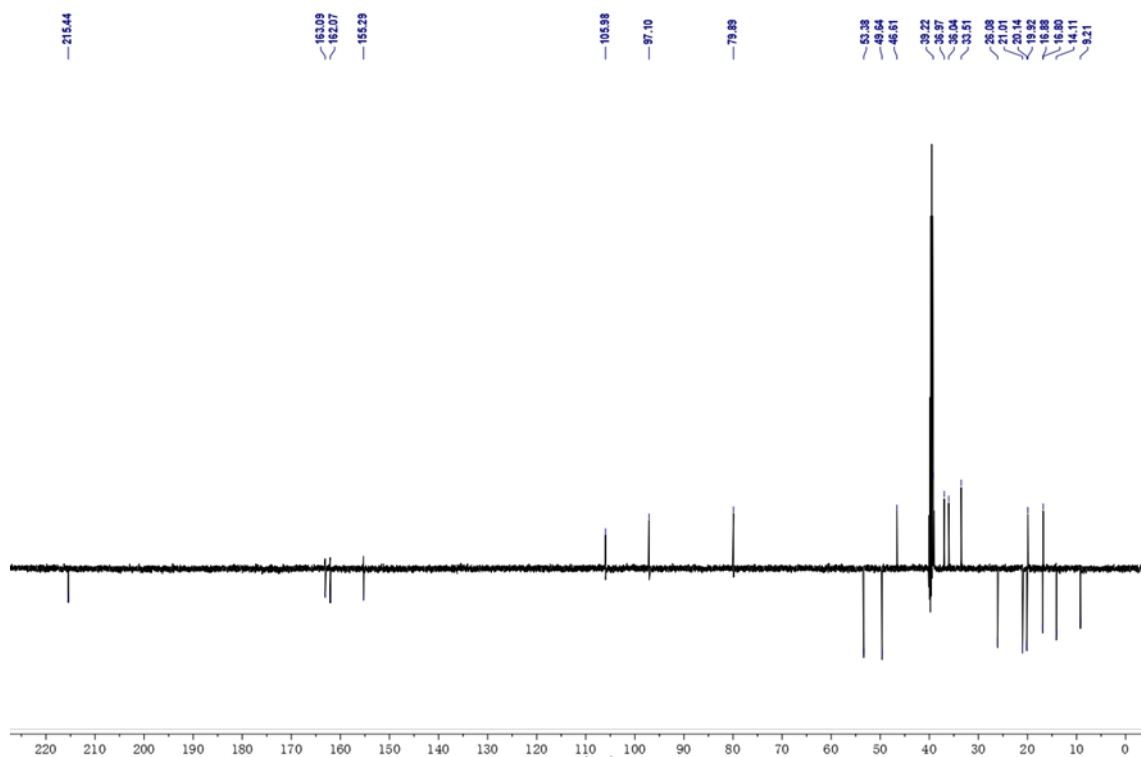


Figure S32. ¹³C NMR spectrum of 7 (DMSO-*d*₆, 125 MHz).

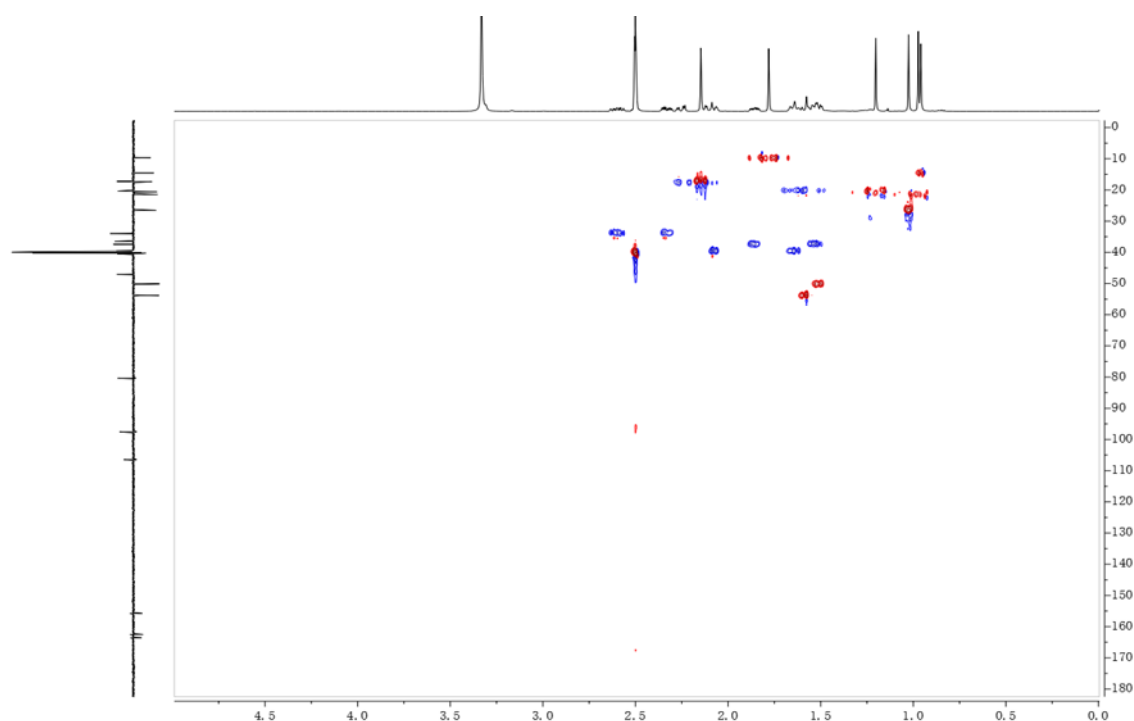


Figure S33. HSQC spectrum of 7.

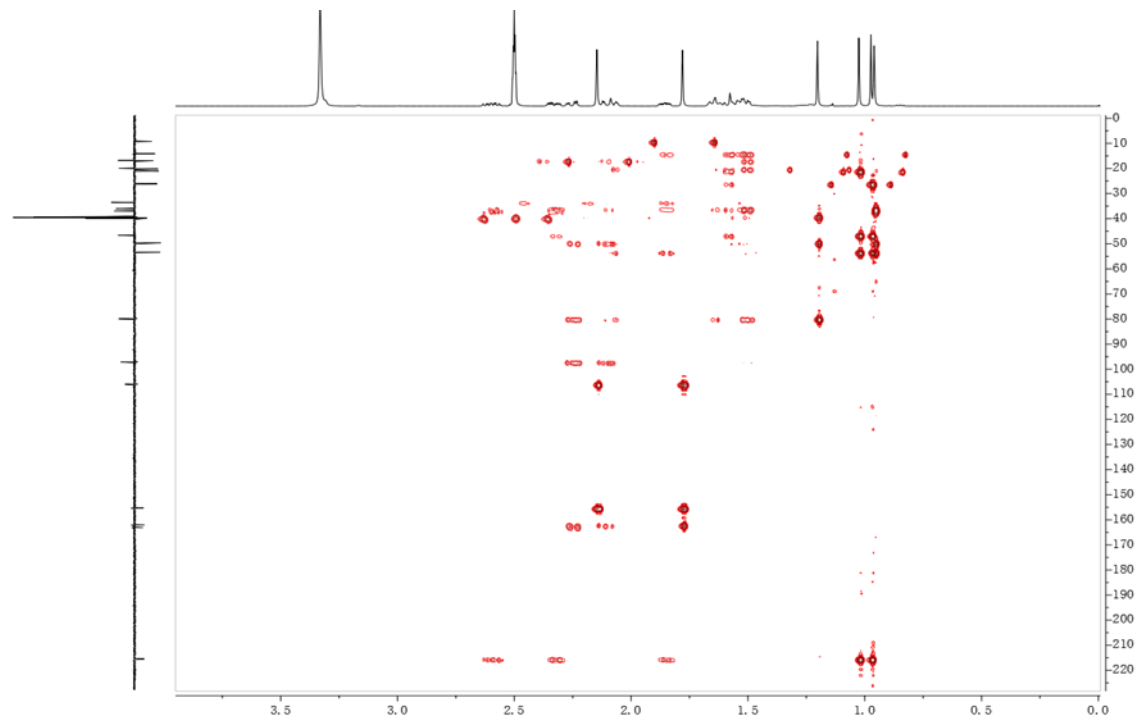


Figure S34. HMBC spectrum of 7.

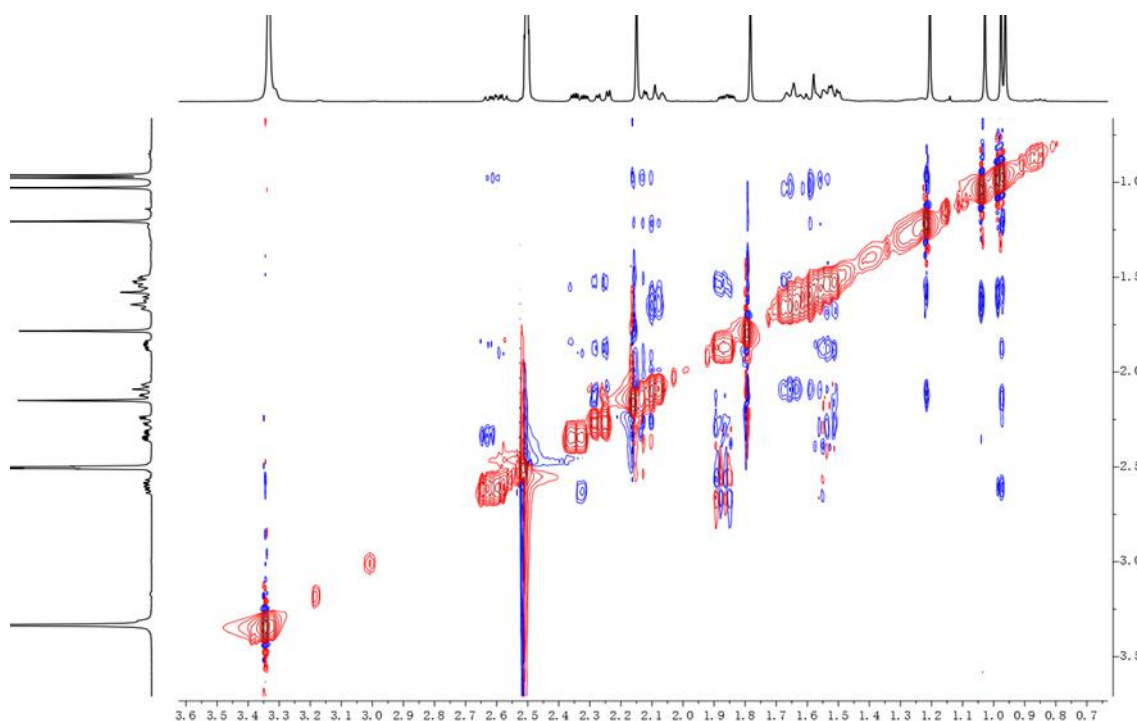


Figure S35. ROESY spectrum of 7.

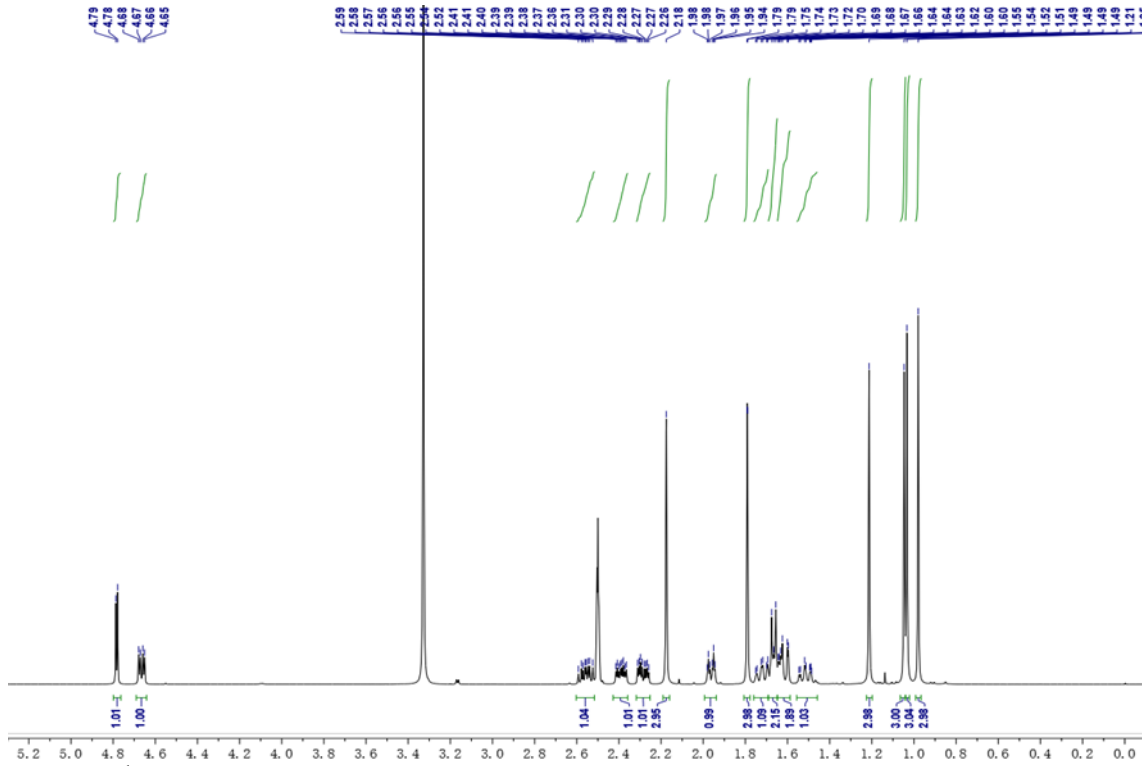


Figure S36. ^1H NMR spectrum of 8 (DMSO- d_6 , 500 MHz).

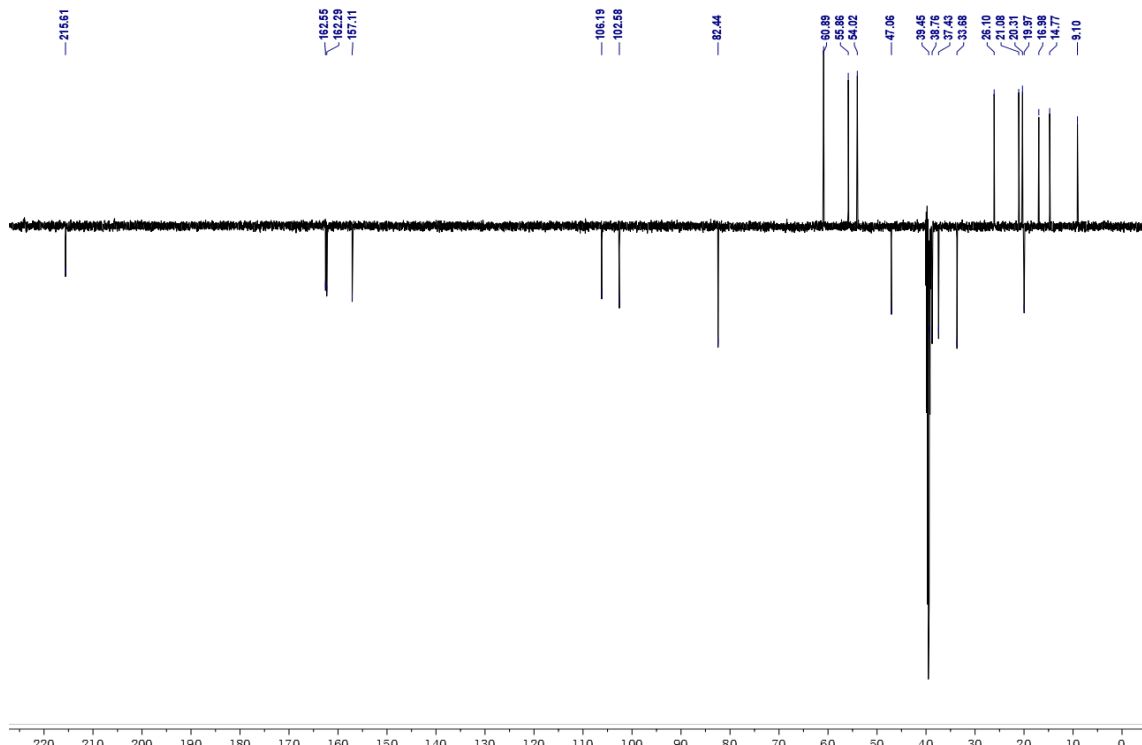


Figure S37. ^{13}C NMR spectrum of **8** (DMSO- d_6 , 125 MHz).

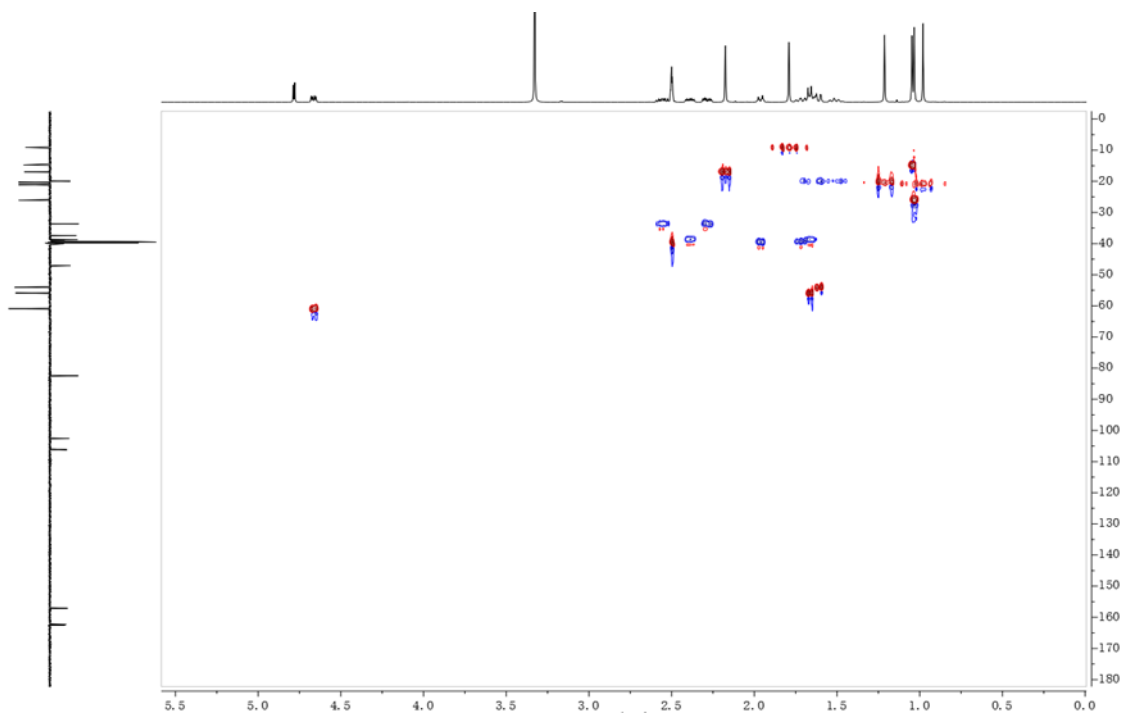


Figure S38. HSQC spectrum of 8.

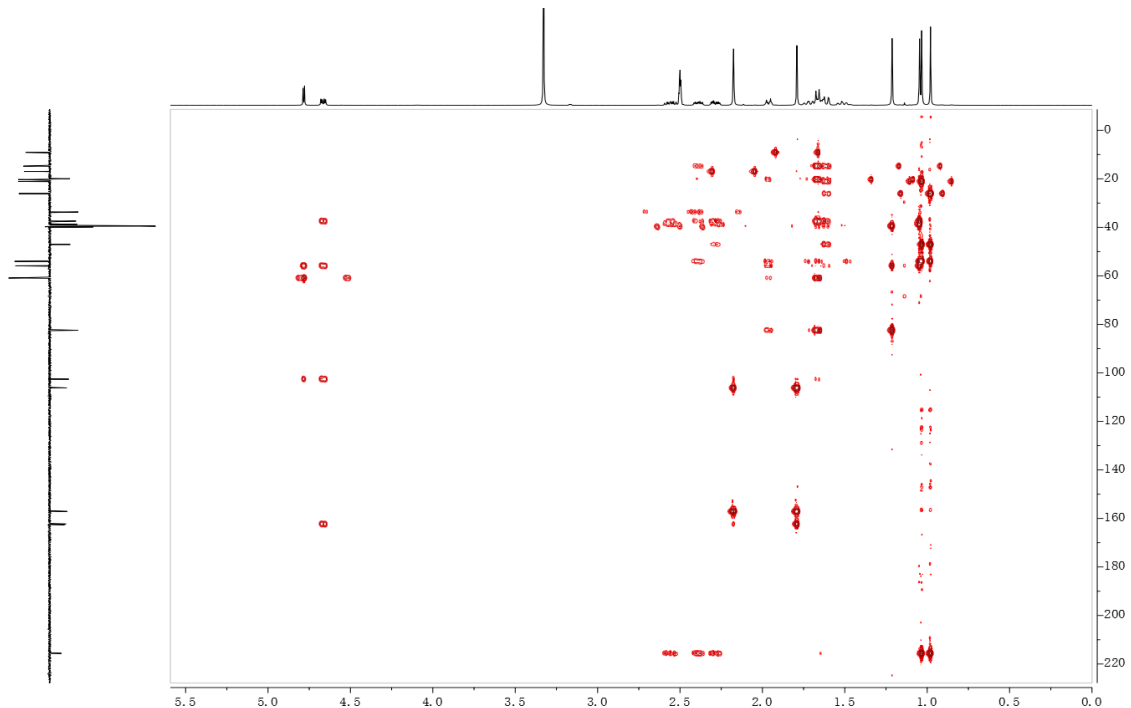


Figure S39. HMBC spectrum of 8.

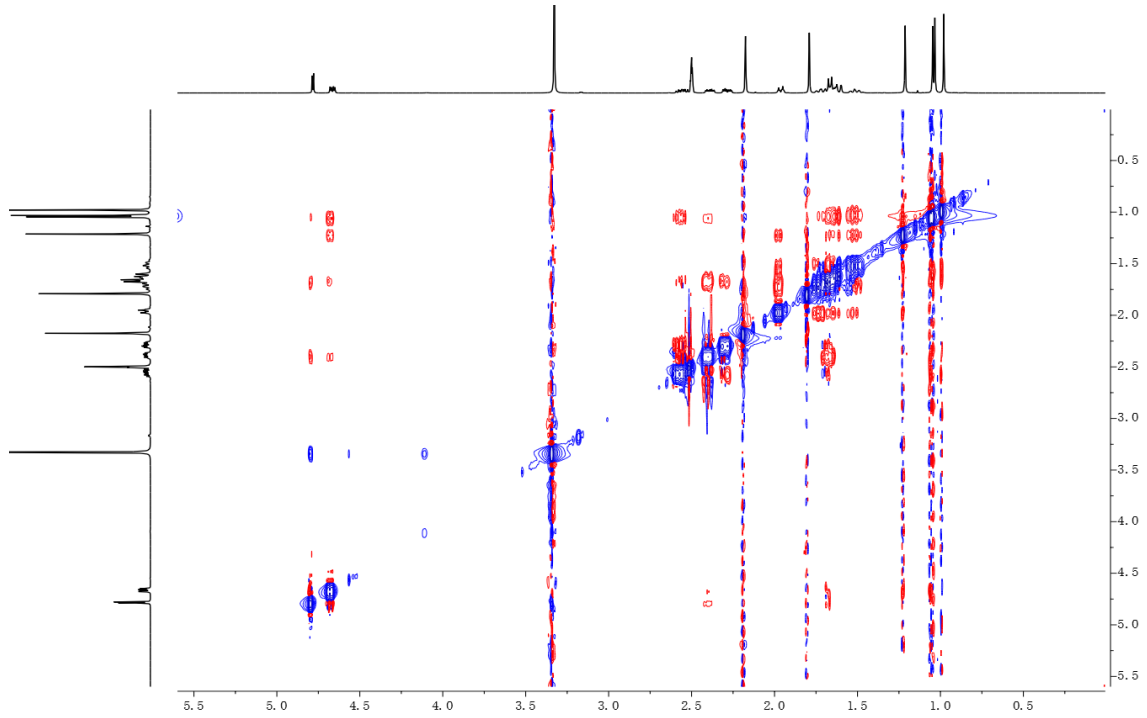


Figure S40. ROESY spectrum of **8**.

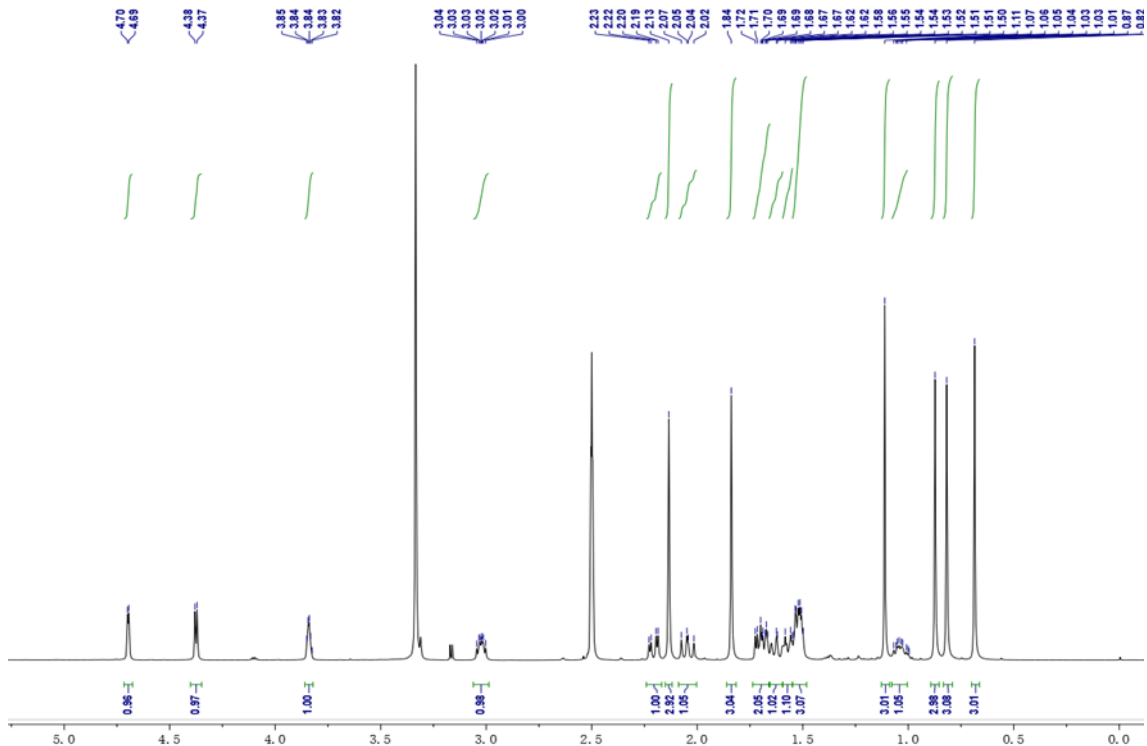


Figure S41. ^1H NMR spectrum of 9 (DMSO- d_6 , 500 MHz).

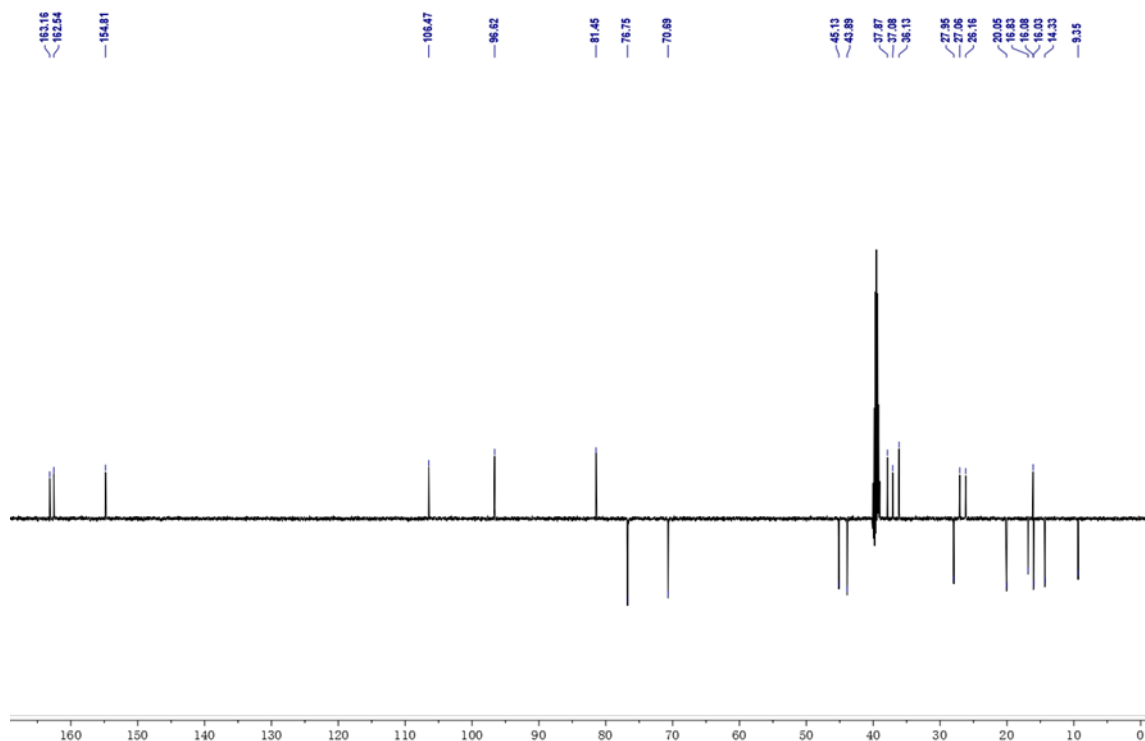


Figure S42. ^{13}C NMR spectrum of 9 (DMSO- d_6 , 125 MHz).

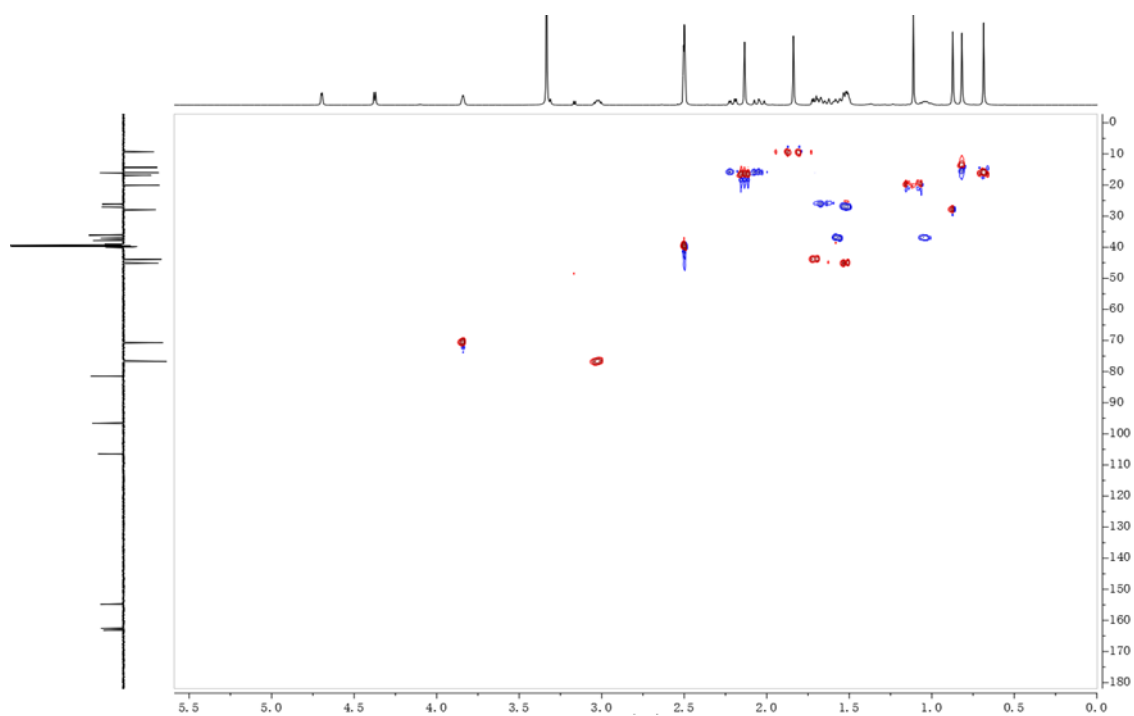


Figure S43. HSQC spectrum of 9.

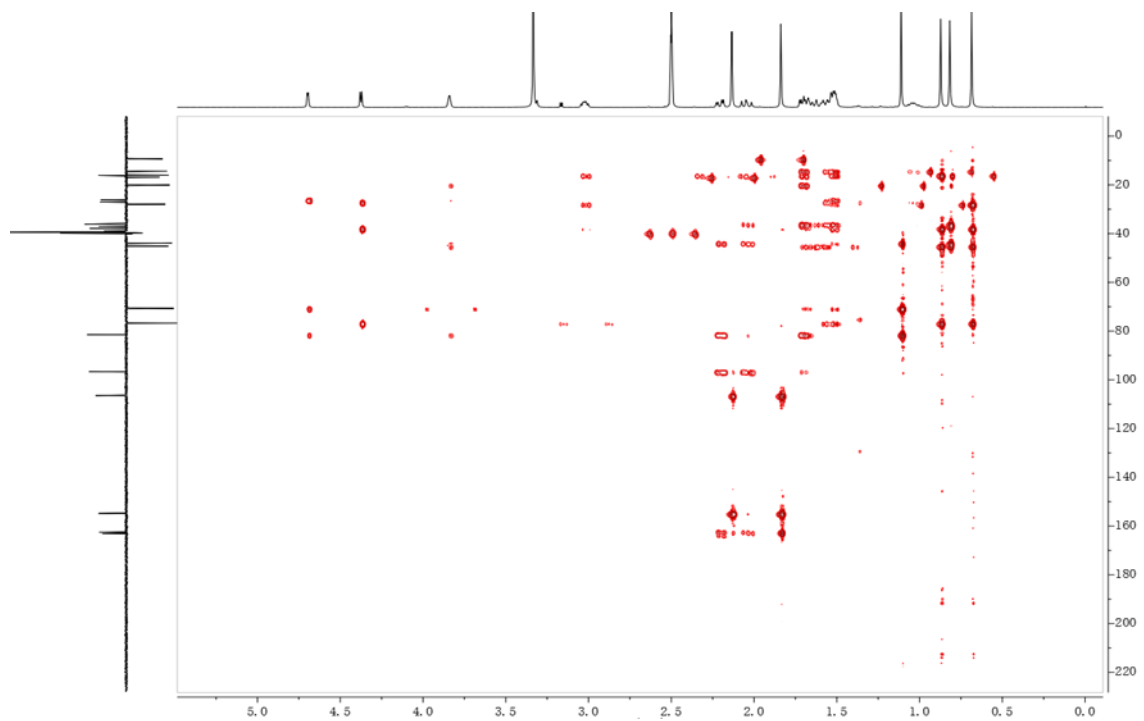


Figure S44. HMBC spectrum of 9.

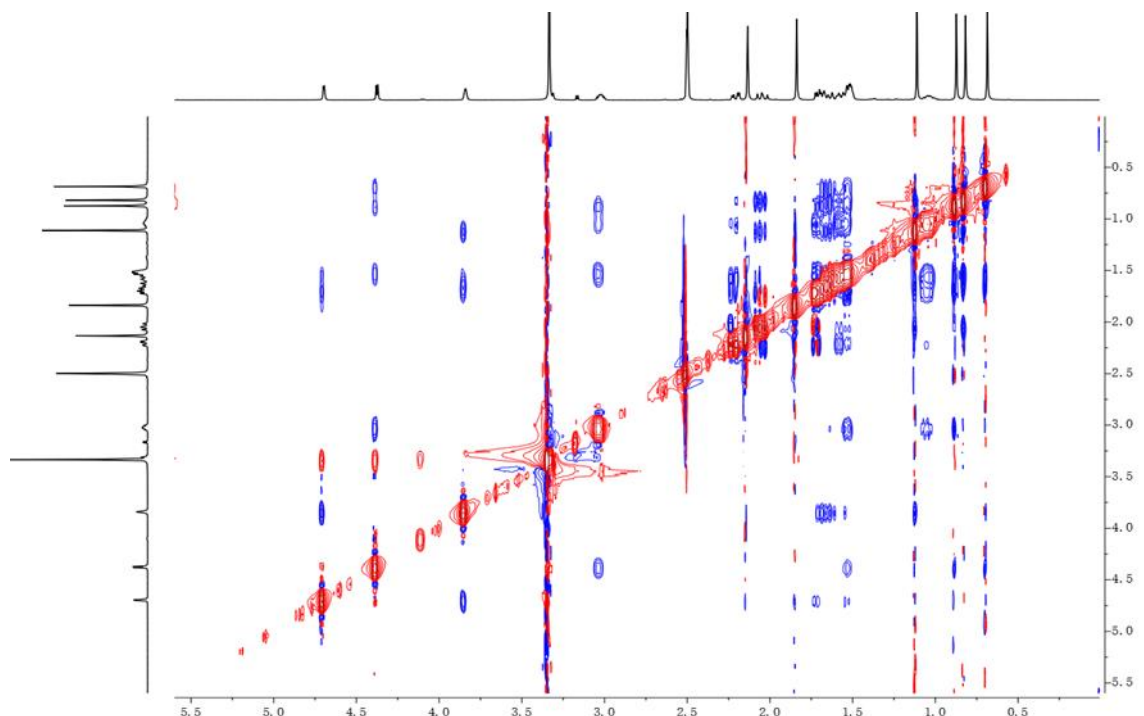


Figure S45. ROESY spectrum of 9.

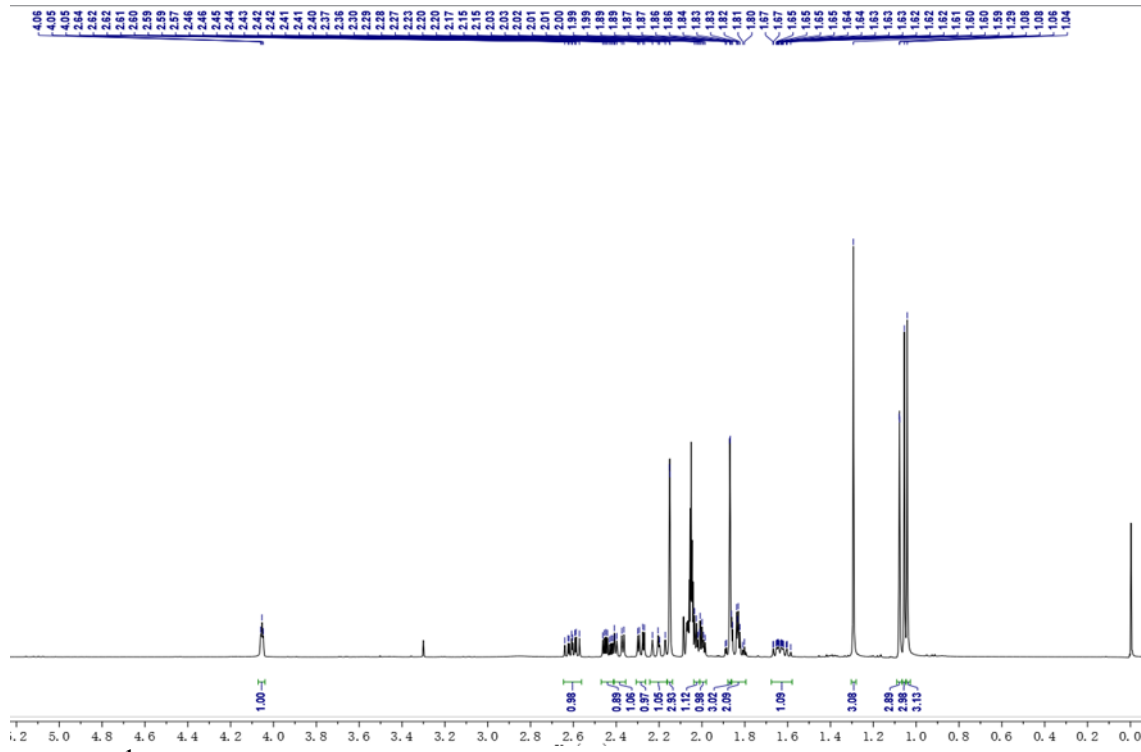


Figure S46. ^1H NMR spectrum of 10 (acetone- d_6 , 500 MHz).

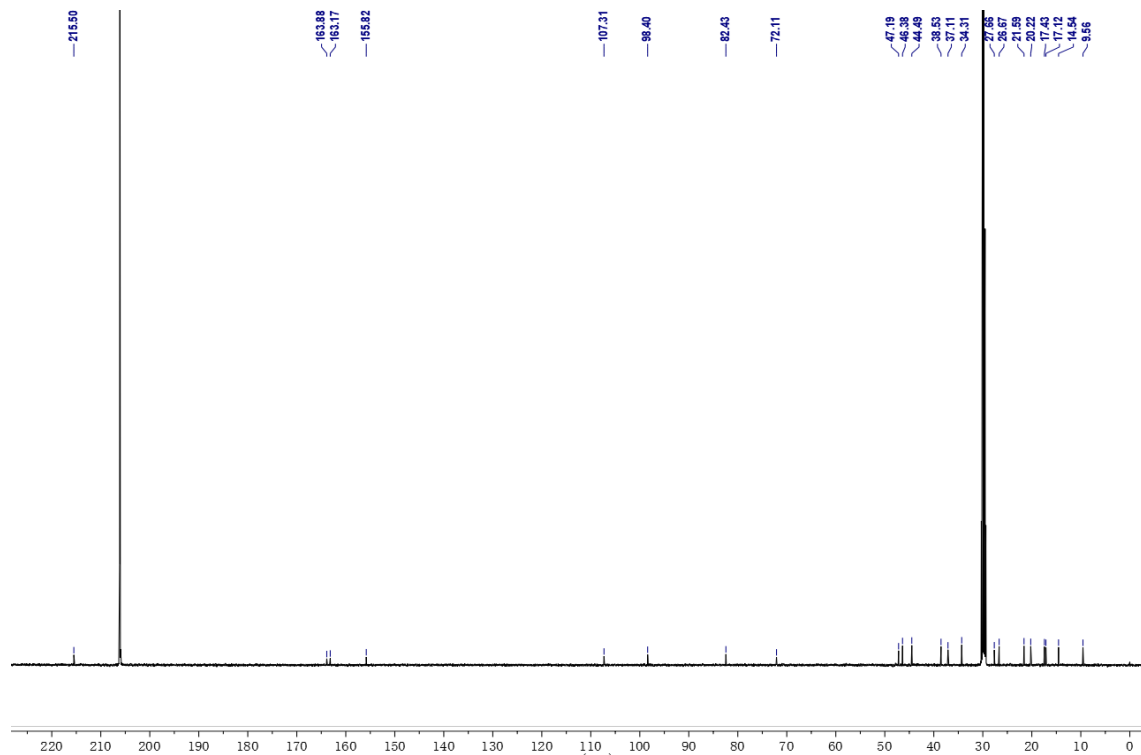


Figure S47. ^{13}C NMR spectrum of **10** (acetone- d_6 , 125 MHz).

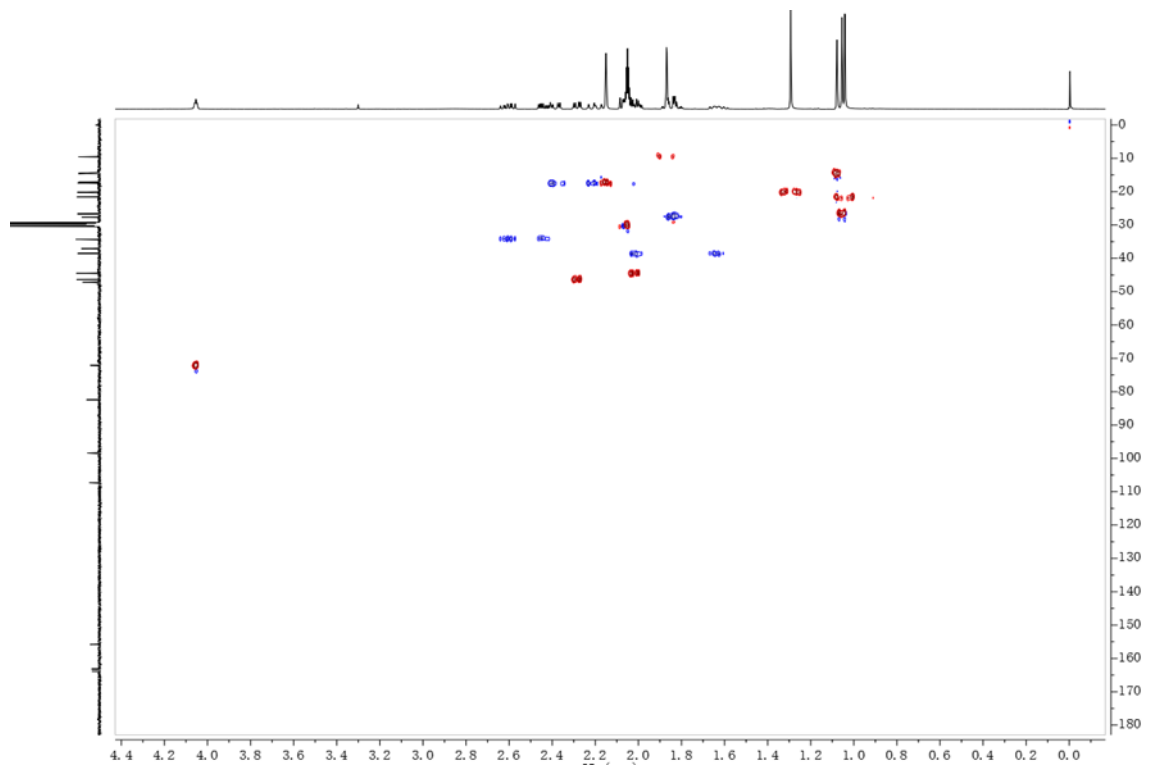


Figure S48. HSQC spectrum of 10.

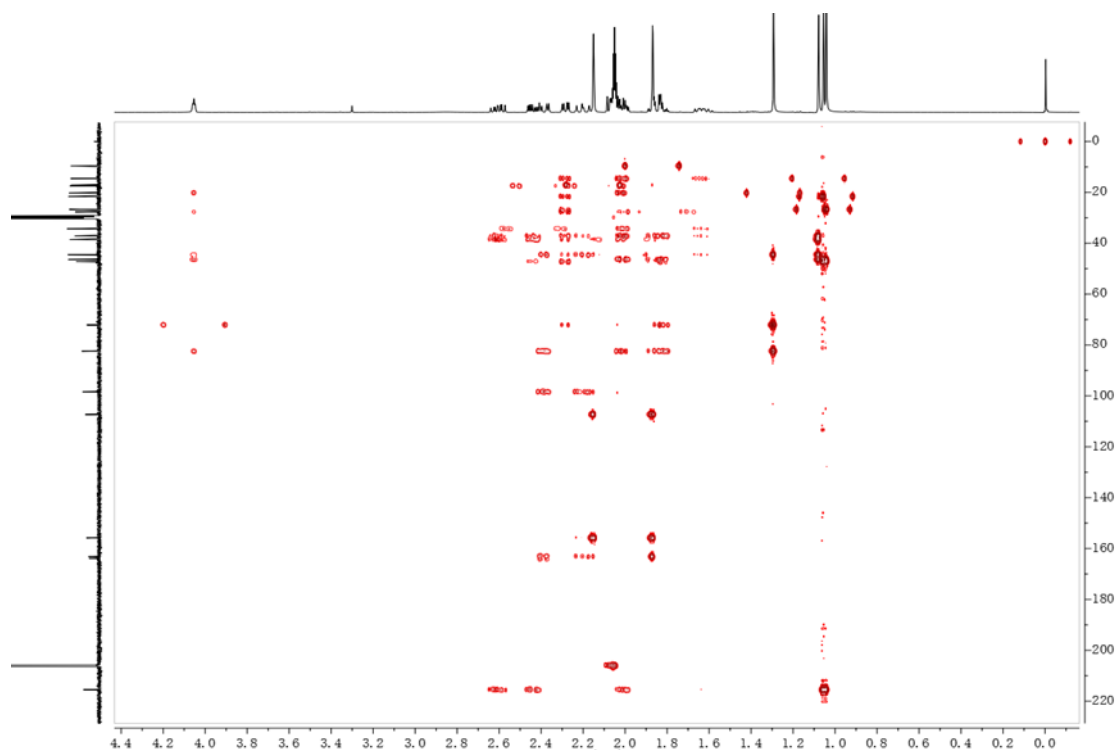


Figure S49. HMBC spectrum of 10.

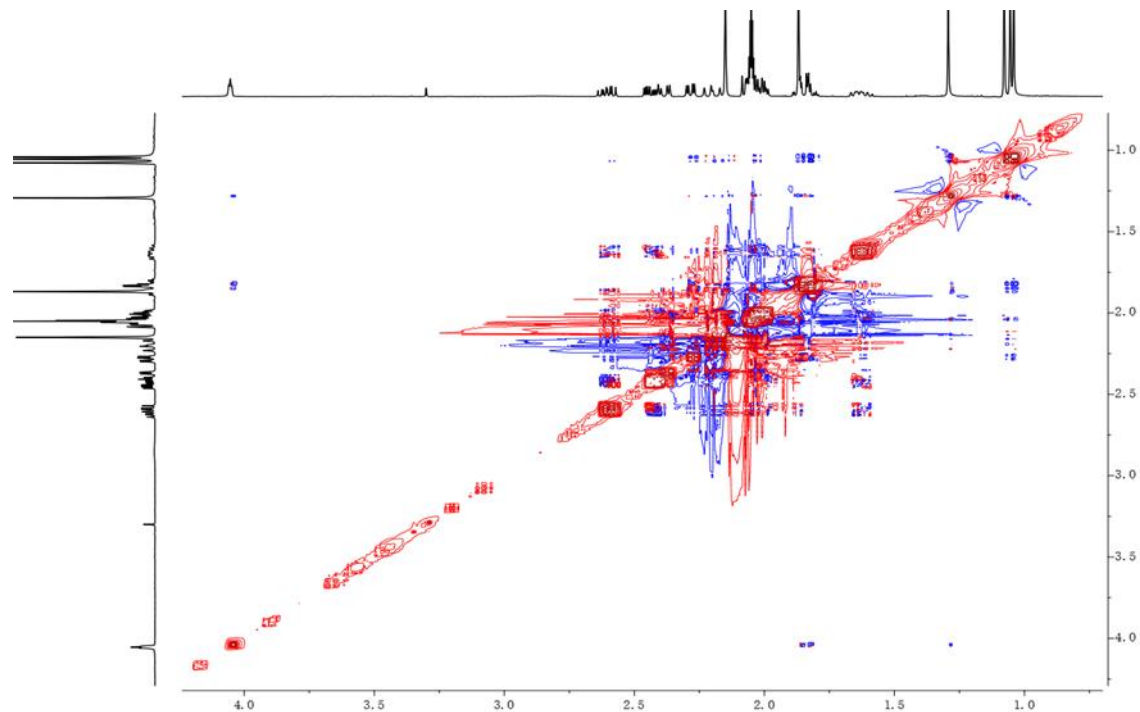


Figure S50. ROESY spectrum of **10**.

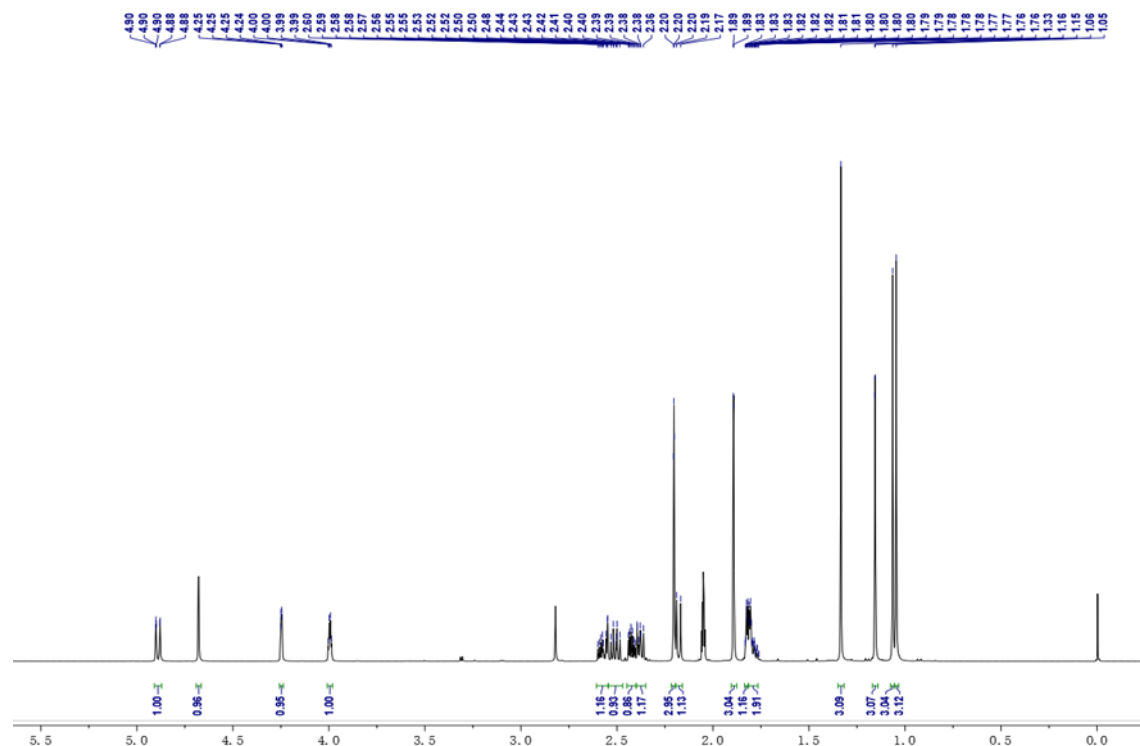


Figure S51. ^1H NMR spectrum of 11 (acetone- d_6 , 500 MHz).

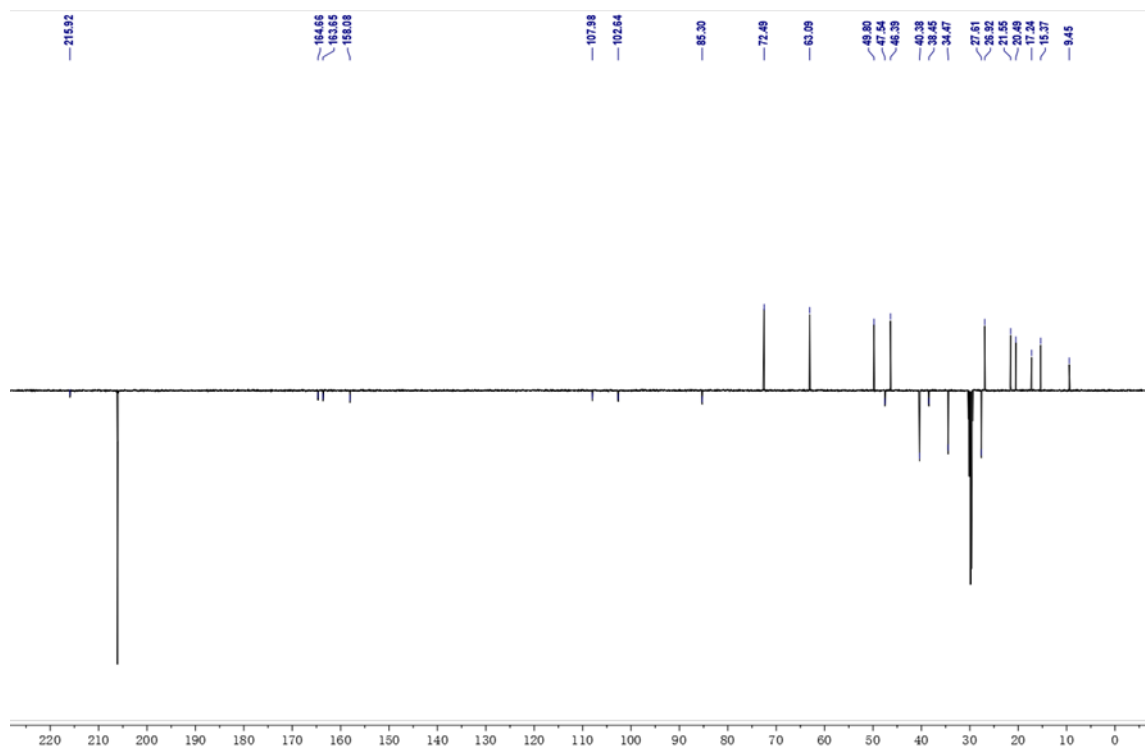


Figure S52. ¹³C NMR spectrum of 11 (acetone-*d*₆, 125 MHz).

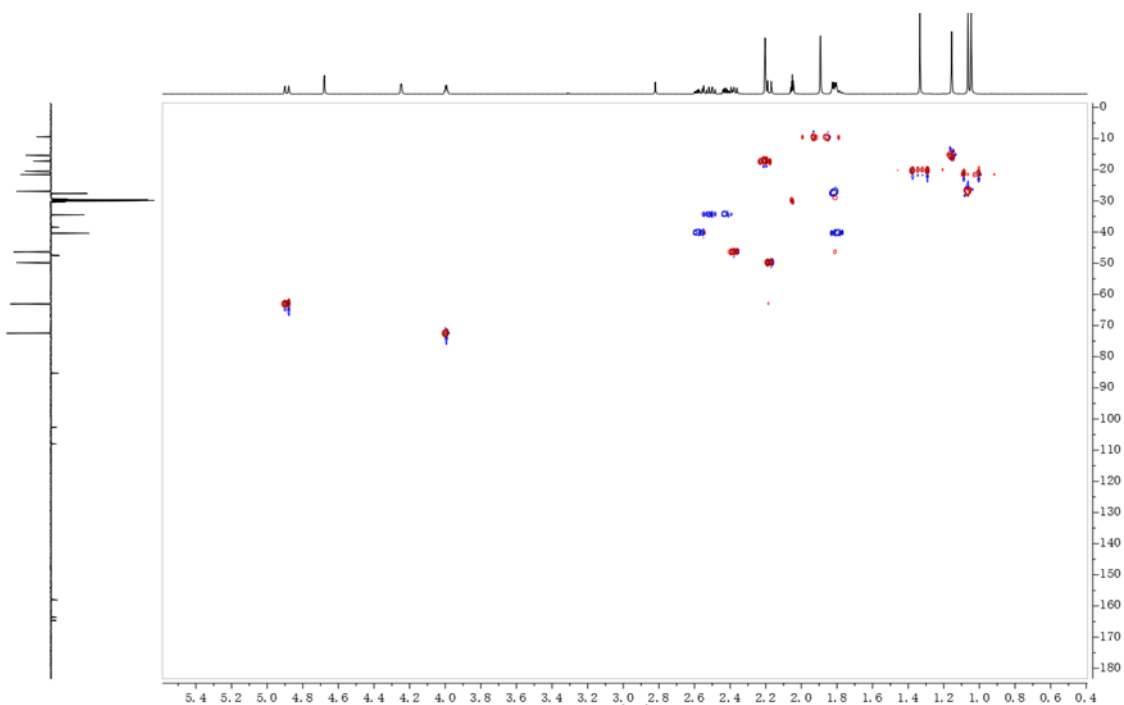


Figure S53. HSQC spectrum of 11.

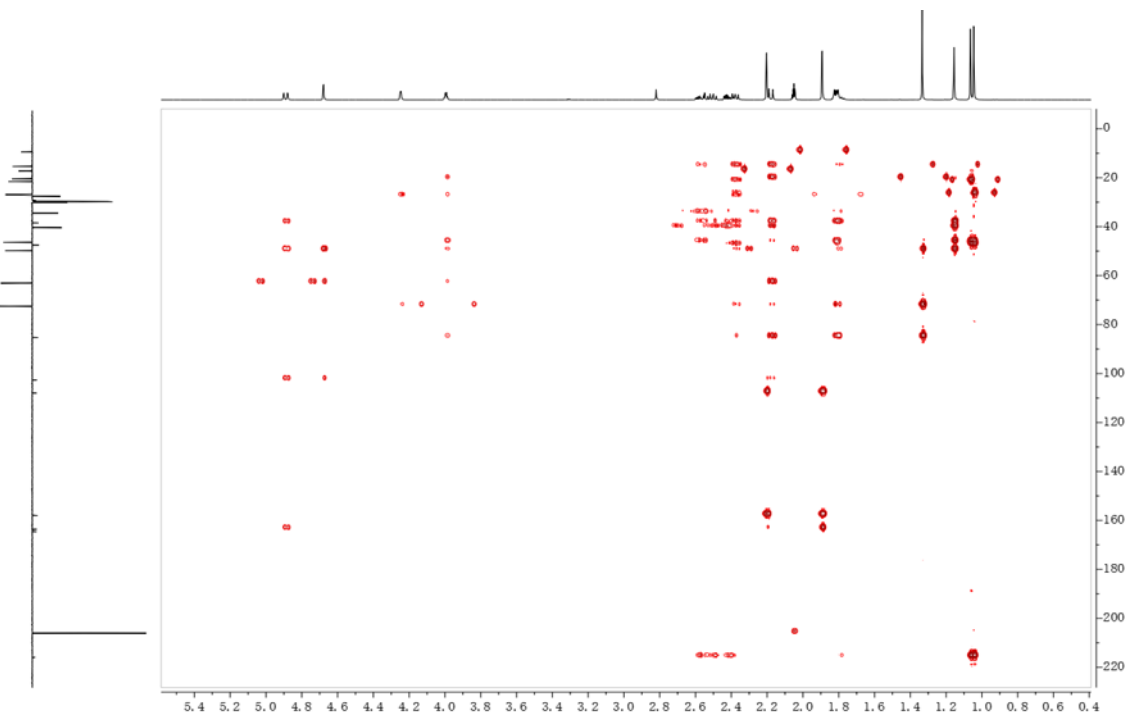


Figure S54. HMBC spectrum of 11.

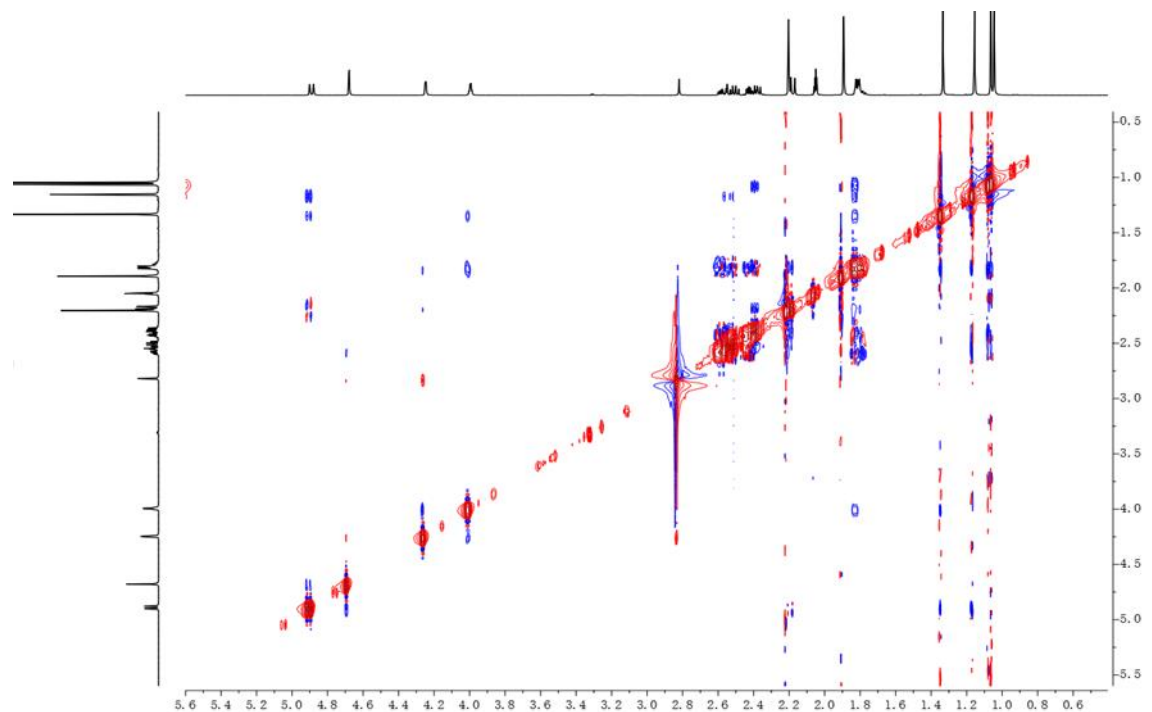


Figure S55. ROESY spectrum of 11.

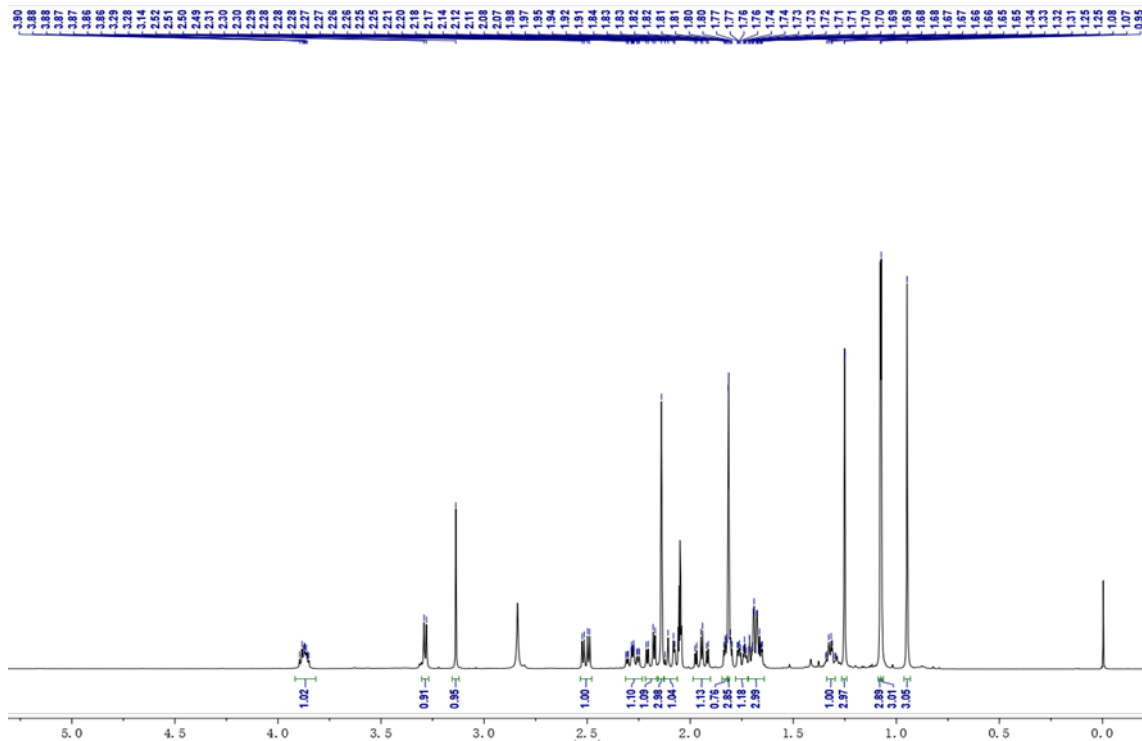


Figure S56. ^1H NMR spectrum of 12 (acetone- d_6 , 500 MHz).

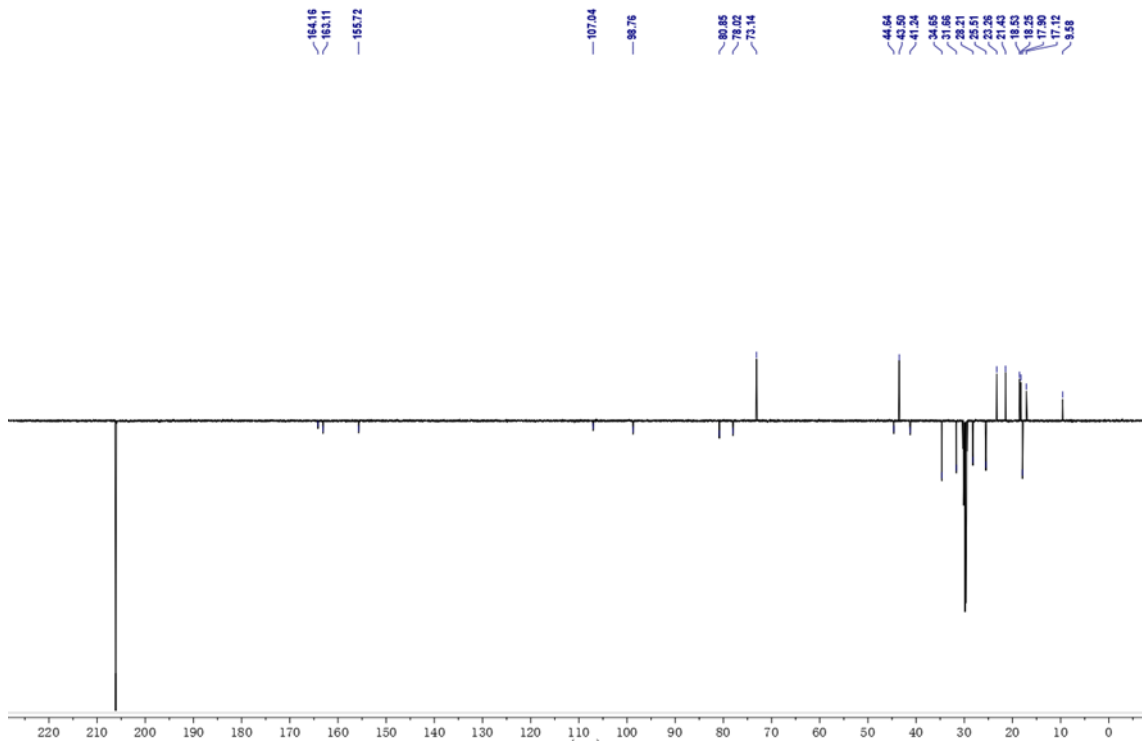


Figure S57. ^{13}C NMR spectrum of **12** (acetone- d_6 , 125 MHz).

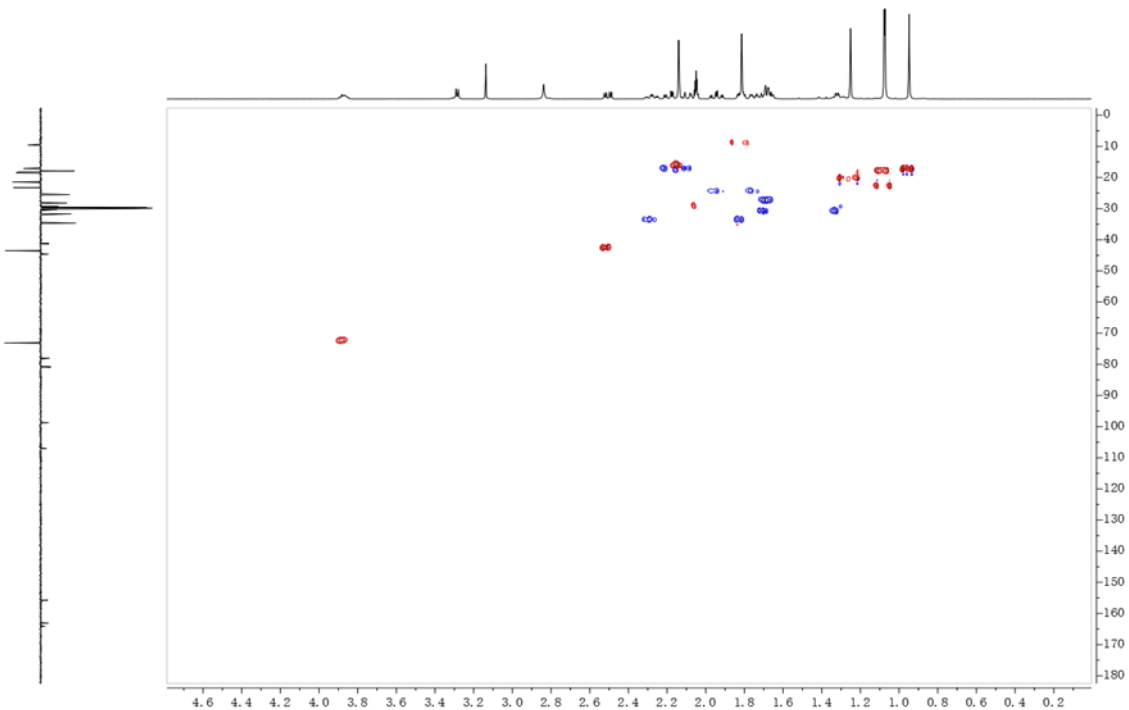


Figure S58. HSQC spectrum of 12.

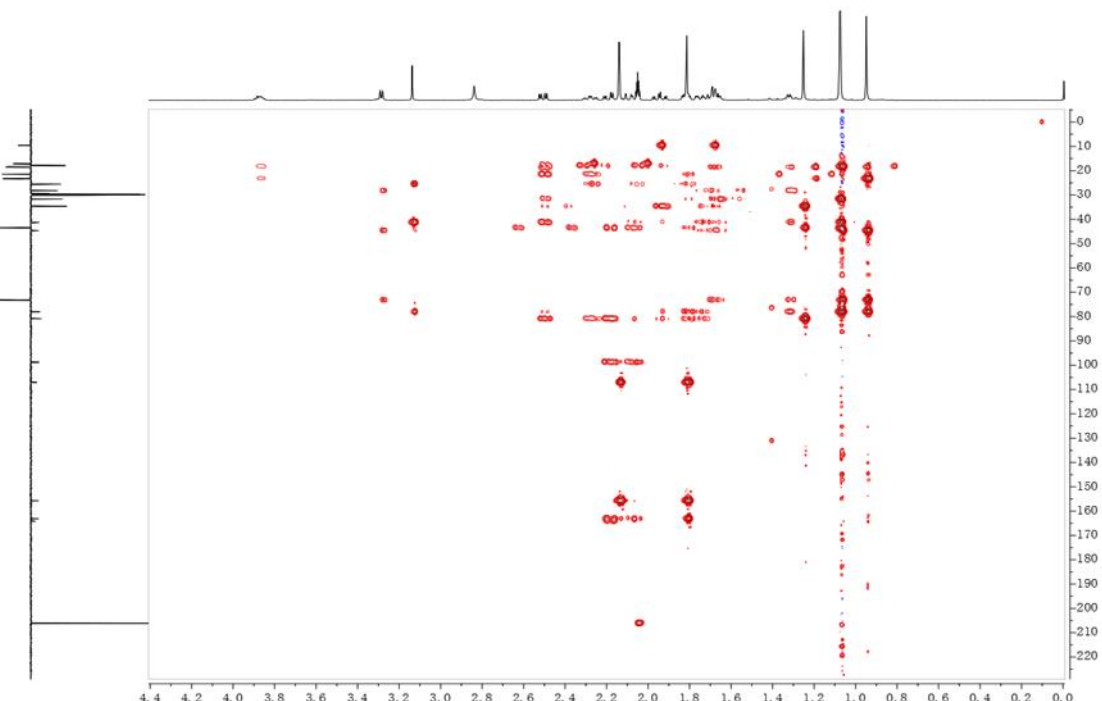


Figure S59. HMBC spectrum of 12.

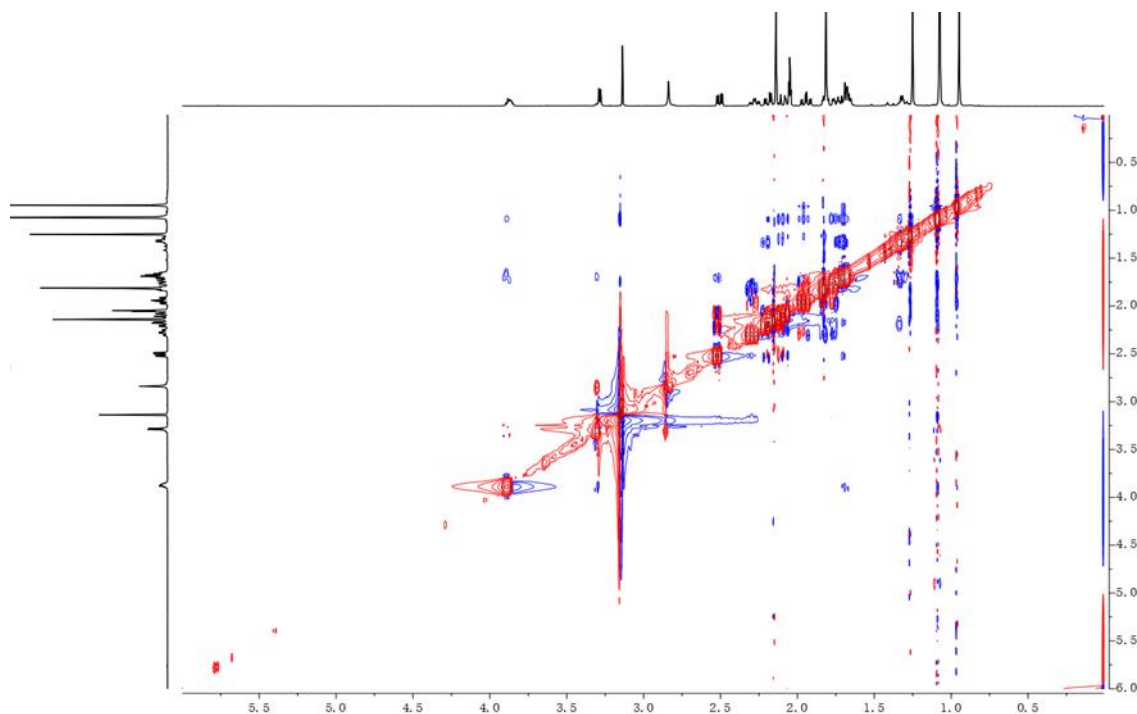


Figure S60. ROESY spectrum of 12.

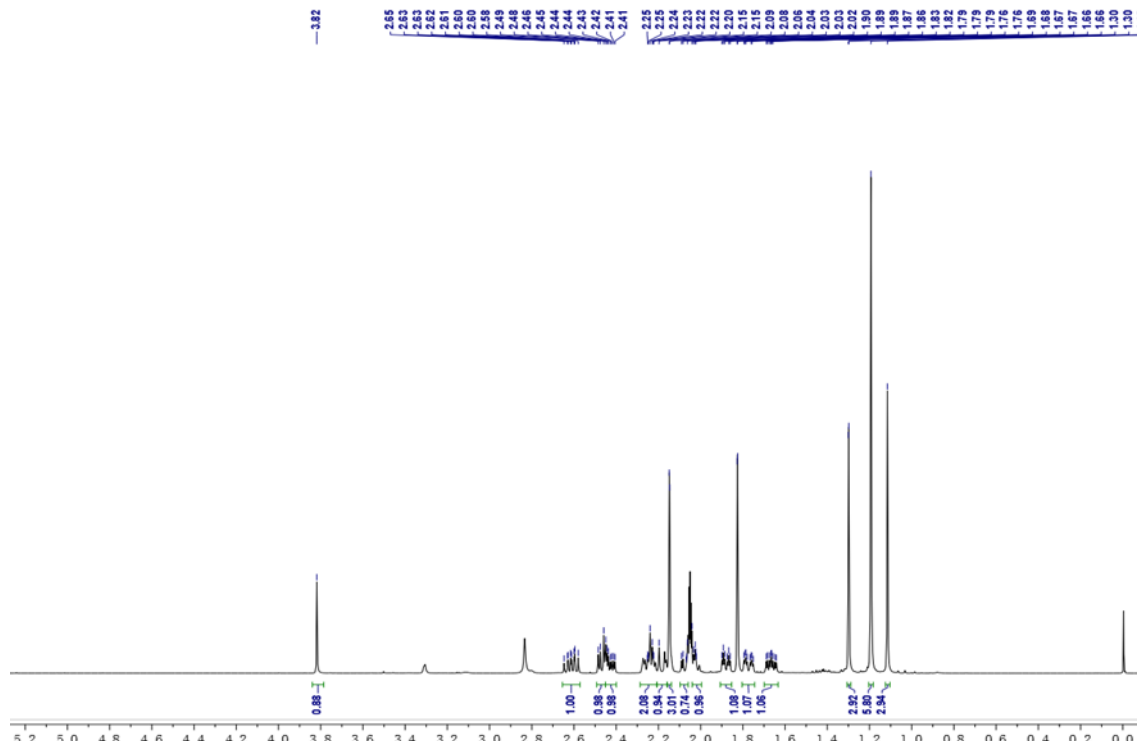


Figure S61. ^1H NMR spectrum of 13 (acetone- d_6 , 500 MHz).

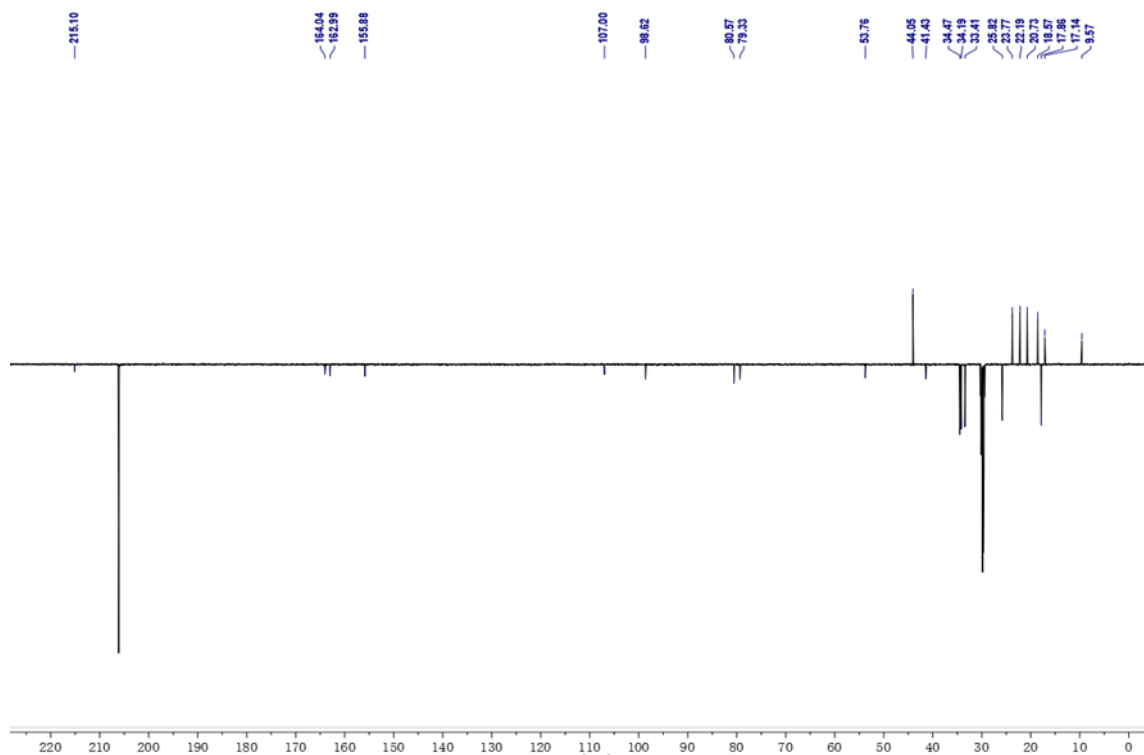


Figure S62. ^{13}C NMR spectrum of 13 (acetone- d_6 , 125 MHz).

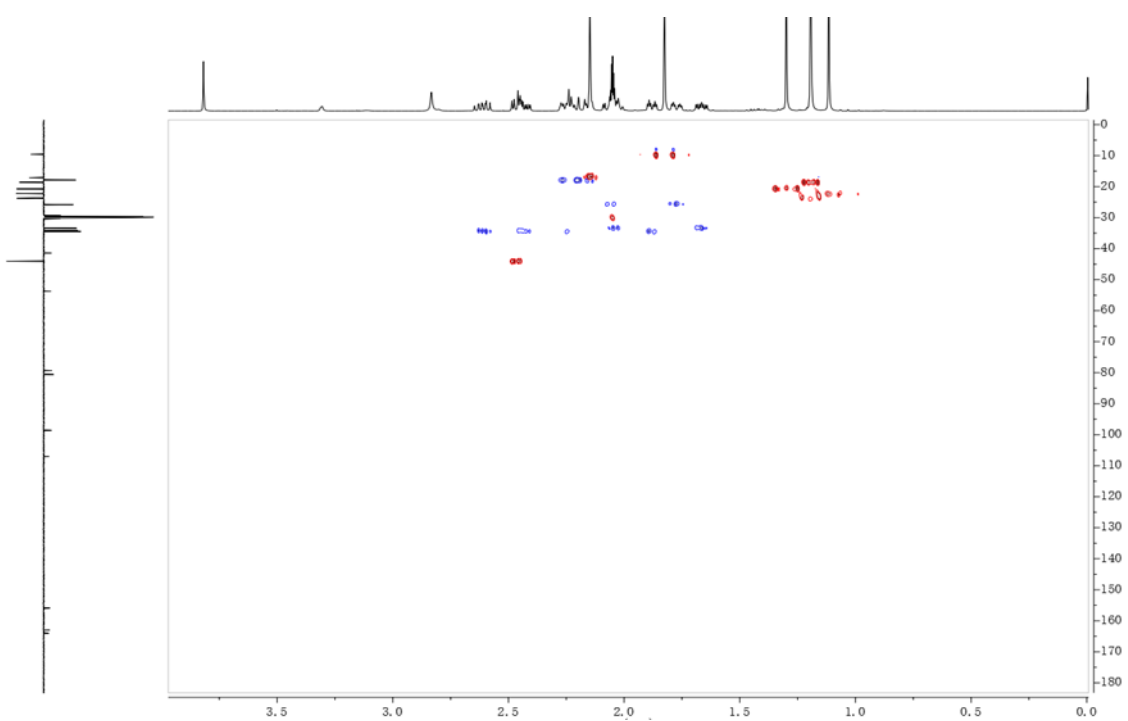


Figure S63. HSQC spectrum of 13.

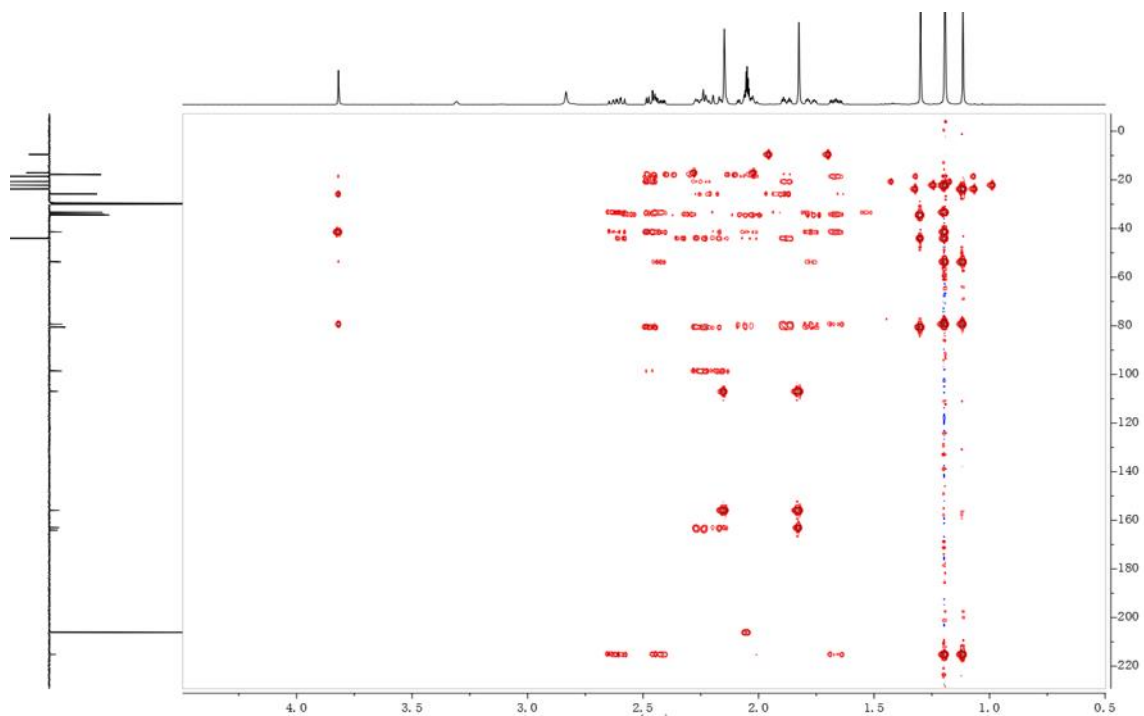


Figure S64. HMBC spectrum of 13.

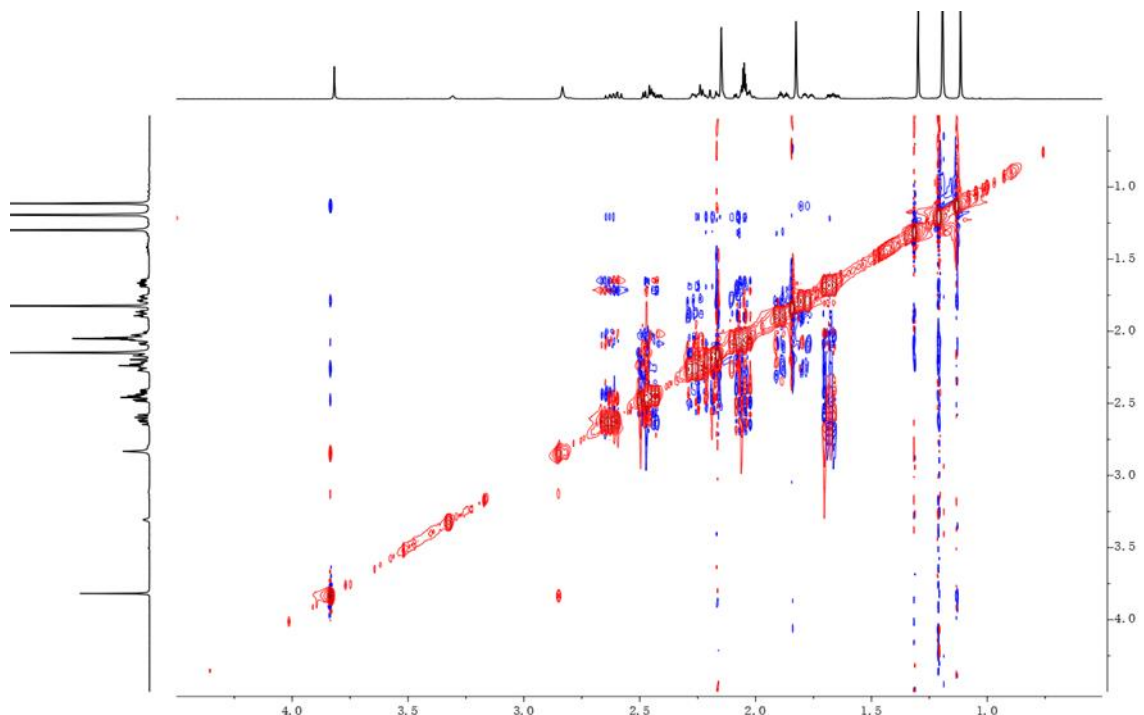


Figure S65. ROESY spectrum of 13.

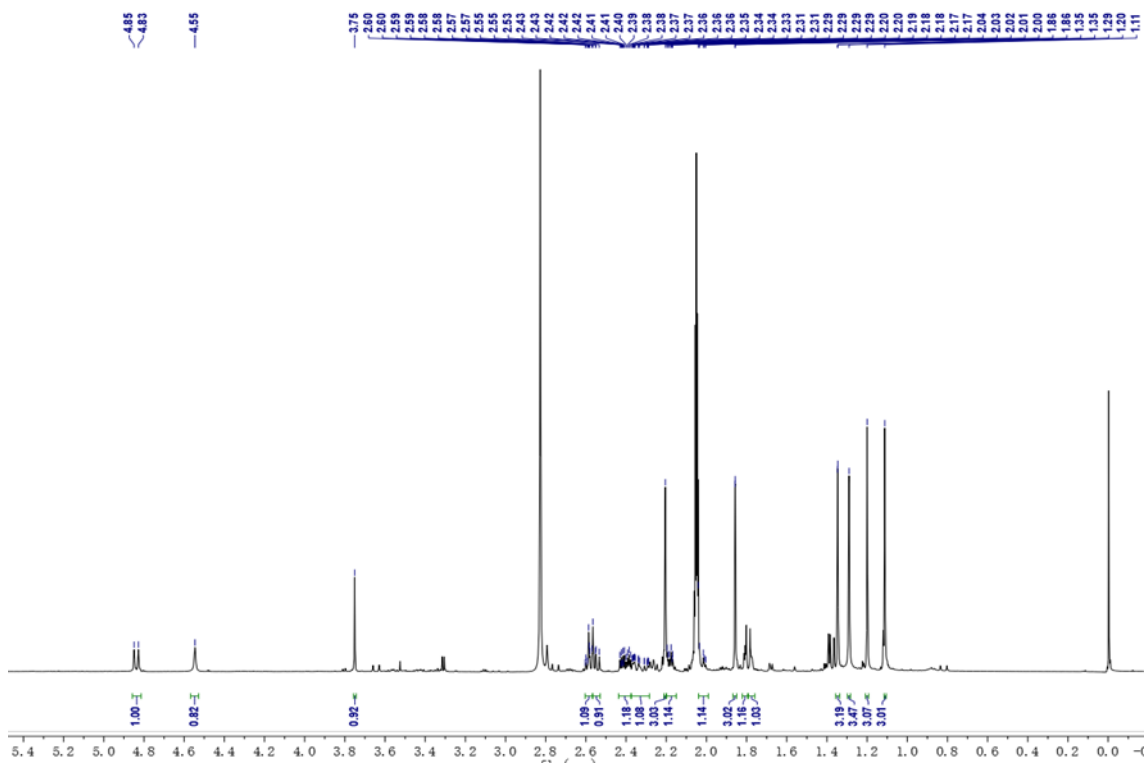


Figure S66. ^1H NMR spectrum of 14 (acetone- d_6 , 500 MHz).

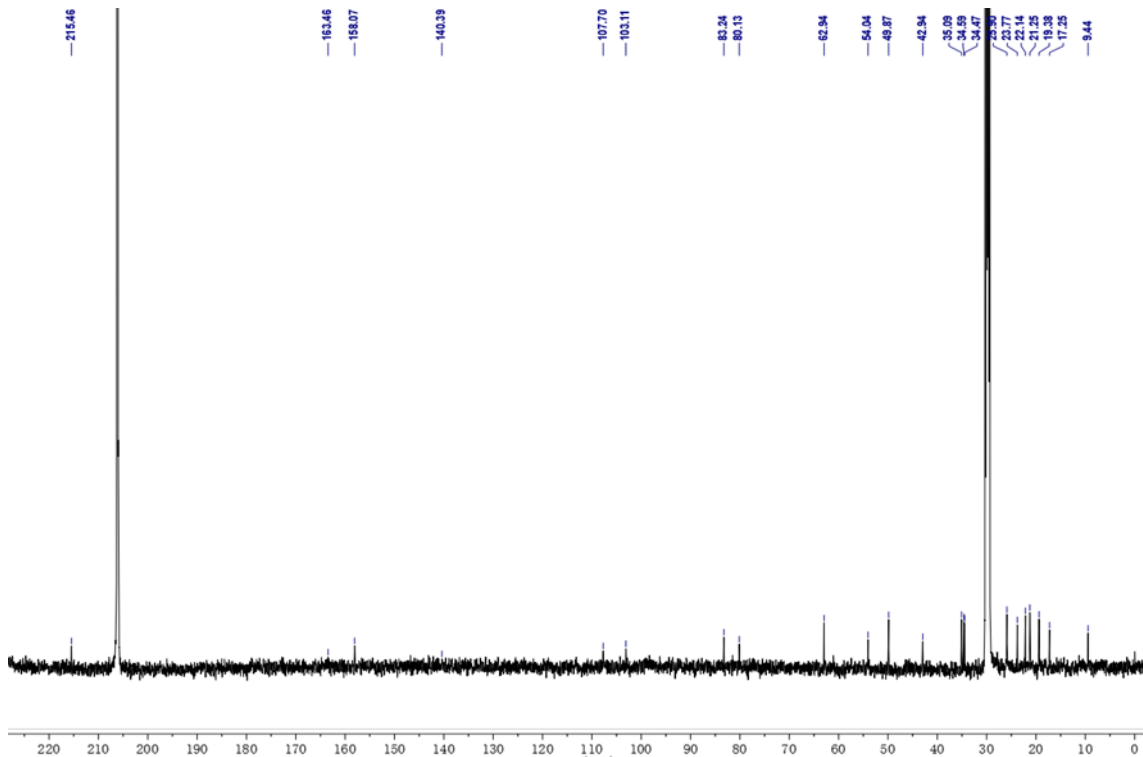


Figure S67. ^{13}C NMR spectrum of 14 (acetone- d_6 , 125 MHz).

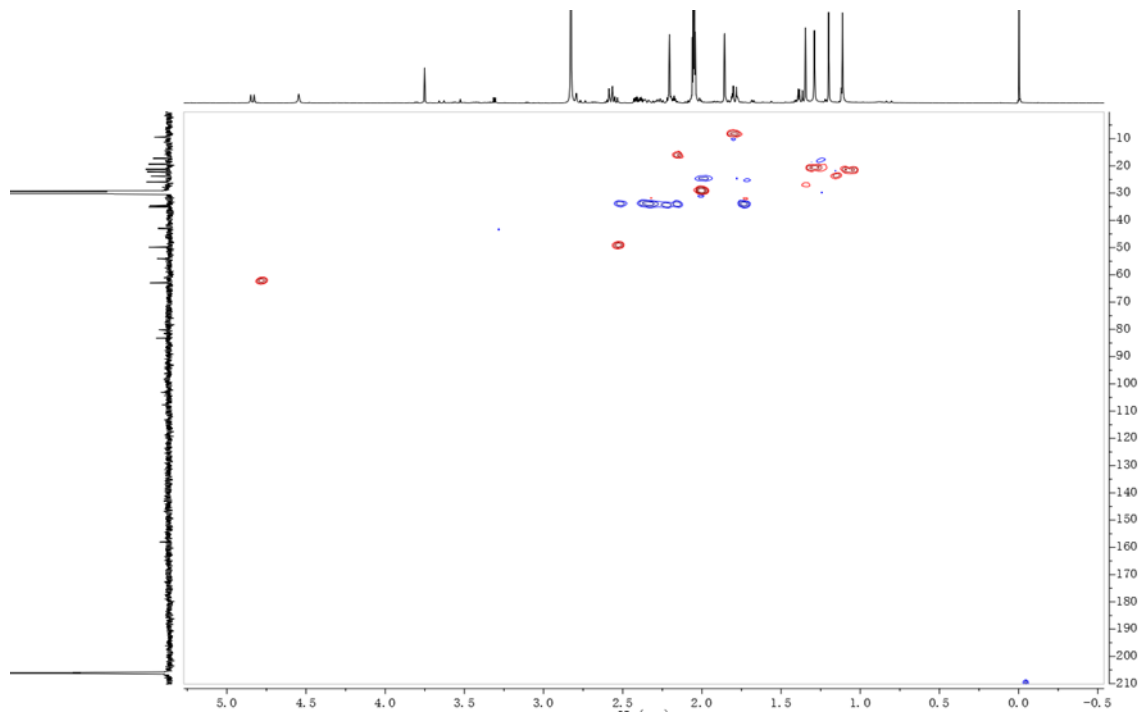


Figure S68. HSQC spectrum of 14.

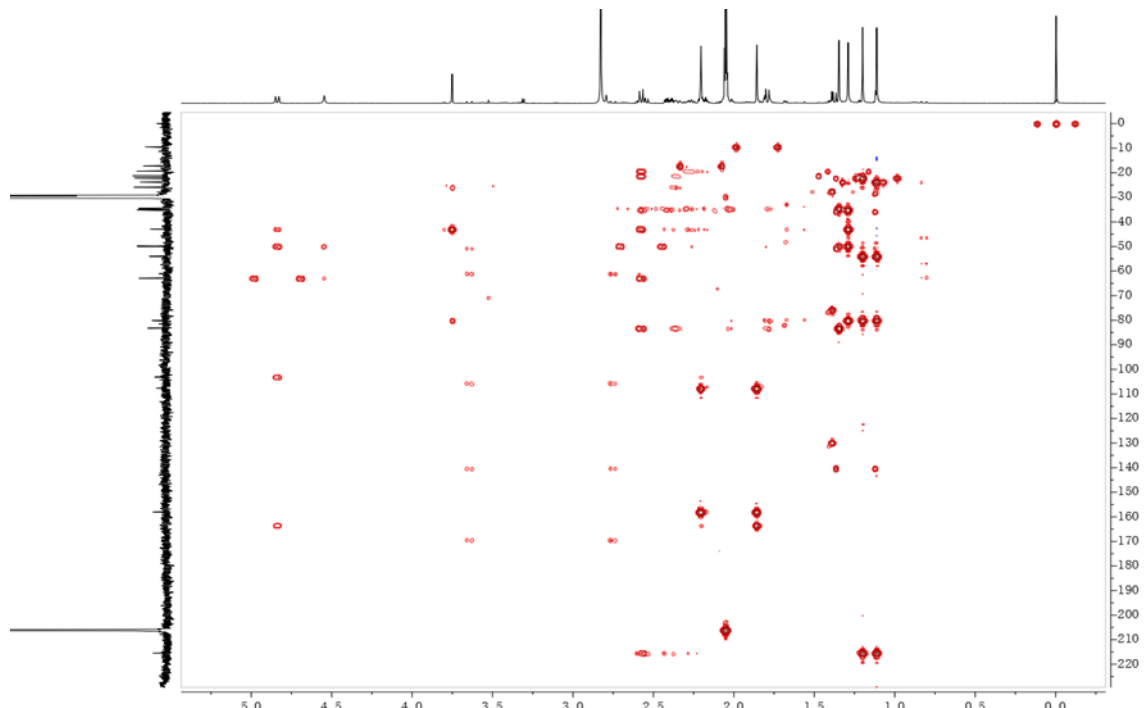


Figure S69. HMBC spectrum of 14.

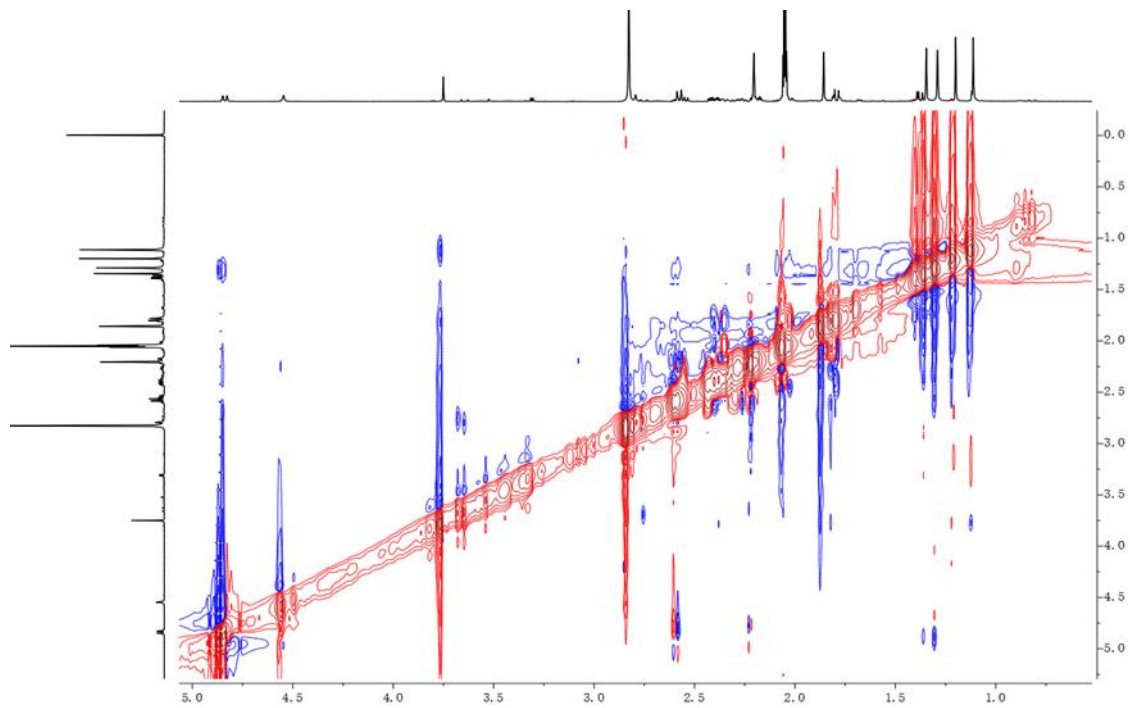


Figure S70. ROESY spectrum of 14.

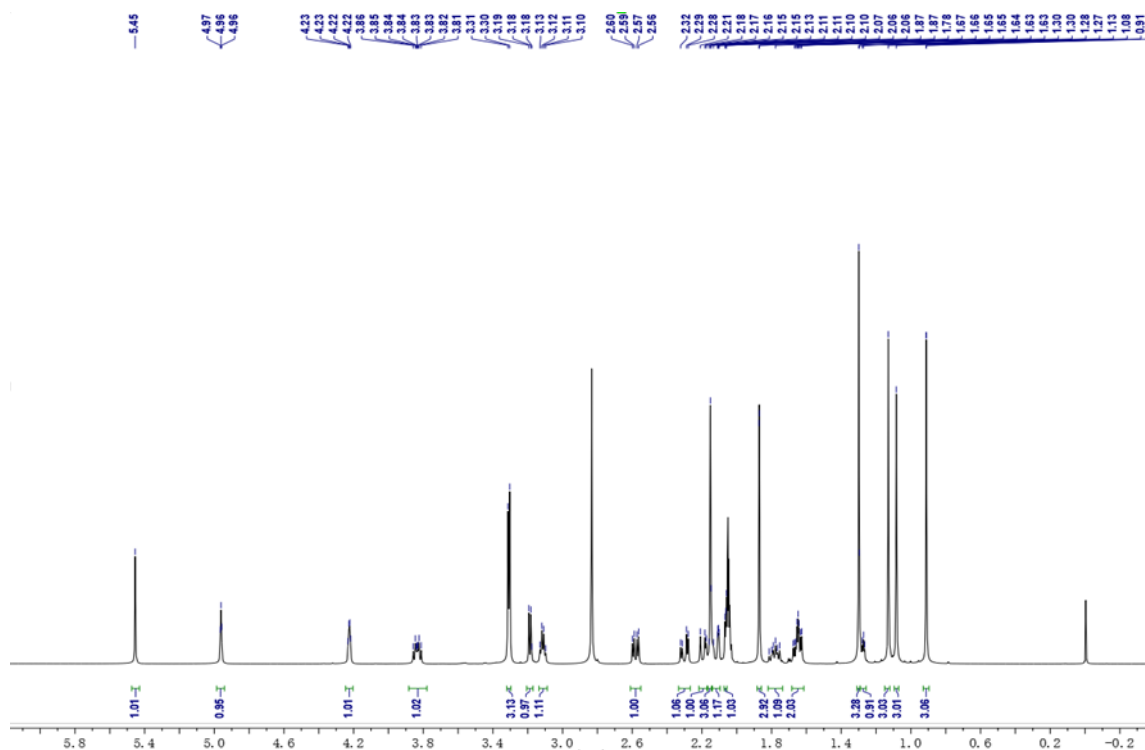


Figure S71. ^1H NMR spectrum of 15 (acetone- d_6 , 500 MHz).

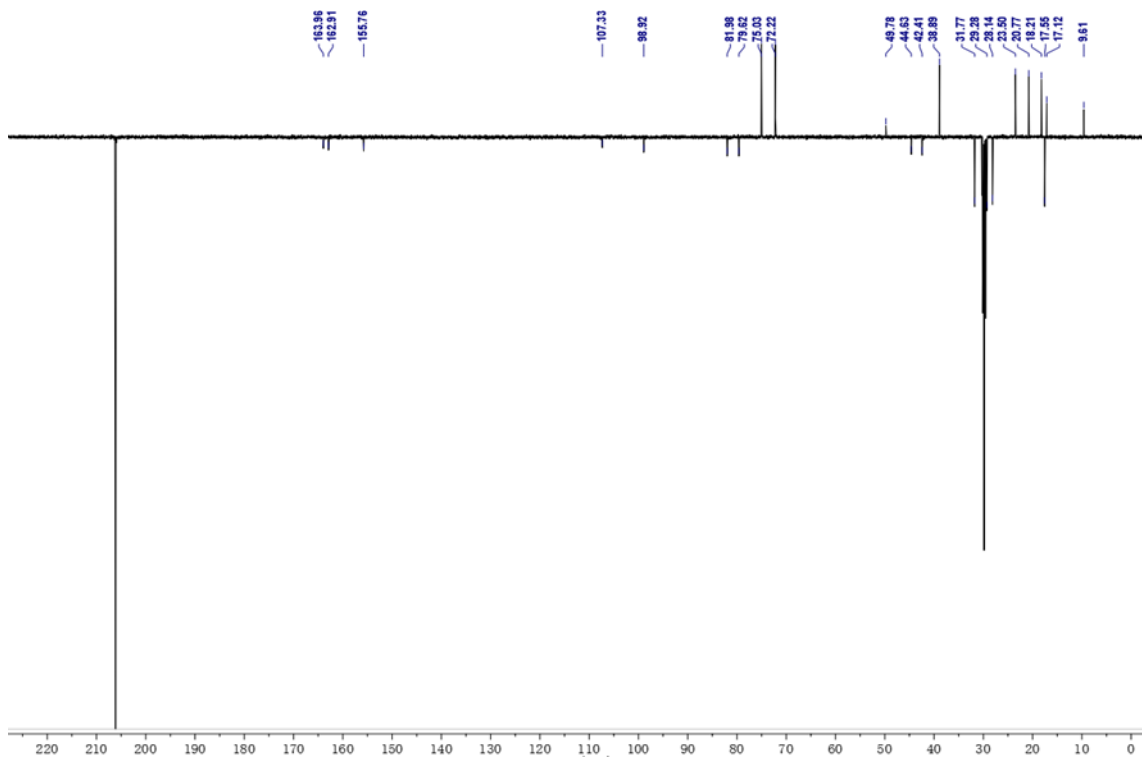


Figure S72. ¹³C NMR spectrum of 15 (acetone-*d*₆, 125 MHz).

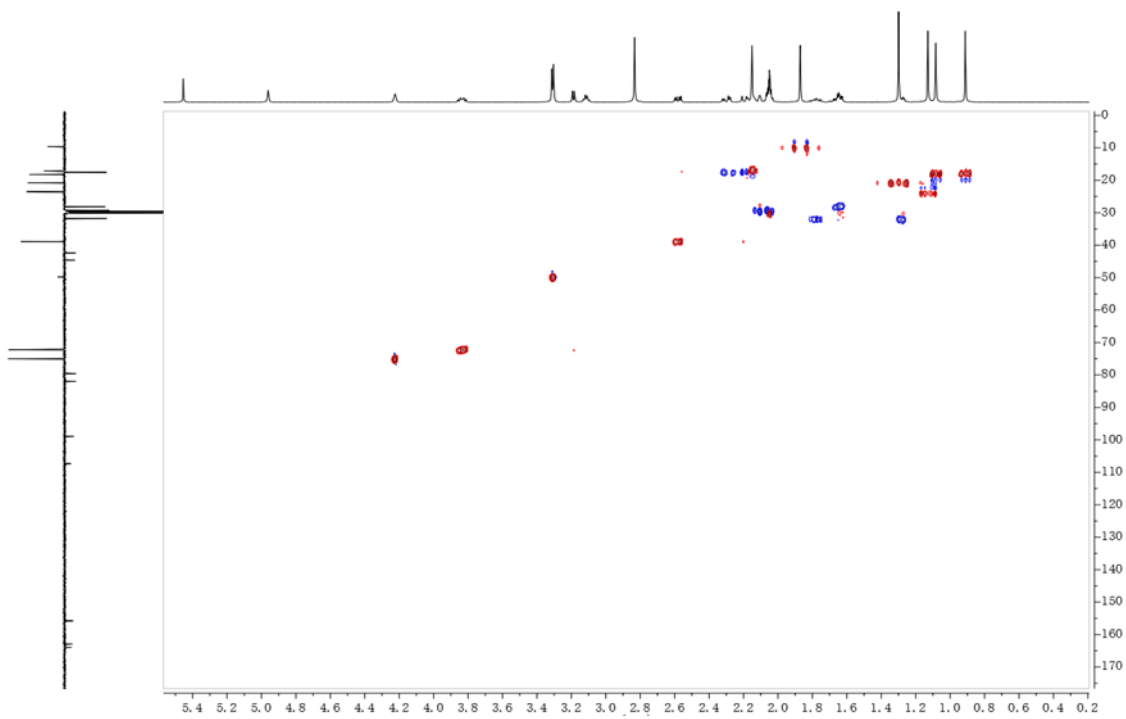


Figure S73. HSQC spectrum of 15.

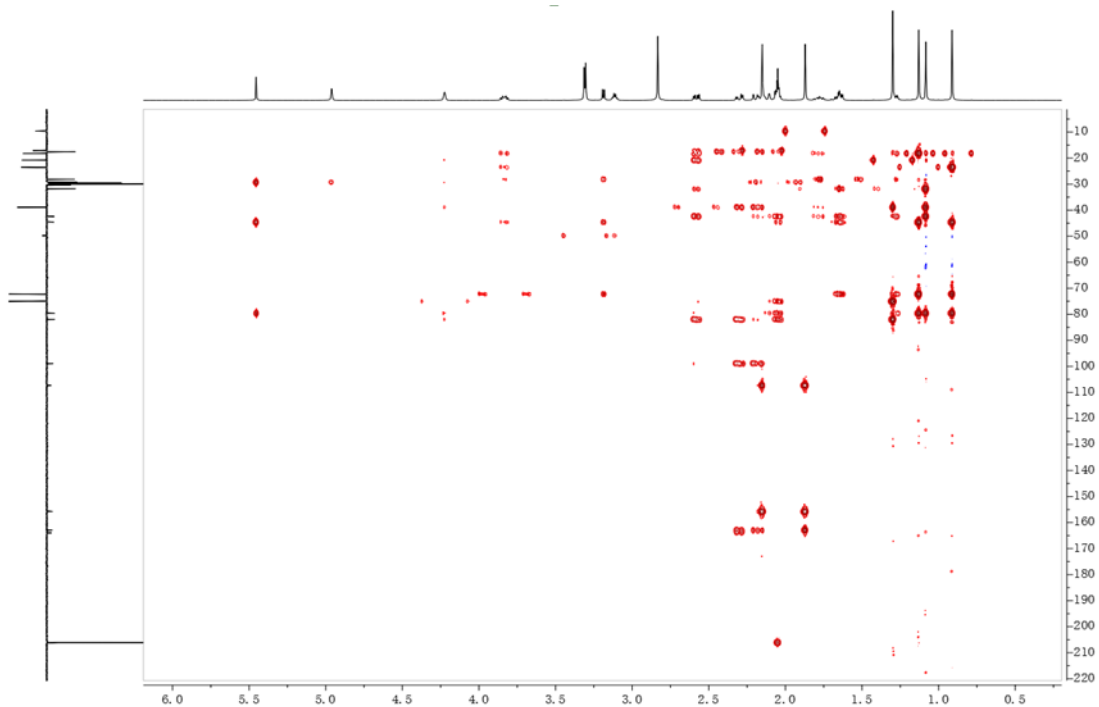


Figure S74. HMBC spectrum of 15.

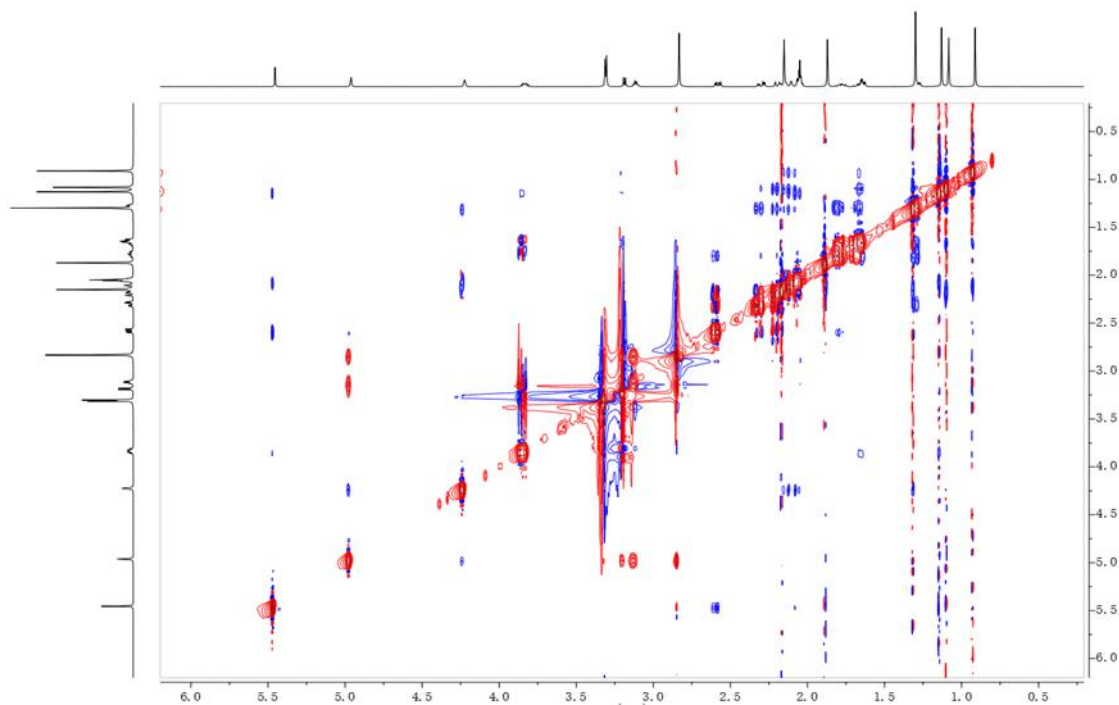


Figure S75. ROESY spectrum of 15.

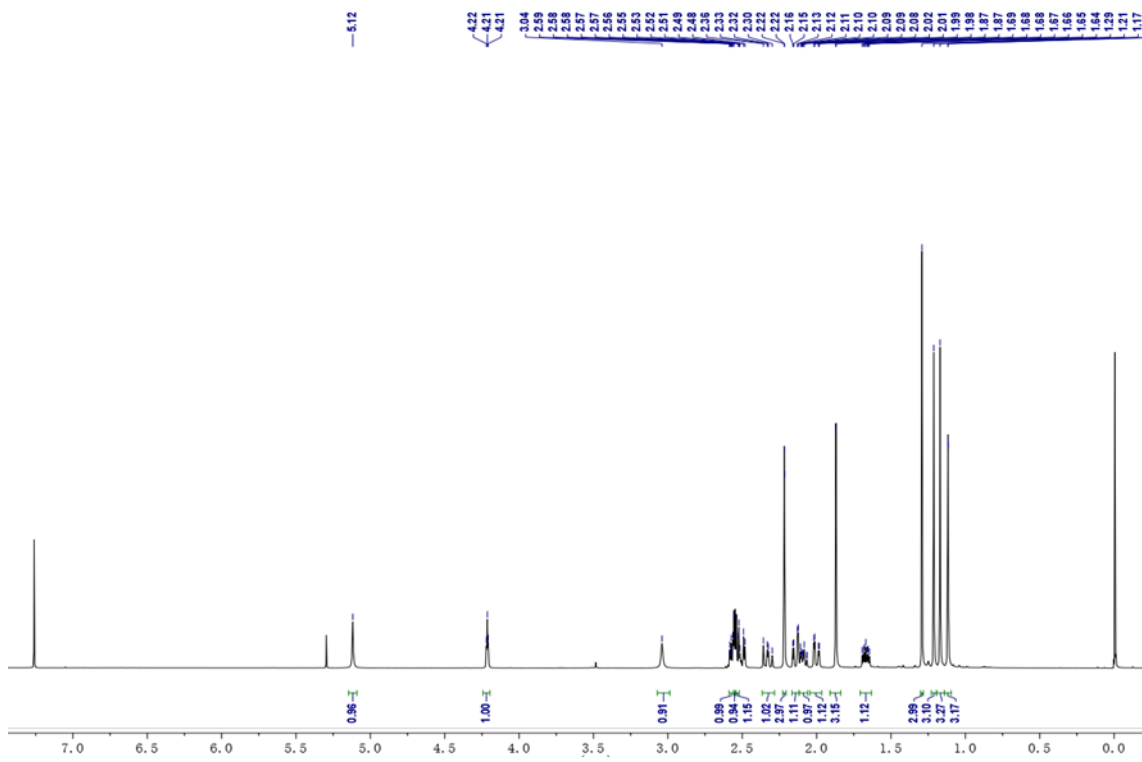


Figure S76. ^1H NMR spectrum of 16 (chloroform-*d*, 500 MHz).

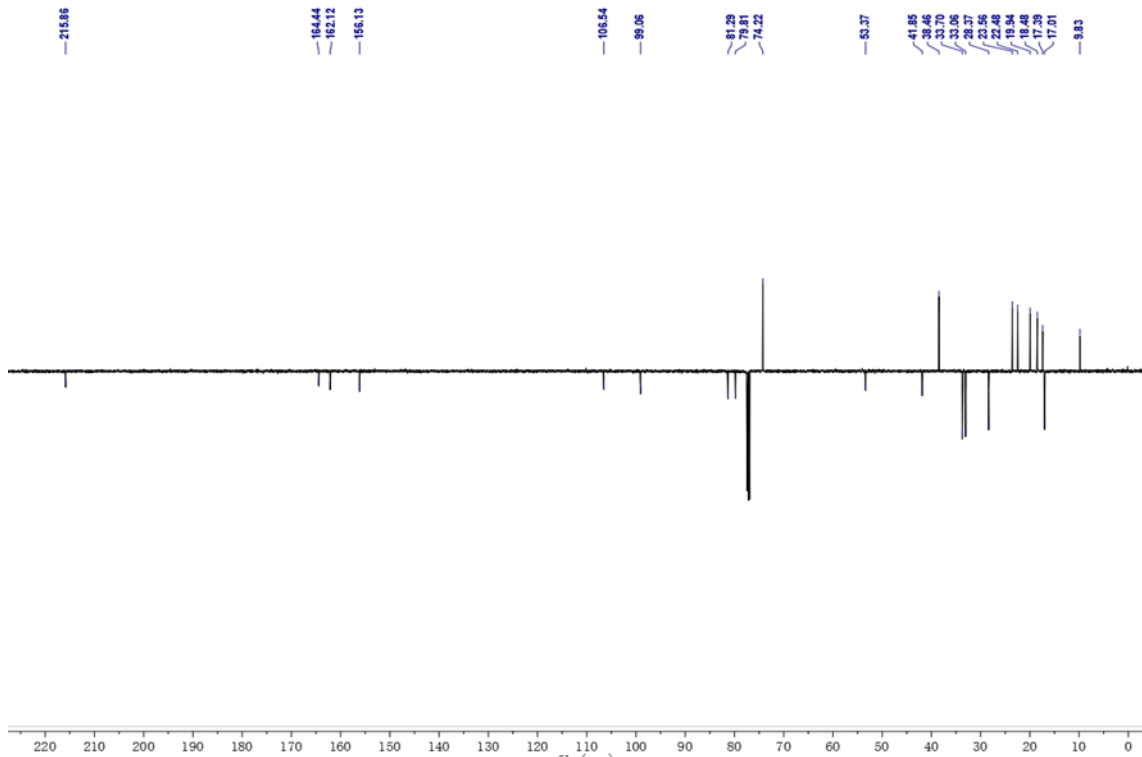


Figure S77. ^{13}C NMR spectrum of 16 (chloroform-*d*, 125 MHz).

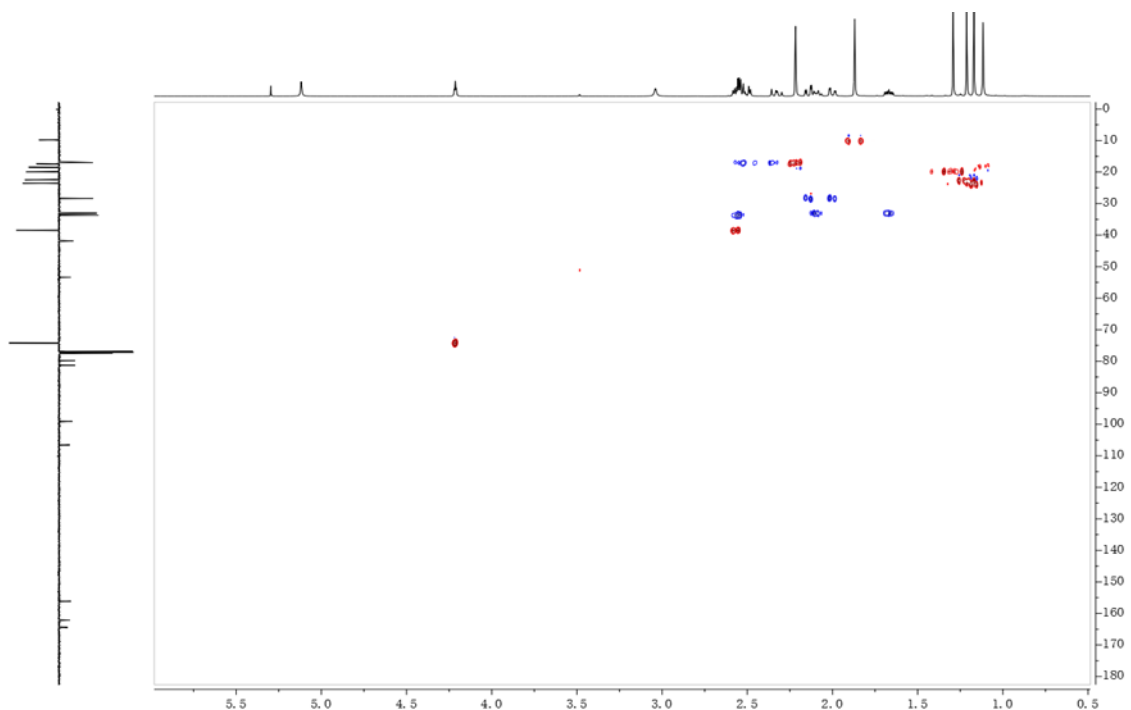


Figure S78. HSQC spectrum of 16.

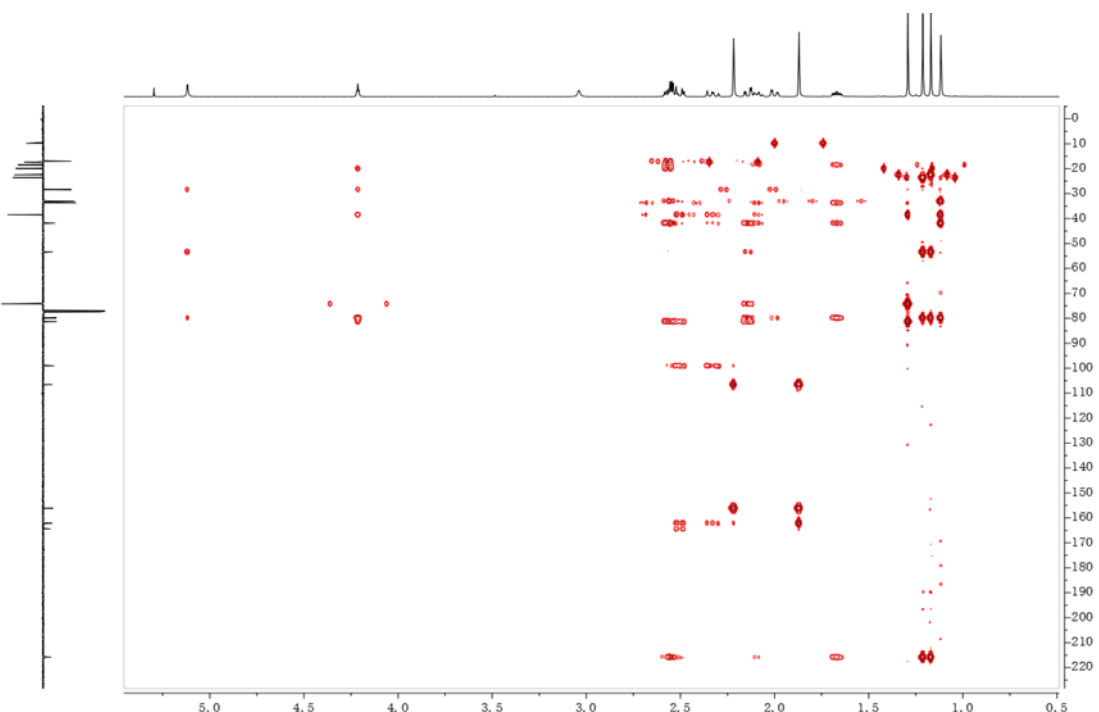


Figure S79. HMBC spectrum of 16.

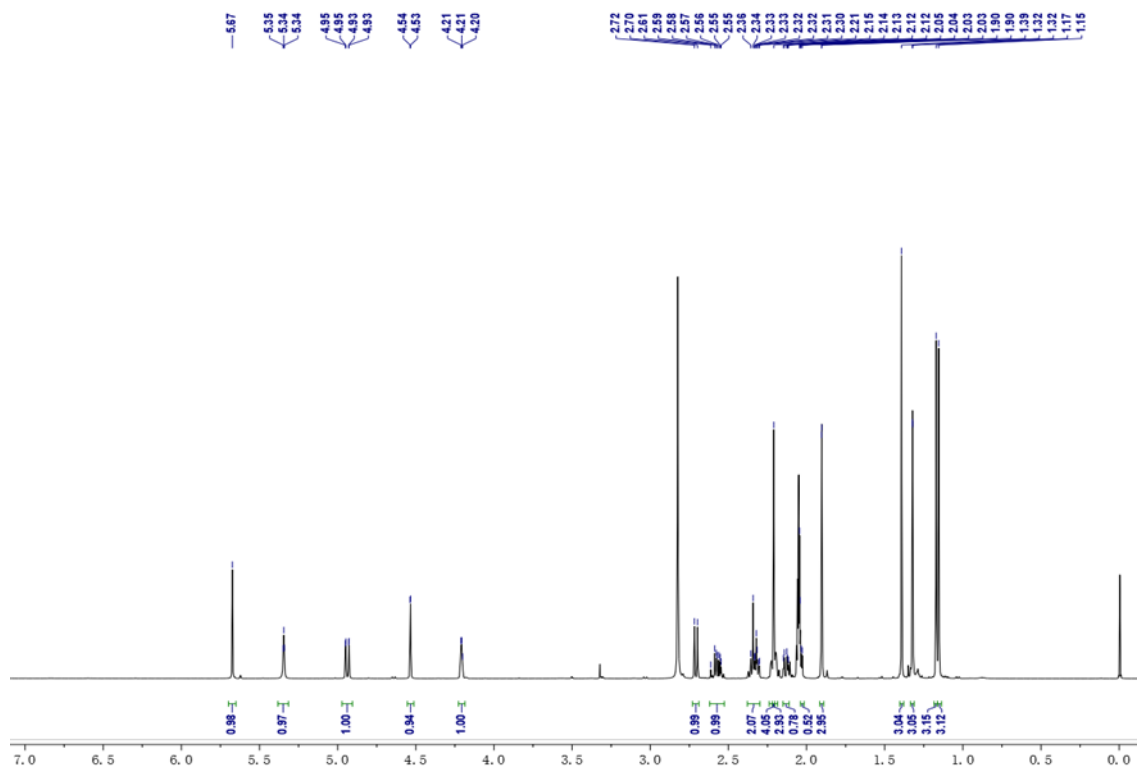


Figure S80. ^1H NMR spectrum of 17 (acetone- d_6 , 500 MHz).

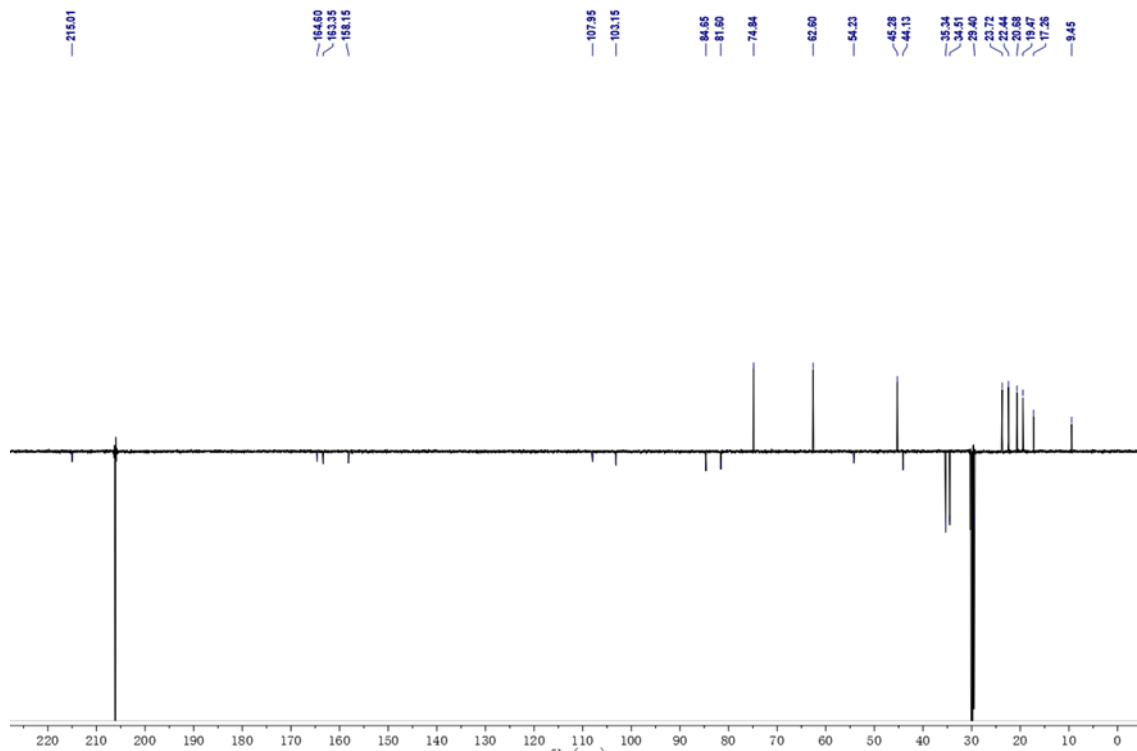


Figure S81. ^{13}C NMR spectrum of 17 (acetone- d_6 , 125 MHz).

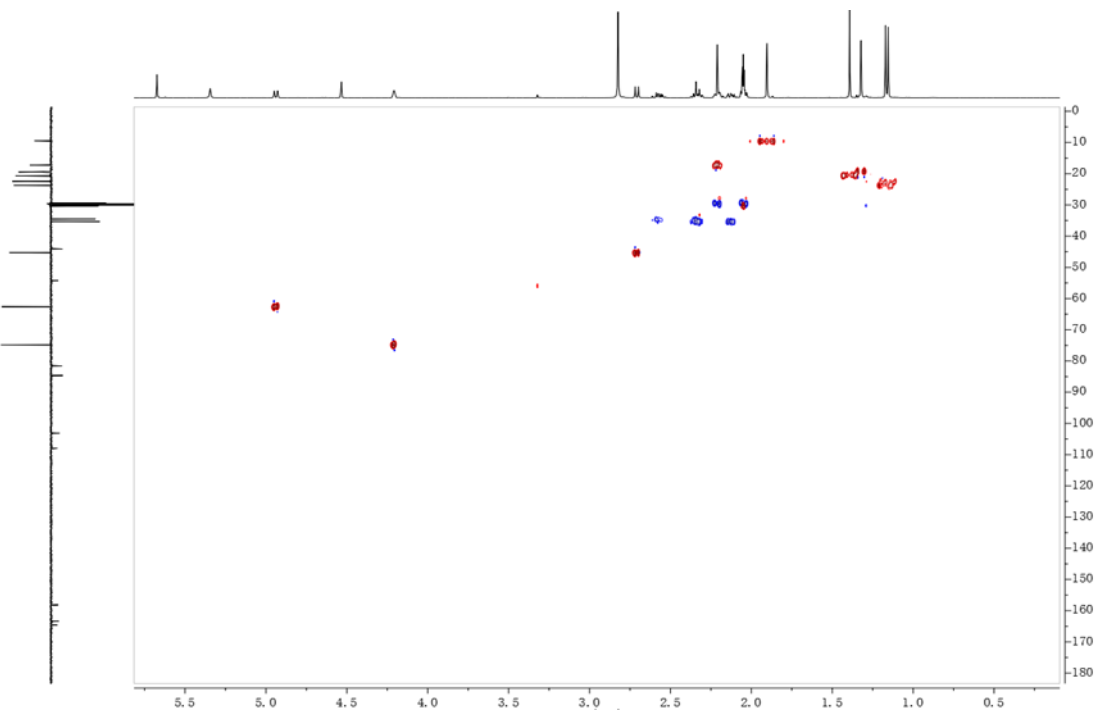


Figure S82. HSQC spectrum of 17.

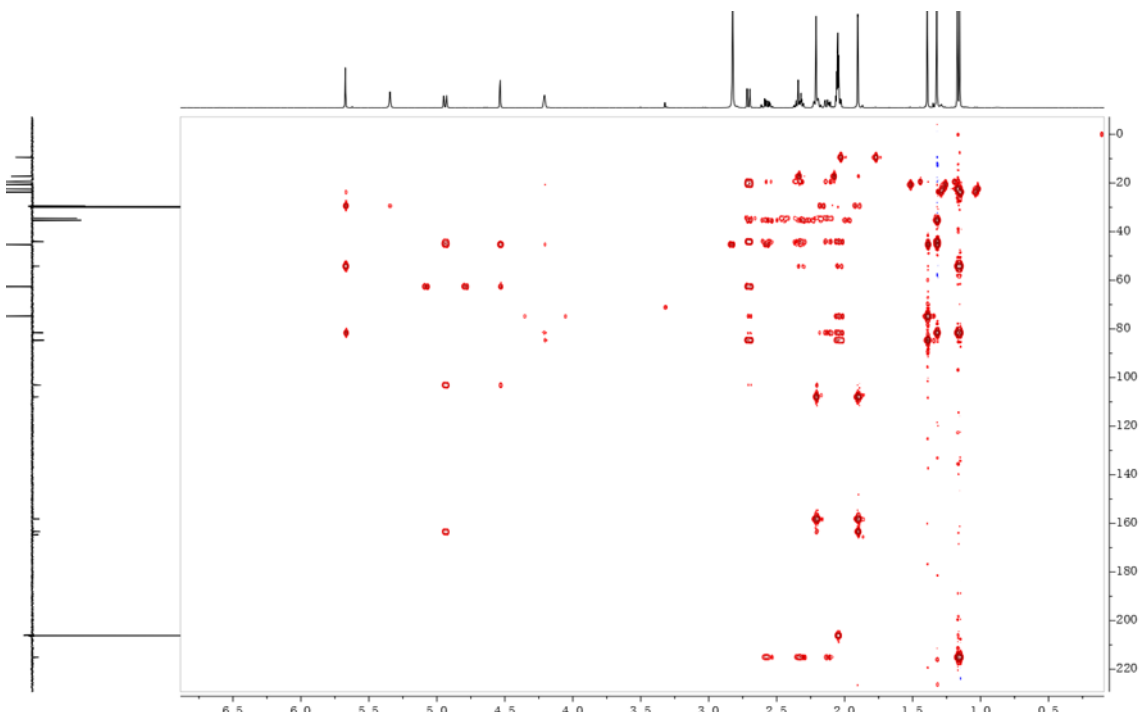


Figure S83. HMBC spectrum of 17.

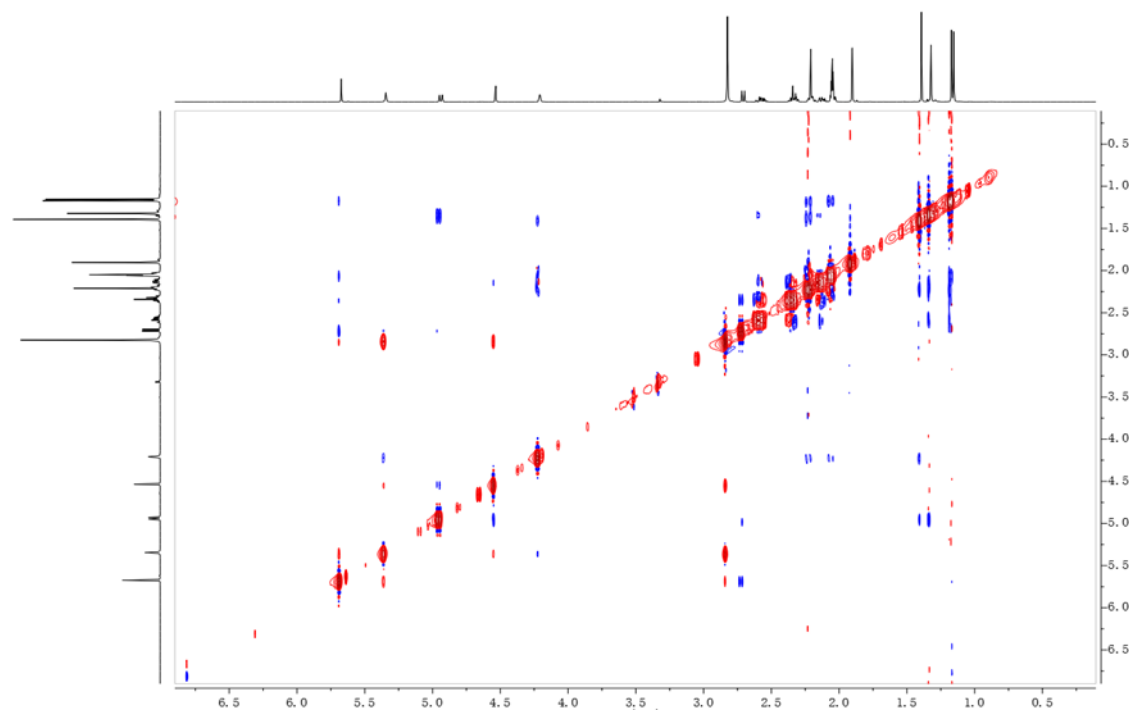


Figure S84. ROESY spectrum of 17.

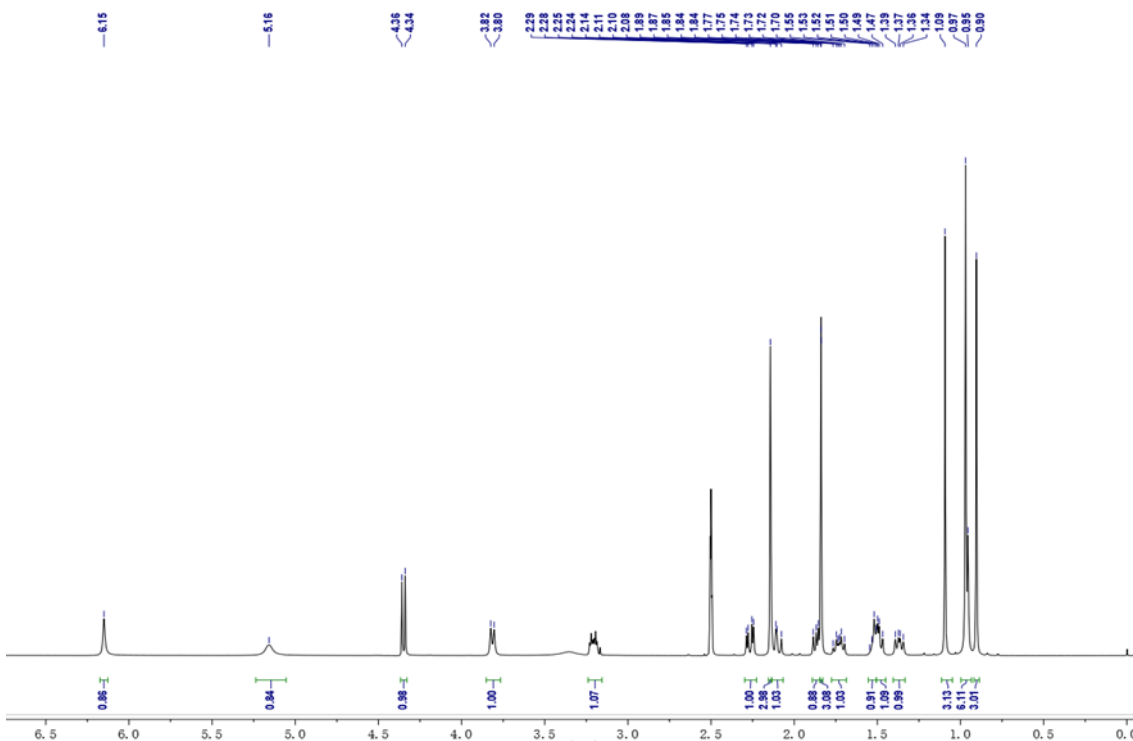


Figure S85. ^1H NMR spectrum of 19 (DMSO- d_6 , 500 MHz).

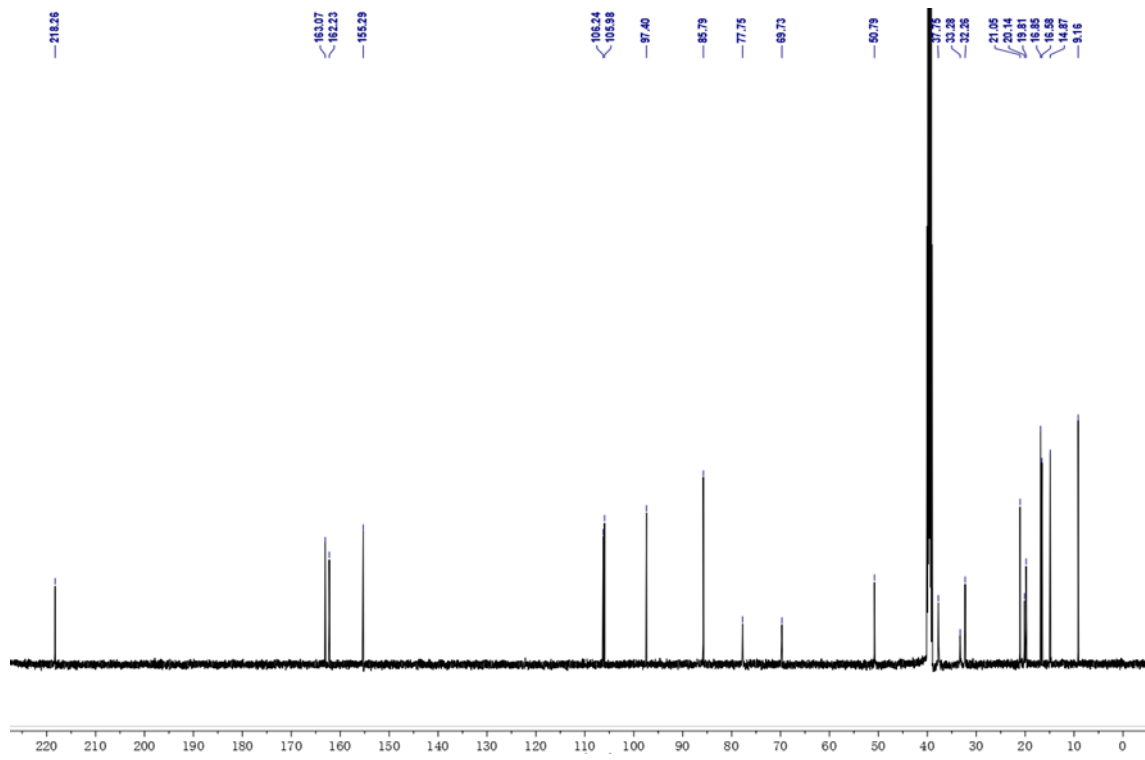


Figure S86. ¹³C NMR spectrum of 19 (DMSO-*d*₆, 125 MHz).

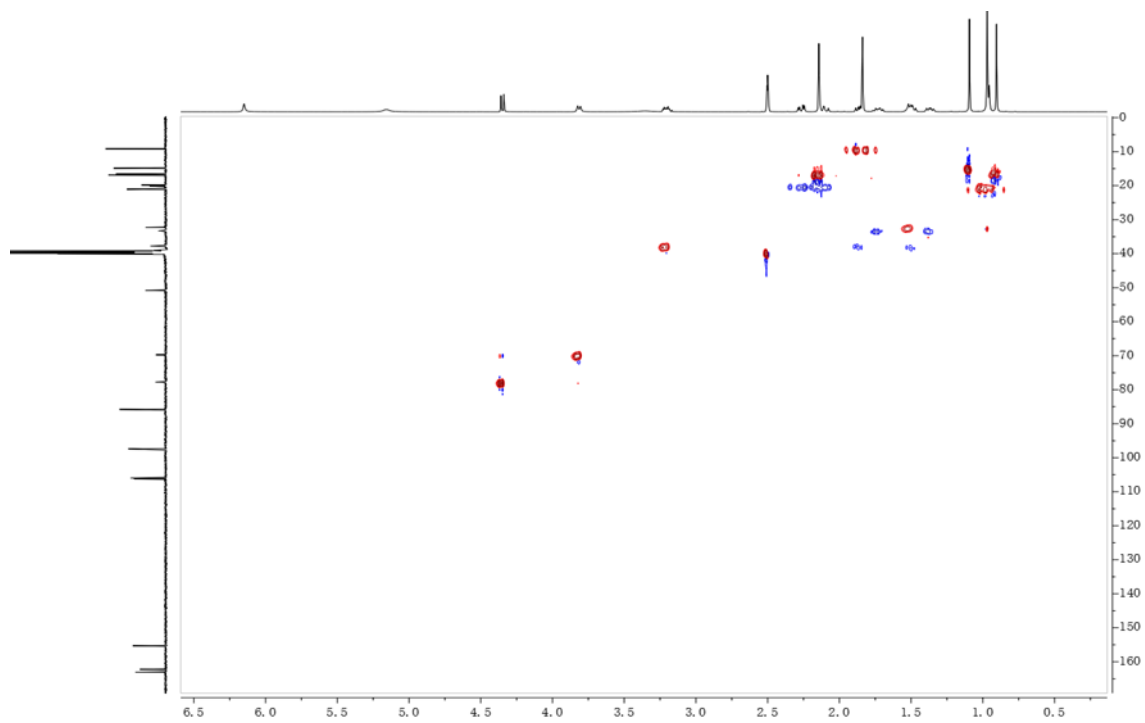


Figure S87. HSQC spectrum of 19.

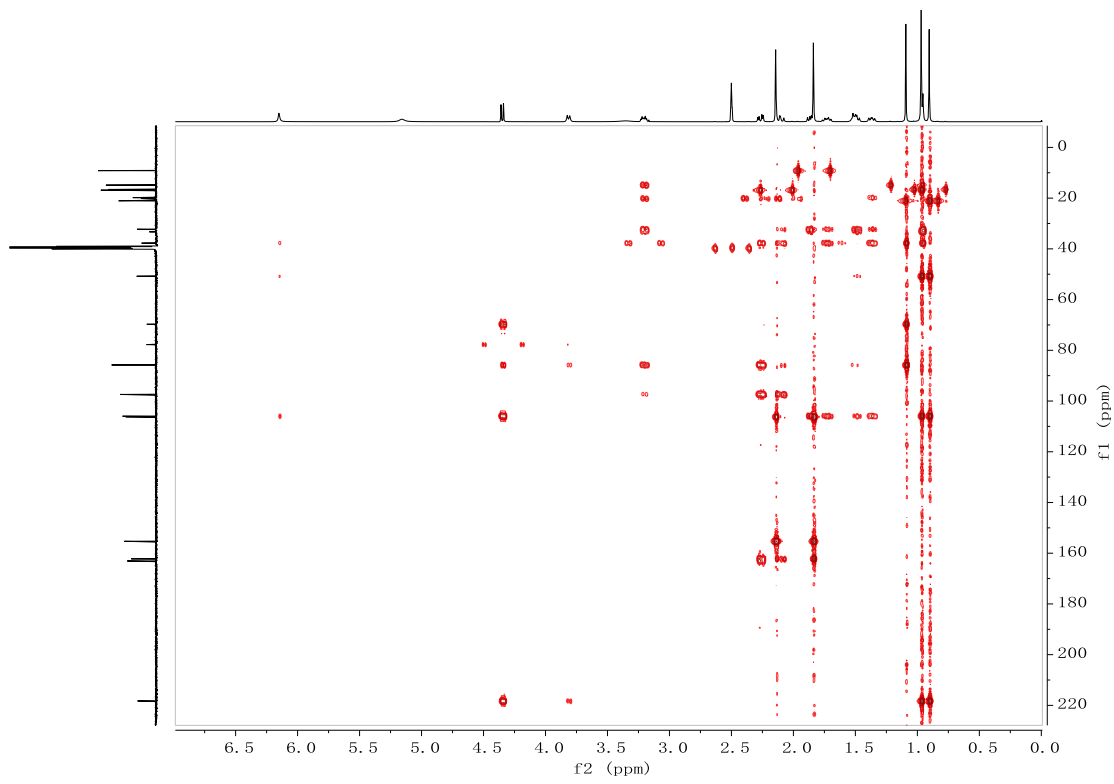


Figure S88. HMBC spectrum of 19.

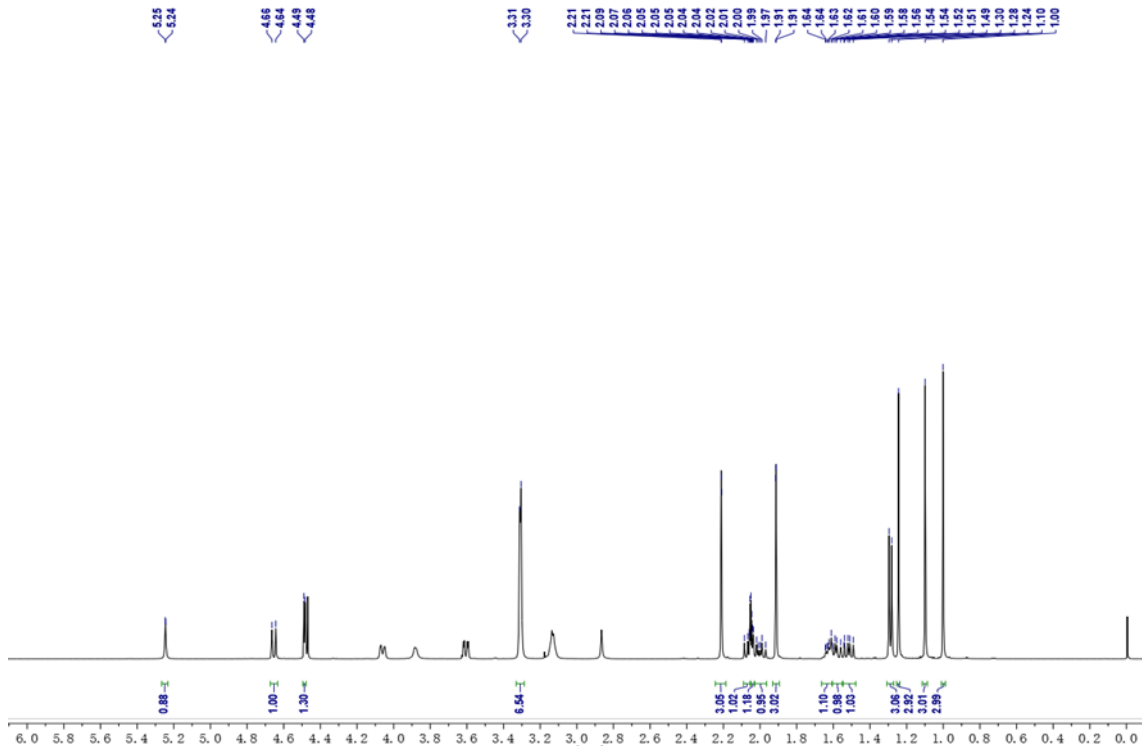


Figure S89. ^1H NMR spectrum of 21 (acetone- d_6 , 500 MHz).

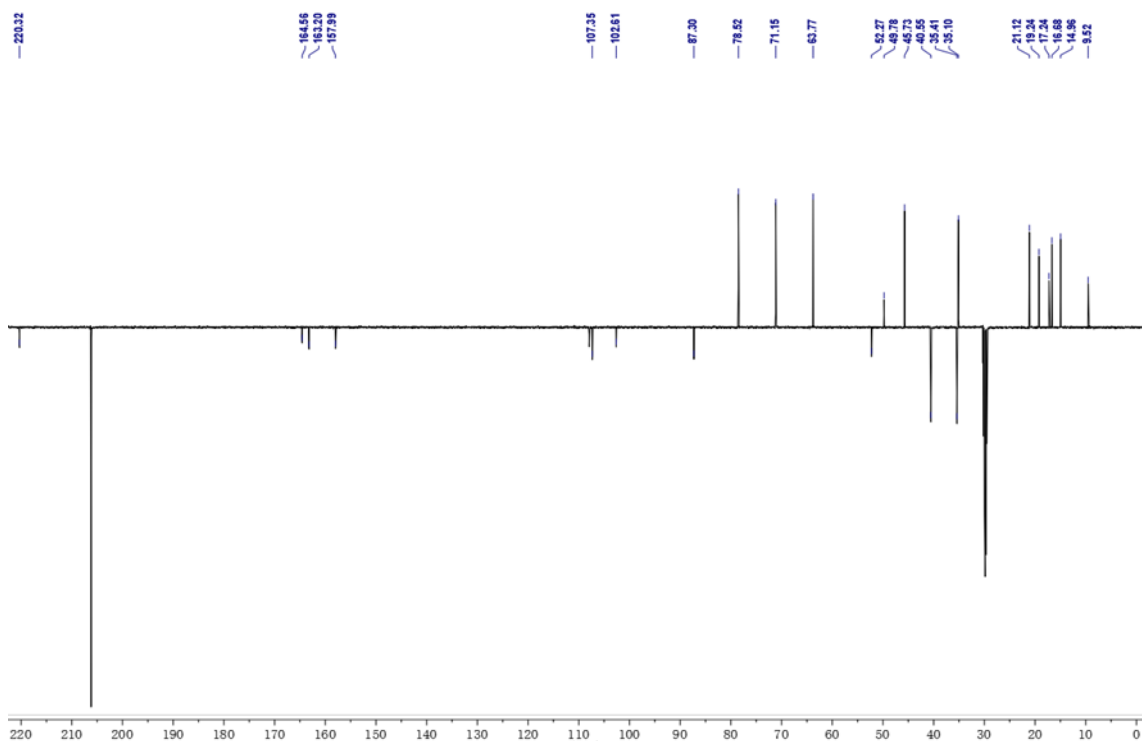


Figure S90. ¹³C NMR spectrum of 21 (acetone-*d*₆, 125 MHz).

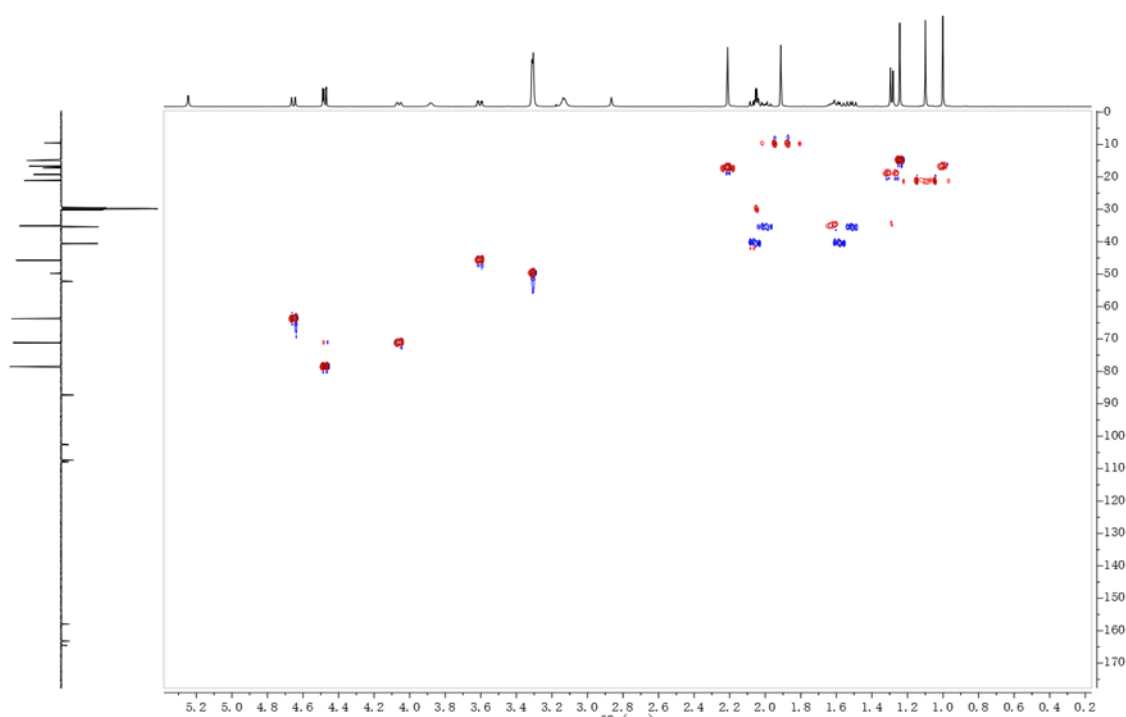


Figure S91. HSQC spectrum of 21.

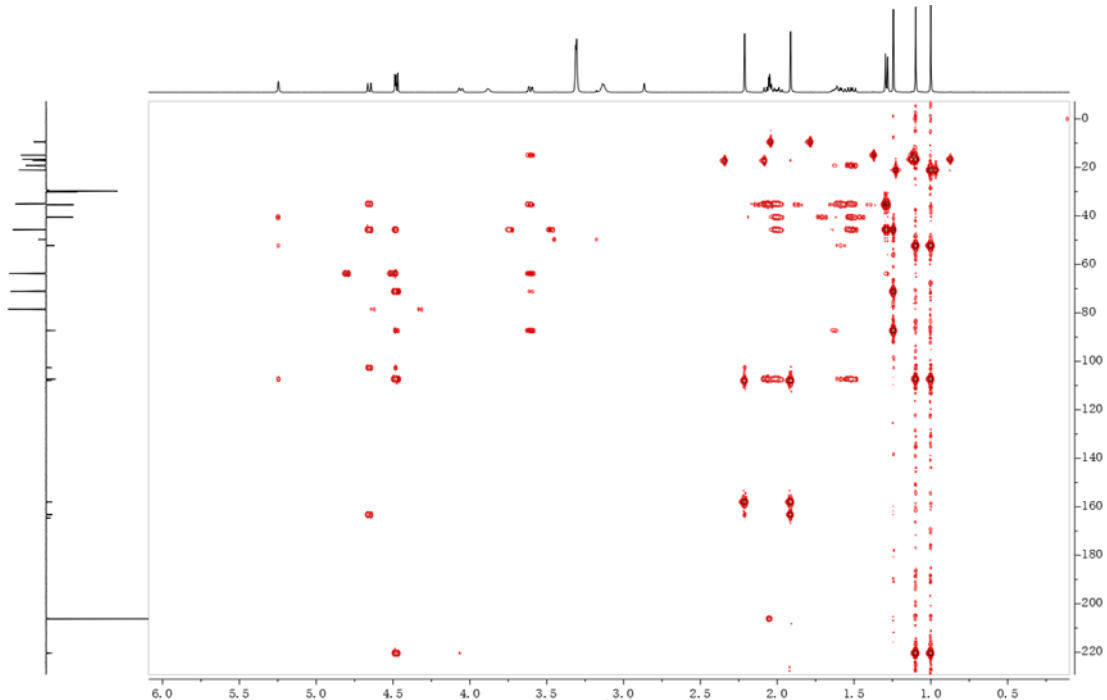


Figure S92. HMBC spectrum of 21.

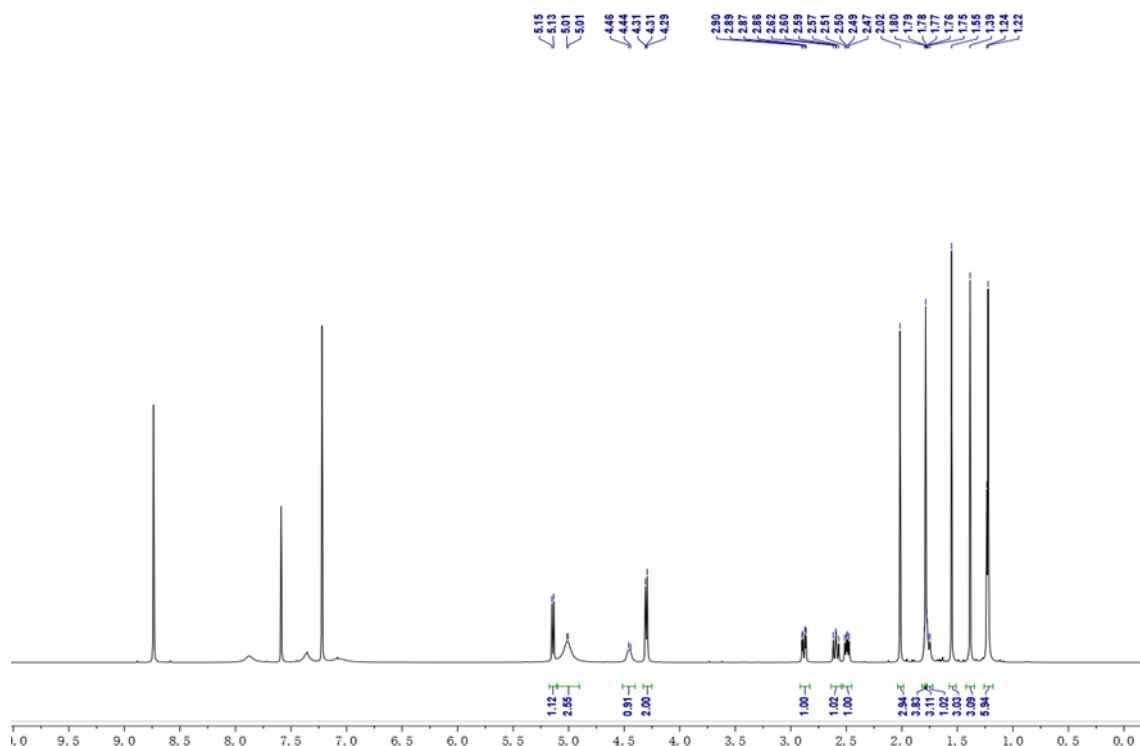


Figure S93. ^1H NMR spectrum of 23 (pyridine- d_5 , 500 MHz).

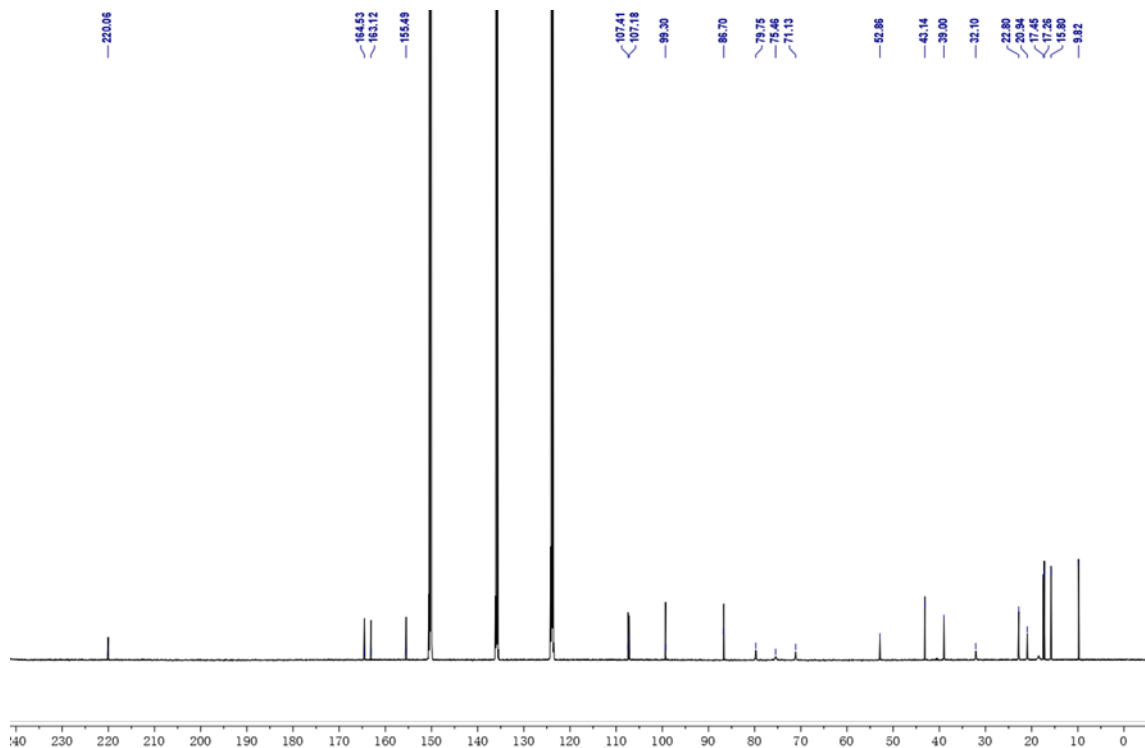


Figure S94. ¹³C NMR spectrum of 23 (pyridine-*d*₅, 125 MHz).

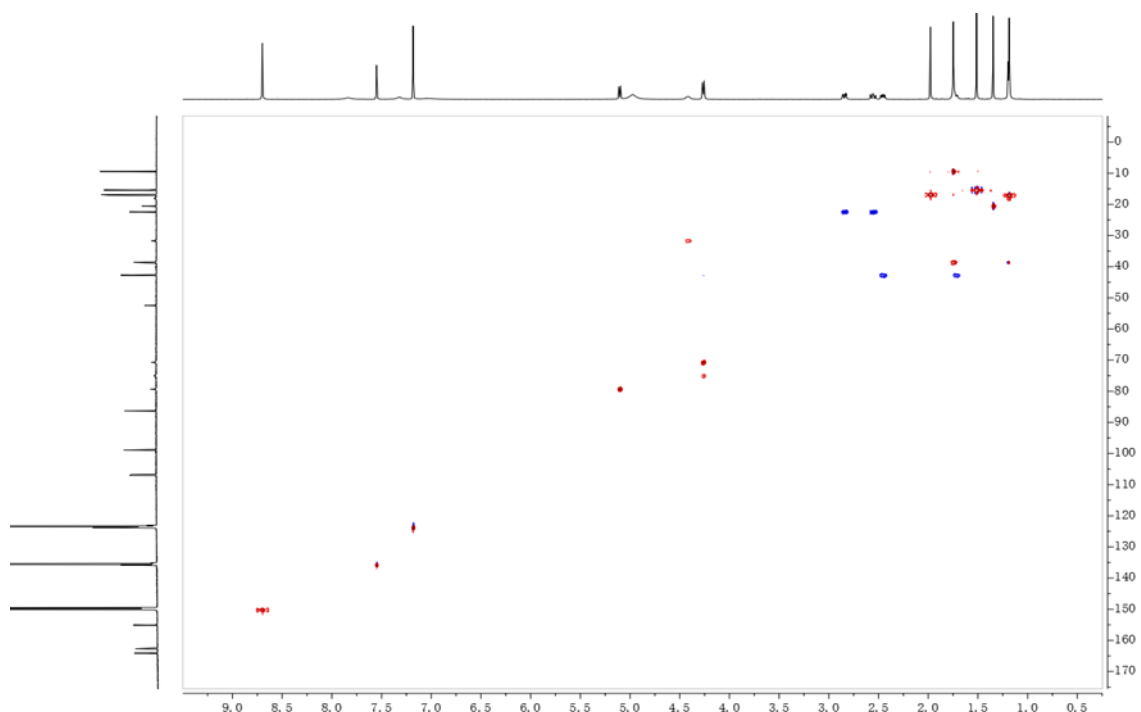


Figure S95. HSQC spectrum of 23.

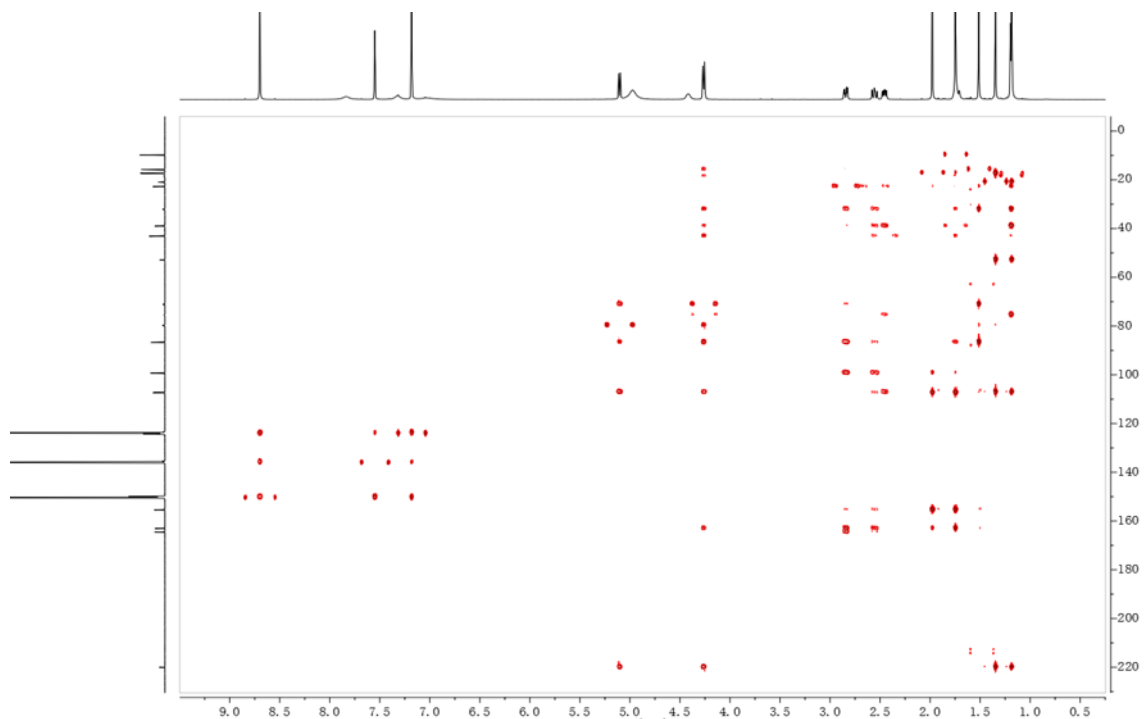


Figure S96. HMBC spectrum of 23.

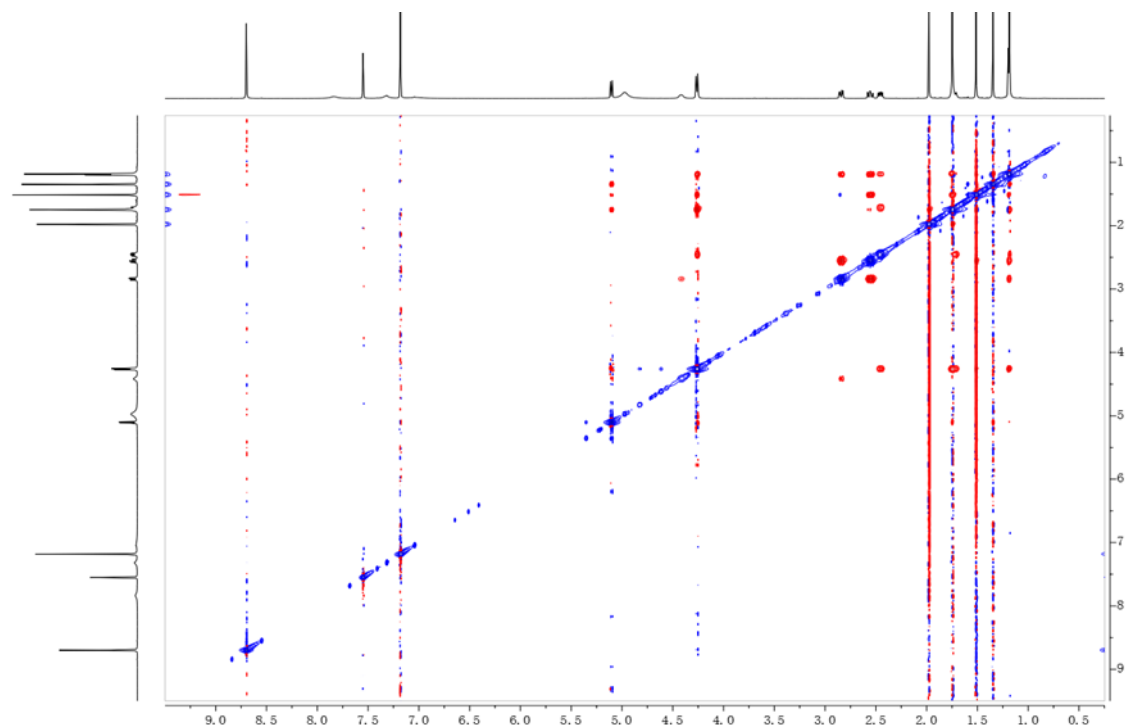


Figure S97. ROESY spectrum of 23.

References

1. Y.-M. Chiang, M. Ahuja, C. E. Oakley, R. Entwistle, A. Asokan, C. Zutz, C. C. C. Wang and B. R. Oakley, Development of Genetic Dereplication Strains in *Aspergillus nidulans* Results in the Discovery of Aspercryptin, *Angew. Chem.-Int. Edit.*, 2016, **55**, 1662-1665.
2. J. H. Yu, Z. Hamari, K. H. Han, J. A. Seo, Y. Reyes-Domínguez and C. Scazzocchio, Double-joint PCR:: a PCR-based molecular tool for gene manipulations in filamentous fungi, *Fungal Genet. Biol.*, 2004, **41**, 973-981.
3. J. W. Bok and N. P. Keller, Fast and easy method for construction of plasmid vectors using modified quick-change mutagenesis, *Methods in molecular biology (Clifton, N.J.)*, 2012, **944**, 163-174.
4. M. Baek, F. DiMaio, I. Anishchenko, J. Dauparas, S. Ovchinnikov, G. R. Lee, J. Wang, Q. Cong, L. N. Kinch, R. D. Schaeffer, C. Millan, H. Park, C. Adams, C. R. Glassman, A. DeGiovanni, J. H. Pereira, A. V. Rodrigues, A. A. van Dijk, A. C. Ebrecht, D. J. Opperman, T. Sagmeister, C. Buhlheller, T. Pavkov-Keller, M. K. Rathinaswamy, U. Dalwadi, C. K. Yip, J. E. Burke, K. C. Garcia, N. V. Grishin, P. D. Adams, R. J. Read and D. Baker, Accurate prediction of protein structures and interactions using a three-track neural network, *Science*, 2021, **373**, 871-876.
5. M. van Kempen, S. S. Kim, C. Tumescheit, M. Mirdita, J. Lee, C. L. M. Gilchrist, J. Soeding and M. Steinegger, Fast and accurate protein structure search with Foldseek, *Nat. Biotechnol.*, 2023, DOI: 10.1038/s41587-023-01773-0.
6. F. Gabler, S.-Z. Nam, S. Till, M. Mirdita, M. Steinegger, J. Soding, A. N. Lupas and V. Alva, Protein Sequence Analysis Using the MPI Bioinformatics Toolkit, *Curr. Protoc. Bioinformatics*, 2020, **72**, e108-e108.
7. M. N. Price, P. S. Dehal and A. P. Arkin, FastTree: Computing Large Minimum Evolution Trees with Profiles instead of a Distance Matrix, *Mol. Biol. Evol.*, 2009, **26**, 1641-1650.
8. W. Kabsch, XDS, *Acta Crystallogr. Sect. D-Biol. Crystallogr.*, 2010, **66**, 125-132.
9. P. Emsley, B. Lohkamp, W. G. Scott and K. Cowtan, Features and development of Coot, *Acta Crystallogr. Sect. D-Biol. Crystallogr.*, 2010, **66**, 486-501.
10. P. D. Adams, P. V. Afonine, G. Bunkoczi, V. B. Chen, I. W. Davis, N. Echols, J. J. Headd, L.-W. Hung, G. J. Kapral, R. W. Grosse-Kunstleve, A. J. McCoy, N. W. Moriarty, R. Oeffner, R. J. Read, D. C. Richardson, J. S. Richardson, T. C. Terwilliger and P. H. Zwart, PHENIX: a comprehensive Python-based system for macromolecular structure solution, *Acta Crystallogr. Sect. D-Struct. Biol.*, 2010, **66**, 213-221.
11. A. J. McCoy, R. W. Grosse-Kunstleve, P. D. Adams, M. D. Winn, L. C. Storoni and R. J. Read, Phaser crystallographic software, *J. Appl. Crystallogr.*, 2007, **40**, 658-674.
12. L. Hu, T. Zhang, D. Liu, G. Guan, J. Huang, P. Proksch, X. Chen and W. Lin, Notoamide-type alkaloid induced apoptosis and autophagy via a P38/JNK signaling pathway in hepatocellular carcinoma cells, *RSC Adv.*, 2019, **9**, 19855-19868.
13. J. Xie, Y. Chen, G. Cai, R. Cai, Z. Hu and H. Wang, Tree Visualization By One Table (tvBOT): a web application for visualizing, modifying and annotating phylogenetic trees, *Nucleic Acids Res.*, 2023, **51**, W587-W592.